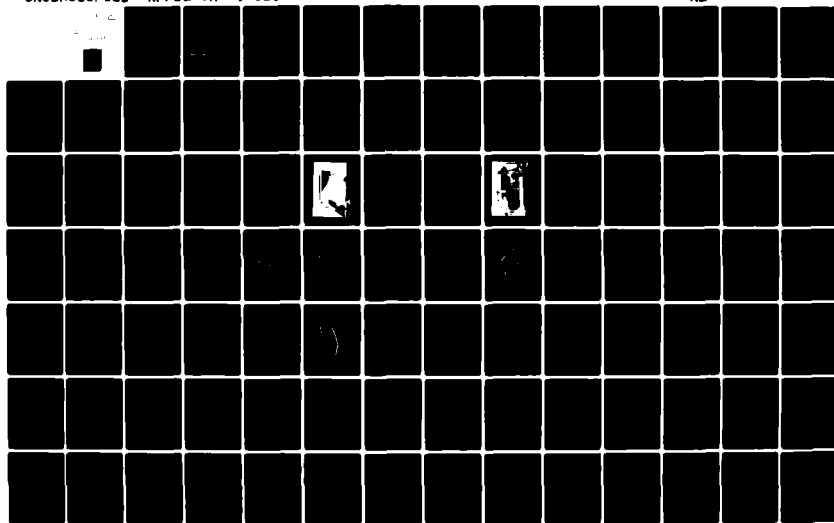
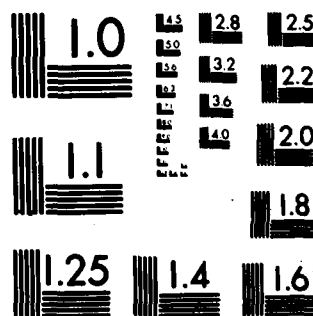


AD-A091 051

AIR FORCE FLIGHT DYNAMICS LAB WRIGHT-PATTERSON AFB OH F/6 1/3
EVALUATION OF THE IMPACT COMPUTER PROGRAM AS A LINEAR DESIGN TO--ETC(U)
MAR 80 R E MCCARTY
UNCLASSIFIED AFFDL-TR-79-3103

NL





MICROCOPY RESOLUTION TEST CHART
NATIONAL BUREAU OF STANDARDS-1963-A

C
LEVEL II (2)
AFFDL-TR-79-3103

EVALUATION OF THE IMPACT COMPUTER PROGRAM AS A LINEAR
DESIGN TOOL FOR BIRD-RESISTANT AIRCRAFT TRANSPARENCIES

Robert E. McCarty
Crew Escape and Subsystems Branch
Vehicle Equipment Division

March 1980
TECHNICAL REPORT AFFDL-TR-79-3103
Final Report for Period 1 January - 1 August 1978

Approved for public release; distribution unlimited.

AIR FORCE FLIGHT DYNAMICS LABORATORY
AIR FORCE WRIGHT AERONAUTICAL LABORATORIES
AIR FORCE SYSTEMS COMMAND
WRIGHT-PATTERSON AIR FORCE BASE, OHIO 45433

DTIC
ELECTE
OCT 31 1980
A

80 10 30 094

AD A091051

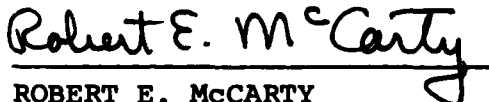
DDC FILE COPY

NOTICE

When Government drawings, specifications, or other data are used for any purpose other than in connection with a definitely related Government procurement operation, the United States Government thereby incurs no responsibility nor any obligation whatsoever; and the fact that the Government may have formulated, furnished, or in any way supplied the said drawings, specifications, or other data, is not to be regarded by implication or otherwise as in any manner licensing the holder or any other person or corporation, or conveying any rights or permission to manufacture, use or sell any patented invention that may in any way be related thereto.

This report has been reviewed by the Information Office (IO) and is releasable to the National Technical Information Service (NTIS). At NTIS, it will be available to the general public, including foreign nations.

This technical report has been reviewed and is approved for publication.

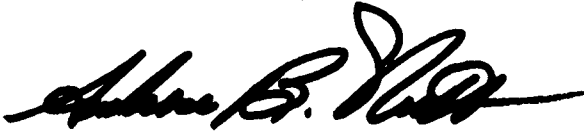


ROBERT E. MCCARTY
Project Engineer



R. HARLEY WALKER
Group Leader
Subsystems Development
Group

FOR THE COMMANDER



AMBROSE B. NUTT
Director
Vehicle Equipment Division

"If your address has changed, if you wish to be removed from our mailing list, or if the addressee is no longer employed by your organization, please notify AFFDL/FER, W-PAFB, OH 45433 to help us maintain a current mailing list."

Copies of this report should not be returned unless return is required by security considerations, or notice on a specific document.

UNCLASSIFIED

SECURITY CLASSIFICATION OF THIS PAGE (When Data Entered)

REPORT DOCUMENTATION PAGE		READ INSTRUCTIONS BEFORE COMPLETING FORM
1. REPORT NUMBER AFFDL-TR-79-3163	2. GOVT ACCESSION NO. AD-A091051	3. REPORT'S CATALOG NUMBER 0519
4. TITLE (and Subtitle) EVALUATION OF THE IMPACT COMPUTER PROGRAM AS A LINEAR DESIGN TOOL FOR BIRD-RESISTANT AIRCRAFT TRANSPARENCIES.		5. TYPE OF REPORT & PERIOD COVERED Final Report 1 Jan 78 - 1 Aug 78
6. AUTHOR(s) Robert E. McCarty		7. PERFORMING ORG. REPORT NUMBER
8. CONTRACT OR GRANT NUMBER(s)		9. PROGRAM ELEMENT PROJECT, TASK AND A WORK UNIT NUMBERS Project 2402 Task 240203 Work Unit 24020305
10. CONTROLLING OFFICE NAME AND ADDRESS Air Force Flight Dynamics Laboratory Wright-Patterson Air Force Base, OH 45433		11. REPORT DATE March 1980
12. MONITORING AGENCY NAME & ADDRESS (if different from Controlling Office) 12-166		13. NUMBER OF PAGES 165
14. DISTRIBUTION STATEMENT (of this Report) Approved for public release; distribution unlimited.		15. SECURITY CLASS. (of this report) Unclassified
16. DISTRIBUTION STATEMENT (of the abstract entered in Block 20, if different from Report)		15a. DECLASSIFICATION/DOWNGRADING SCHEDULE
17. SUPPLEMENTARY NOTES		
18. KEY WORDS (Continue on reverse side if necessary and identify by block number) Finite Element Analysis Structural Analysis Aircraft Windshields Bird Impact Computed Aided Design		
19. ABSTRACT (Continue on reverse side if necessary and identify by block number) The use of a finite element structural analysis computer program called IMPACT to simulate the transient response of B-1 aircraft windshield panels to bird impact is discussed. For the two simulations accomplished, computed results were compared to experimental data acquired during bird impact tests of actual windshield panels. For the first case of a panel tested at ambient temperature the computed results were qualitatively accurate. Strain levels		

DD FORM 1473

EDITION OF 1 NOV 65 IS OBSOLETE

UNCLASSIFIED

SECURITY CLASSIFICATION OF THIS PAGE (When Data Entered)

012070

UNCLASSIFIED

SECURITY CLASSIFICATION OF THIS PAGE(When Data Entered)

measured during the test exceeded those calculated by IMPACT, however, and the disagreement was attributed to the presence of geometric nonlinearities in the test structure the effects of which were not accounted for in the IMPACT analysis. For the second case of a panel heated to an outer surface temperature of 220 deg F the computed results were unreasonable. Disagreement between computed and experimental data was attributed to errors in the theoretical formulation or coding of IMPACT relating to its capability to account for the effects of elevated temperatures or temperature gradients within the structure. Continued development of IMPACT is not recommended; a currently available fully nonlinear finite element program is identified which has more potential of serving as a transparency birdstrike analysis tool.

UNCLASSIFIED

SECURITY CLASSIFICATION OF THIS PAGE(When Data Entered)

FOREWORD

This report describes an in-house work effort conducted by the Crew Escape and Subsystems Branch (FER), Vehicle Equipment Division (FE), Air Force Flight Dynamics Laboratory, Air Force Wright Aeronautical Laboratories, Wright-Patterson Air Force Base, Ohio, under Project 2402, "Vehicle Equipment Technology," Task 240203, "Aerospace Vehicle Recovery and Escape Subsystems," Work Unit 24020305, "Survivable Aircraft Transparent Enclosures."

The work reported herein was performed during the period of 1 January 1978 to 1 August 1978 by the author, Mr. Robert E. McCarty (AFFDL/FER), project engineer. The report was released by the author in June 1979. All illustrations for the report were done by Mrs. In Sook Oh.

This report is the first of a planned series dealing with finite element design and analysis of various Air Force aircraft transparency systems. Later reports will follow as portions of the work planned are completed. The overall goal of this work is to develop and apply finite element analysis computer programs capable of simulating accurately the transient structural response of aircraft transparency systems to bird impact.

Accession For	
NTIS GRA&I	<input checked="checked" type="checkbox"/>
DTIC TAB	<input type="checkbox"/>
Unannounced	
Justification	
By	
Distribution/	
Availability Codes	
Dist	Avail and/or
	Special
A	

TABLE OF CONTENTS

SECTION		PAGE
I	INTRODUCTION	1
	1. Background	1
	2. Approach	3
	3. Scope	4
II	'IMPACT' COMPUTER PROGRAM	5
	1. Capabilities	5
	2. Architecture	6
	3. Operation	10
III	EXPERIMENTAL DATA	11
	1. Simulated B-1 Windshield Tests	11
	2. B-1 X-5 Module Tests	16
IV	STRUCTURAL MODELING	22
	1. Test Case Selection	22
	2. Test BM14	23
	3. Test BM19	36
	4. Test BM18	36
	5. Test BM006	38
	6. Test BM004	46
V	BIRDSTRIKE LOADS	47
	1. Theory	47
	2. Birdstrike Loads Data - Test BM14	54
	3. Birdstrike Loads Data - Test BM19	71
VI	COMPUTER ANALYSES	79
	1. Assumptions	79
	2. Test BM14	83
	3. Test BM19	86
	4. Tests BM006 and BM004	87
	5. Boundary Conditions Study	91
	6. Interlayer Properties Study	93

TABLE OF CONTENTS (Concluded)

SECTION		PAGE
VII	RESULTS	96
	1. Accuracy of IMPACT Results	96
	2. Efficiency of IMPACT	135
	3. Usability of IMPACT	137
VIII	CONCLUSIONS	139
IX	RECOMMENDATIONS	143
	REFERENCES	146

LIST OF ILLUSTRATIONS

FIGURE		PAGE
1	IMPACT Architecture	7
2	Simulated B-1 Windshield Test Setup	13
3	Simulated B-1 Windshield Test Fixture	14
4	Simulated B-1 Windshield Test Fixture Photo	15
5	B-1 X-5 Module Test Setup	17
6	B-1 X-5 Module Test Setup Photo	18
7	Elevation View of Impact Location	19
8	Plan View of Impact Location	20
9	Simulated Windshield Support Structure	24
10	Test BM14/BM19 Simulated B-1 Windshield	25
11	Test BM14/BM19 Center Member Support Structure	26
12	Test BM14/BM19 Side Post Support Structure	27
13	Test BM14/BM19 Forward Longeron Support Structure	28
14	Test BM14/BM19 Aft Longeron Support Structure	29
15	-49 Laminate Partial Windshield Panel in Support Fixture	30
16	Test BM14/BM19 Finite Element Model	32
17	BM19 Windshield Temperature Distribution Assumed	37
18	Test BM18 Simulated B-1 Windshield	39
19	Test BM18 Center Member Support Structure	40
20	Test BM006 B-1 X-5 Module Windshield	41
21	Test BM006 Finite Element Model	43

LIST OF ILLUSTRATIONS (Continued)

FIGURE		PAGE
22	Motion of a Bird Before and After Impact	49
23	Oblique Impact Effective Bird Length	51
24	Generalized Bird Impact Force-Time Profile	53
25	Camera Locations for Shots BM-14 through BM-19	55
26	Camera Number 2 Record of Test BM14	57
27	Camera Number 4 Record of Test BM14	58
28	Axial View of BM14 Test Fixture	59
29	Determination of Angle Theta, θ	61
30	Bird Impact Force-Time Distribution for Test BM14	63
31	Determination of Angle Gamma, γ	64
32	Layout for Bird Impact Loads, Test BM14	66
33	Bird Impact Footprint for Test BM14	67
34	BM14 Bird Footprint at Time Increment 1	68
35	BM14 Bird Footprint at Time Increment 2	68
36	BM14 Bird Footprint at Time Increment 3	68
37	BM14 Bird Footprint at Time Increment 4	68
38	BM14 Bird Footprint at Time Increment 5	69
39	BM14 Bird Footprint at Time Increment 6	69
40	BM14 Bird Footprint at Time Increment 7	69
41	BM14 Bird Footprint at Time Increment 8	69
42	BM14 Bird Footprint at Time Increment 9	70
43	BM14 Bird Footprint at Time Increment 10	70
44	Camera Number 2 Record of Test BM19	72
45	Camera Number 1 Record of Test BM19	73

LIST OF ILLUSTRATIONS (Continued)

FIGURE		PAGE
46	Bird Impact Footprint for Test BM19	75
47	BM19 Bird Footprint at Time Increment 1	76
48	BM19 Bird Footprint at Time Increment 2	76
49	BM19 Bird Footprint at Time Increment 3	76
50	BM19 Bird Footprint at Time Increment 4	76
51	BM19 Bird Footprint at Time Increment 5	77
52	BM19 Bird Footprint at Time Increment 6	77
53	BM19 Bird Footprint at Time Increment 7	77
54	BM19 Bird Footprint at Time Increment 8	77
55	BM19 Bird Footprint at Time Increment 9	78
56	BM19 Bird Footprint at Time Increment 10	78
57	Shear Stress-Strain Characteristics for PPG 112 Interlayer	80
58	Static Analysis of Pinned-Pinned Laminated Beam	94
59	Static Analysis of Fixed-Fixed Laminated Beam	94
60	Strain Gage Locations for Tests BM14 and BM19	97
61	X Strain for the Outer Face of Cell Number 66	98
62	Y Strain for the Outer Face of Cell Number 66	98
63	X Strain for the Inner Face of Cell Number 66	98
64	Y Strain for the Inner Face of Cell Number 66	99
65	X Strain for the Outer Face of Cell Number 110	99

LIST OF ILLUSTRATIONS (Continued)

FIGURE		PAGE
66	Y Strain for the Outer Face of Cell Number 110	99
67	X Strain for the Inner Face of Cell Number 110	100
68	Y Strain for the Inner Face of Cell Number 110	100
69	X Strain for the Outer Face of Cell Number 115	100
70	Y Strain for the Outer Face of Cell Number 115	101
71	X Strain for the Inner Face of Cell Number 115	101
72	Y Strain for the Inner Face of Cell Number 115	101
73	X Strain for the Outer Face of Cell Number 124	102
74	Y Strain for the Outer Face of Cell Number 124	102
75	X Strain for the Inner Face of Cell Number 124	102
76	Y Strain for the Inner Face of Cell Number 124	103
77	X Strain for the Outer Face of Cell Number 164	103
78	Y Strain for the Outer Face of Cell Number 164	103
79	X Strain for the Inner Face of Cell Number 164	104
80	Y Strain for the Inner Face of Cell Number 164	104
81	Bending Wave Propagation	106
82	Locations for BM14 and BM19 at which IMPACT Calculated Strains	107

LIST OF ILLUSTRATIONS (Continued)

FIGURE		PAGE
83	Static Strains at Center Cross Section of Pinned-Pinned Beam	110
84	Static Strains at Center Cross Section of Fixed-Fixed Beam	111
85	Static Strains at Center Cross Section of Hot Pinned-Pinned Beam	113
86	Shallow Spherical Cap Under Apex Loading	116
87	Linear and Nonlinear Analysis Results for Shallow Cap	117
88	Cross Section of BM14 Windshield Panel	117
89	Z Deflection for Node 447	119
90	Z Deflection of Nodes Along Longitudinal Section for Test BM14	120
91	BM14 Structural Failure Predicted by IMPACT	122
92	X Strain for the Outer Face of Cell Number 66	123
93	Y Strain for the Outer Face of Cell Number 66	123
94	X Strain for the Inner Face of Cell Number 66	123
95	Y Strain for the Inner Face of Cell Number 66	124
96	X Strain for the Inner Face of Cell Number 110	124
97	X Strain for the Outer Face of Cell Number 115	124
98	Y Strain for the Outer Face of Cell Number 115	125
99	X Strain for the Inner Face of Cell Number 115	125

LIST OF ILLUSTRATIONS (Concluded)

FIGURE		PAGE
100	Y Strain for the Inner Face of Cell Number 115	125
101	X Strain for the Outer Face of Cell Number 124	126
102	Y Strain for the Outer Face of Cell Number 124	126
103	X Strain for the Inner Face of Cell Number 124	127
104	Y Strain for the Inner Face of Cell Number 124	127
105	Z Deflection of BM14 Node 447 and BM19 Node 359	130
106	Z Deflection for Node 359	131
107	Z Deflection of Nodes Along a Longitudinal Section for Test BM19	132
108	Equivalent Stress for Outer Surface of Cell 394	134
109	Equivalent Stress for Inner Surface of Cell 394	134

LIST OF TABLES

TABLE		PAGE
1	Simulated B-1 Windshield Tests	12
2	B-1 X-5 Module Tests	21
3	Mechanical Properties of Materials BM14/ BM19 Finite Element Models	34
4	Mechanical Properties of Materials BM006 Finite Element Model	44
5	Computer Resources Required for IMPACT Analysis of Test BM14	84
6	Computer Resources Required for IMPACT Analysis of Test BM19	86
7	Computer Resources Required for IMPACT Analysis of Test BM006	88

LIST OF SYMBOLS

<u>Symbol</u>	<u>Units</u>	<u>Definition</u>
A	in ²	Cross sectional area.
BB	in	Width of ply in laminated beam.
CP	-	Central processor.
d	ft	Bird diameter.
E	psi	Young's Modulus.
F	lb	Force.
F _{avg}	lb	Average force exerted by bird on target over period of impact.
G	psi	Shear modulus.
h	in	Height.
H	lb	Axial force in ply of laminated beam.
I	lb sec	Impulse.
I	in ⁴	Area moment of inertia.
I _p	in ⁴	Polar area moment of inertia.
I _{xx}	in ⁴	Area moment of inertia.
I _{yy}	in ⁴	Area moment of inertia.
I/O	-	Input/Output.
JCL	-	Job control language.
L	ft	Bird length.
L _{eff}	ft	Effective bird length.
m	slugs	Mass.
MXJ	lb in	Bending moment in ply of laminated beam.
n	ft	Inward unit surface normal located at target point on aircraft windshield.

LIST OF SYMBOLS (Continued)

<u>Symbol</u>	<u>Units</u>	<u>Definition</u>
R	in	Radius.
S	in	Circular arc length.
t	sec	Time.
t	in	Thickness.
T	sec	Period of impact.
T	in	Thickness of ply in laminated beam.
TL	-	True length.
V	ft/sec	Velocity, bird velocity.
V _B	ft/sec	Bird velocity.
V _r	ft/sec	Radial velocity.
w	in	Deflection.
x	in	Cartesian coordinate.
y	in	Cartesian coordinate.
z	in	Cartesian coordinate.
α	deg	Alpha, the angle between the windshield centerline and the bird path measured in the aircraft plane of symmetry.
β	deg	Beta, the angle between the surface normal at the target point and the aircraft right hand direction measured in the plane normal to the windshield centerline.
δ	-	Time increment number.
γ	deg	Gamma, the angle between the major axis of the bird impact footprint ellipse and the centerline of the windshield measured in the plane tangent to the surface at the impact point.

LIST OF SYMBOLS (Concluded)

<u>Symbol</u>	<u>Units</u>	<u>Definition</u>
δ	deg	Delta, the complement of theta.
δ_{ij}	-	Kronecker delta.
ϵ	in/in	Normal axial strain at the top and bottom edges of a ply cross section in a laminated beam.
ϵ_{ij}	in/in	Strain tensor.
ϵ_{kk}	in/in	Dilatation
ϵ_X	in/in	Normal strain in the X direction.
ϵ_Y	in/in	Normal strain in the Y direction.
θ	deg	Theta, the angle between the target surface and the bird path measured in the plane normal to the surface at the impact point.
μ	-	Micro; prefix for 10^{-6} .
ν	-	Poisson's ratio.
σ_{ij}	psi	Stress tensor.

SECTION I INTRODUCTION

1. BACKGROUND

Current flight missions for United States Air Force aircraft involve high speed, low altitude operations. Under these conditions, bird impacts on aircraft transparent crew enclosures pose a significant hazard and have resulted in unacceptable losses of aircraft and aircrew.

The F-111 aircraft has proven particularly vulnerable to the transparency birdstrike hazard primarily as a result of its transonic nap-of-the earth penetration mission and its brittle, tempered glass windshield. As of June 1978, five USAF and one Royal Australian F-111 aircraft had been destroyed as a result of confirmed windshield birdstrike at a cost of approximately \$78 million.

During 1972, the Improved Windshield Protection Program Office was established within the Air Force Flight Dynamics Laboratory to develop new transparency technology providing improved birdstrike protection for F-111 aircrew members. Laminated plastic windshields and canopies were developed and qualified by this office and are being retrofitted on several series of the F-111 aircraft (References 1-4).

(1) H. E. Littel, Improved Windshield and Canopy Protection Development Program, Air Force Flight Dynamics Laboratory, Wright-Patterson Air Force Base, Ohio 45433, AFFDL-TR-74-75, June 1974.

(2) A. L. Lewis and K. W. Cooke, F-111 Bird Resistant Windshield Support Structures, Air Force Flight Dynamics Laboratory, Wright-Patterson Air Force Base, Ohio 45433, AFFDL-TR-74-40, 10 May 1974.

(3) B. S. West, Design and Testing of F-111 Bird Resistant Windshield/Support Structure: Volume 1 - Design and Verification Testing, Air Force Flight Dynamics Laboratory, Wright-Patterson Air Force Base, Ohio 45433, AFFDL-TR-76-101, October 1976.

(4) J. B. Olson, Design, Development and Testing of a Light-Weight Bird-Proof Cockpit Enclosure for the F-111, 1978 Conference on Aerospace Transparent Materials and Enclosures, Air Force Materials Laboratory, Wright-Patterson Air Force Base, Ohio 45433, AFFDL-TR-76-168.

To date, more than ten retrofit aircraft have experienced windshield birdstrikes and have been recovered safely. In most cases, impact velocities exceeded 450 KIAS.

The approach taken in this development of improved F-111 transparencies was empirical in nature and, as a result, quite costly. By 1975, strong interest had surfaced in developing a finite element computer program capability to analyze aircraft transparency response to birdstrike. Such a tool could be used, it was hoped, in the design process to reduce the number of experimental tests required and, as a consequence, reduce overall program cost.

The result of this interest was the development of the IMPACT computer program by the Douglas Aircraft Company, Long Beach, California, under contract number F33615-75-C-3105 (References 5-7). Since the main objective of this Douglas work effort originally was the design of an improved windshield system for the B-1 aircraft, a number of full-scale birdstrike tests were performed with a variety of candidate B-1 windshield designs (References 8-10). It had been intended to validate the IMPACT

(5) P. H. Denke, Aircraft Windshield Bird Impact Math Model, Part 1 Theory and Application, Air Force Flight Dynamics Laboratory, Wright-Patterson Air Force Base, Ohio 45433, AFFDL-TR-77-99, Part 1, December 1977.

(6) G. R. Eide, Aircraft Windshield Bird Impact Math Model - Part 2 -User's Manual, Air Force Flight Dynamics Laboratory, Wright-Patterson Air Force Base, Ohio 45433, AFFDL-TR-77-99, Part 2, December 1977.

(7) R. C. Morris, Aircraft Windshield Bird Impact Math Model, Part 3: Programming Manual, Air Force Flight Dynamics Laboratory, Wright-Patterson Air Force Base, Ohio 45433, AFFDL-TR-77-99, Part 3, December 1977.

(8) R. H. Magnusson, High Speed Bird Impact Testing of Aircraft Transparencies, Air Force Flight Dynamics Laboratory, Wright-Patterson Air Force Base, Ohio 45433, AFFDL-TR-77-98, February 1978.

(9) E. J. Sanders, Results of Further Tests to Evaluate the Bird Impact Resistance of Windshields for the B-1 Aircraft, AEDC-DR-76-43, Arnold Engineering Development Center, Arnold Air Force Station, Tennessee 37389.

(10) E. J. Sanders, Results of Bird Impact Testing of Prototype B-1 Windshields and Supporting Structure Design, AEDC-DR-76-100, Arnold Engineering Development Center, Arnold Air Force Station, Tennessee 37389.

computer program by performing correlation studies under contract with this B-1 birdstrike data, but redirection of the contract prevented this from ever occurring. When IMPACT was delivered to the USAF in December 1977, it had been validated using only small and moderate-sized structural analysis problems (Reference 5).

The circumstances just described led to a decision by the Crew Escape and Subsystems Branch, Vehicle Equipment Division of the Air Force Flight Dynamics Laboratory to perform in-house B-1 correlation studies with the IMPACT computer program during fiscal year 1978. The approach taken is discussed in the following section.

2. APPROACH

The Douglas Aircraft Company had generated finite element models of the structures used in B-1 birdstrike testing. It was planned to utilize these structural models in conjunction with the IMPACT computer program to simulate several B-1 windshield birdstrike tests. The analyses would be linear since the planned nonlinear version of IMPACT was not operational at delivery time. All materials would be assumed to be linearly elastic and deflections in the structure due to birdstrike loading would be assumed to be small everywhere. The primary objective of the in-house study was to determine whether or not aircraft windshield systems employing relatively stiff structure like the B-1 windshield could be designed with a linear analysis tool such as IMPACT. The secondary objective was to evaluate the efficiency and usability of the IMPACT computer program itself. Conclusions regarding both objectives would be drawn from the study results and recommendations would be made concerning the most promising

(5) P. H. Denke, Aircraft Windshield Bird Impact Math Model, Part 1 Theory and Application, Air Force Flight Dynamics Laboratory, Wright-Patterson Air Force Base, Ohio 45433, AFFDL-TR-77-99, Part 1, December 1977.

paths for further development in the area of aircraft transparency birdstrike analysis.

3. SCOPE

Five B-1 birdstrike simulations were planned. Since knowledge of the mechanical properties of aircraft transparent materials was advancing rapidly at the time, it was planned to update the finite element models prepared by Douglas Aircraft during 1975 and 1976 with current material properties data before initiating analyses with IMPACT (References 12, 13, 23). No modifications would be made to the IMPACT computer program; it would be used in its as-delivered form throughout the conduct of the in-house studies. Correlation between experimental and computed data would be demonstrated in the form of strain-time and deflection-time plots as well as maps of failed areas in the structure.

(12) Military Standardization Handbook-Plastics for Aerospace Vehicles, Part II, Transparent Glazing Materials, MIL-HDBK-17A, Part II, 8 June 1977.

(13) F. E. Greene, Testing for Mechanical Properties of Monolithic and Laminated Polycarbonate Materials, Air Force Flight Dynamics Laboratory, Wright-Patterson Air Force Base, Ohio 45433, AFFDL-TR-77-96, October 1977.

(23) G. F. Rhodes, Damping, Static, Dynamic and Impact Characteristics of Laminated Beams Typical of Windshield Construction, Air Force Flight Dynamics Laboratory, Wright-Patterson Air Force Base, Ohio 45433, AFFDL-TR-76-156, December 1977.

SECTION II

'IMPACT' COMPUTER PROGRAM

1. CAPABILITIES

The IMPACT computer program was intended to be a fully nonlinear, finite element analysis computer program. It was designed to calculate the transient dynamic response of aircraft transparency structures subjected to bird impact loads.

The birdstrike analysis problem becomes especially complex for one-piece, light-weight, doubly-curved, plastic canopies such as that employed on the F-16 aircraft. Since IMPACT was to have been used in a variety of aircraft transparency design applications including F-16 canopy analyses, it was to have included a long list of features required to ensure that capability including the following:

1. Full three-dimensional analysis.
2. Generation of finite element models for laminated transparency structures.
3. General spatial and temporal distributions of loads.
4. Nonlinear elastic-plastic material properties.
5. Temperature effects upon material properties.
6. Strain rate effects upon material properties.
7. Damping due to laminate interlayer materials.
8. Strong geometric nonlinearity (large displacement effects).
9. Coupling between bird impact loading and structural deformation.
10. Thermal loads due to material damping and initial thermal gradients in the structure.
11. Effective postprocessor for graphic analysis of computed results.

Redirection of the work effort and unforeseen problems in the development of IMPACT resulted in the computer program being delivered to the USAF with less than those features just listed. No attempt was made to address load-response coupling due to a lack of available information. Mathematical formulations for nonlinear properties of materials were prepared but not implemented in IMPACT. Attempts were made to account for geometric nonlinearity but were not successful (Reference 5). The thermal loads resulting from interlayer damping were not accounted for and the pre- and postprocessors delivered with IMPACT were rudimentary.

2. ARCHITECTURE

IMPACT was designed to operate in eight serial steps. The eight separate modules are the Laminate Generator, the Loads Generator, the Initial Generator, FORMAT Setup 1, FORMAT Setup 2, FORMAT Setup 3, the Incremental Solution, and the Postprocessor (Figure 1). The three FORMAT steps utilize a previously-developed computer program named FORMAT to perform linear matrix algebra operations (Reference 14). The name FORMAT is an acronym for FORTRAN Matrix Abstraction Technique. The eight modules can be run separately as stand-alone jobs for large problems, or as a continuous series under one job for sufficiently small problems.

(5) P. H. Denke, Aircraft Windshield Bird Impact Math Model, Part 1 Theory and Application, Air Force Flight Dynamics Laboratory, Wright-Patterson Air Force Base, Ohio 45433, AFFDL-TR-77-99, Part 1, December 1977.

(14) J. Pickard, FORMAT - FORTRAN Matrix Abstraction Technique-Volume V, Engineering User and Technical Report, Air Force Flight Dynamics Laboratory, Wright-Patterson Air Force Base, Ohio 45433, AFFDL-TR-66-207, Volume V, October 1968; Volume V Supplement 1, June 1970; Volume V Supplement II, April 1973; Volume V Supplement III, December 1977.

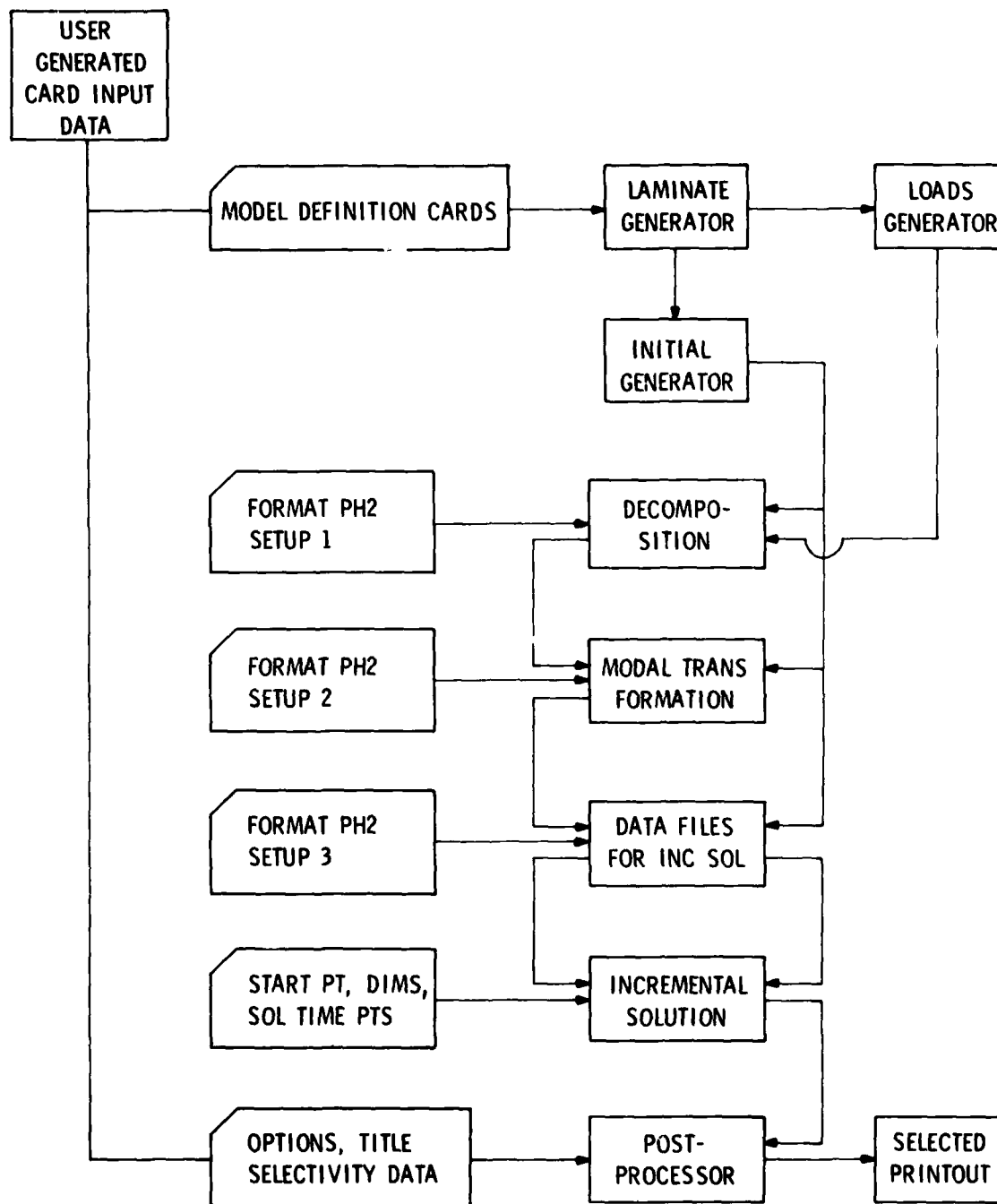


Figure 1. IMPACT Architecture.

The Laminate Generator requires as input a finite element model which is complete except for the definition of joints and elements which are interior to the laminated transparency portion of the model. The Laminate Generator prepares data for all joints and elements through the thickness of the laminate and merges this data with that input for joints and elements lying on the outer surface. The output of the Laminate Generator is a complete finite element model, ready for input to the Loads and Initial Generators. The user is required to utilize means other than IMPACT to prepare the initial finite element model for input to the Laminate Generator. This is not a trivial task and in general requires another computer program to serve as a preprocessor.

The Loads Generator prepares a matrix representing the bird impact loads applied to joints of the model. Several work efforts to develop theoretical models of bird impact loading have been accomplished (References 15-19, 26, 27). The IMPACT

(15) J. P. Barber and J. S. Wilbeck, Characterization of Bird Impacts on a Rigid Plate: Part I, Air Force Flight Dynamics Laboratory, Wright-Patterson Air Force Base, Ohio 45433, AFFDL-TR-75-5, January 1975.

(16) R. L. Peterson and J. P. Barber, Bird Impact Forces in Aircraft Windshield Designs, Air Force Flight Dynamics Laboratory, Wright-Patterson Air Force Base, Ohio 45433, AFFDL-TR-75-150, March 1976.

(17) Y. M. Ito, G. E. Carpenter, and F. W. Perry, Bird Impact Loading Model for Aircraft Windshield Design, CRT 3090-2, California Research & Technology, Inc., Woodland Hills, California 91364, July 1977.

(18) J. P. Barber, J. S. Wilbeck, and H. R. Taylor, Bird Impact Forces and Pressures on Rigid and Compliant Targets, Air Force Flight Dynamics Laboratory, Wright-Patterson Air Force Base, Ohio 45433, AFFDL-TR-77-60, May 1978.

(19) J. S. Wilbeck, Impact Behavior of Low Strength Projectiles, Air Force Materials Laboratory, Wright-Patterson Air Force Base, Ohio 45433, AFML-TR-77-134, July 1978.

(26) A. Challita and J. P. Barber, The Scaling of Bird Impact Loads, Air Force Flight Dynamics Laboratory, Wright-Patterson Air Force Base, Ohio 45433, AFFDL-TR-79-3042, March 1979.

(27) J. Y. Parker, Measurement of Impact Bird Pressure on a Flat Plate, Arnold Engineering Development Center, Arnold Air Force Station, Tennessee 37389, AEDC-TR-79-14.

Loads Generator incorporates a force-time model of bird impact on rigid targets developed by the University of Dayton Research Institute, Dayton, Ohio, (Reference 18). The user inputs parameters including bird mass, bird velocity, and unit vectors for both target surface normal and bird path. The user must also prepare a layout drawing showing the bird loading footprint on the surface of the structure. This layout is used to prepare a list of surface joint numbers which are subject to pressure from bird material during the impact event. These joint numbers are also required as input to the Loads Generator.

The Initial Generator reads the finite element model of the structure as input and generates matrices representing the structure which are required for the analysis. Mass, stiffness, and damping matrices are among those generated.

FORMAT Setup 1 accomplishes decomposition of the structural stiffness matrix. FORMAT Setup 2 solves for and extracts an arbitrary number of free vibration modes for the structure and uses these to transform the structural and loads matrices for modal solution. FORMAT Setup 3 prepares files in sets as required by the Incremental Solution module.

The Incremental Solution module performs a linear incremental solution. The method of integration is direct, not approximate, with data being calculated at time intervals specified by the user.

The Postprocessor reads all the data generated by the Incremental Solution module and selectively prints data at time intervals chosen by the user. The user also specifies those joints for which he wants data printed and whether or not to

(18) J. P. Barber, J. S. Wilbeck, and H. R. Taylor, Bird Impact Forces and Pressures on Rigid and Compliant Targets, Air Force Flight Dynamics Laboratory, Wright-Patterson Air Force Base, Ohio 45433, AFFDL-TR-77-60, May 1978.

have joint displacements, velocities, or accelerations printed for those joints. He may also choose to have printed modal displacements, velocities, or accelerations. In addition, the user may select those elements for which he desires printed data and then may choose that data to be values of force, stress, strain, or equivalent stress for the elements selected. The Postprocessor offers no graphics, or plotting, capability.

Intermediate data between the eight IMPACT modules is voluminous for large problems and must be retained temporarily on magnetic tape.

3. OPERATION

IMPACT was designed to be compatible with Control Data Corporation 6600 series digital computers but may be modified for installation on other systems (Reference 7). It is currently installed on the CDC Cyber 74 at the ASD Computer Center, Area B, Wright-Patterson Air Force Base, Dayton, Ohio.

(7) R. C. Morris, Aircraft Windshield Bird Impact Math Model, Part 3; Programming Manual, Air Force Flight Dynamics Laboratory, Wright-Patterson Air Force Base, Ohio 45433, AFFDL-TR-77-99, Part 3, December 1977.

SECTION III EXPERIMENTAL DATA

1. SIMULATED B-1 WINDSHIELD TESTS

This section outlines in some detail the full-scale bird-strike testing already discussed in Section I.1, which was performed with several candidate B-1 windshield designs. Data acquired during this testing was used in the correlation studies which are the subject of this report.

During the period July through October 1976, 20 bird impact tests were conducted at Arnold Engineering Development Center (AEDC), Tullahoma, Tennessee (Table 1). These tests involved 36-inch-square transparency panels mounted in a larger built-up structure, all intended to simulate the B-1 aircraft windshield and supporting structure (Figures 2, 3, and 4).

The transparency panels tested were of various McDonnell-Douglas designs for an improved B-1 windshield. All were of laminated construction, some having glass structural plies and some polycarbonate.

Bird impact target location A (Figure 3) corresponded to the aft inboard corner of the aircraft left windshield. To shoot target location, C, the windshield support structure fixture was turned end-for-end and then rotated to the alternate position (Figure 3). Location C corresponded to the aft outboard corner of the aircraft right windshield.

Thirty channels of strain gage data were recorded during each test, twenty gages being embedded within the laminated test panel and ten being mounted at various points on the support structure fixture. (Reference 10).

(10) E. J. Sanders, Results of Bird Impact Testing of Prototype B-1 Windshields and Supporting Structure Design, AEDC-DR-76-100, Arnold Engineering Development Center, Arnold Air Force Station, Tennessee 37389.

TABLE 1. SIMULATED B-1 WINDSHIELD TESTS

TEST NO.	BIRD WEIGHT	V (fps)	AMBIENT TEMPERATURE DEG. F	OUTER SURFACE TEMPERATURE DEG. F	SHOT LOCATION (FIG. 3)
BM10	4.08	941	86	-40	A
BM11	4.02	960	80	85	A
BM12	4.00	943	71	-55	A
BM13	4.06	948	80	80	A
BM14	4.04	939	90	87	C
BM15	4.01	515	88	90	E
BM16	4.15	369	92	82	C
BM17	4.00	737	91	97	C
BM18	4.09	847	91	230	C
BM19	4.02	971	89	220	C
BM20	4.02	958	72	74	A
BM21	4.08	960	84	-40	A
BM22	4.05	846	71	75	C
BM23	4.01	953	72	194	C
BM24	4.00	877	58	205	C
BM25	4.00	951	72	200	C
BM26	4.00	939	54	226	C
BM27	4.01	920	78	-36	B
BM28	4.01	940	69	-30	B
BM29	4.00	931	57	-28	B

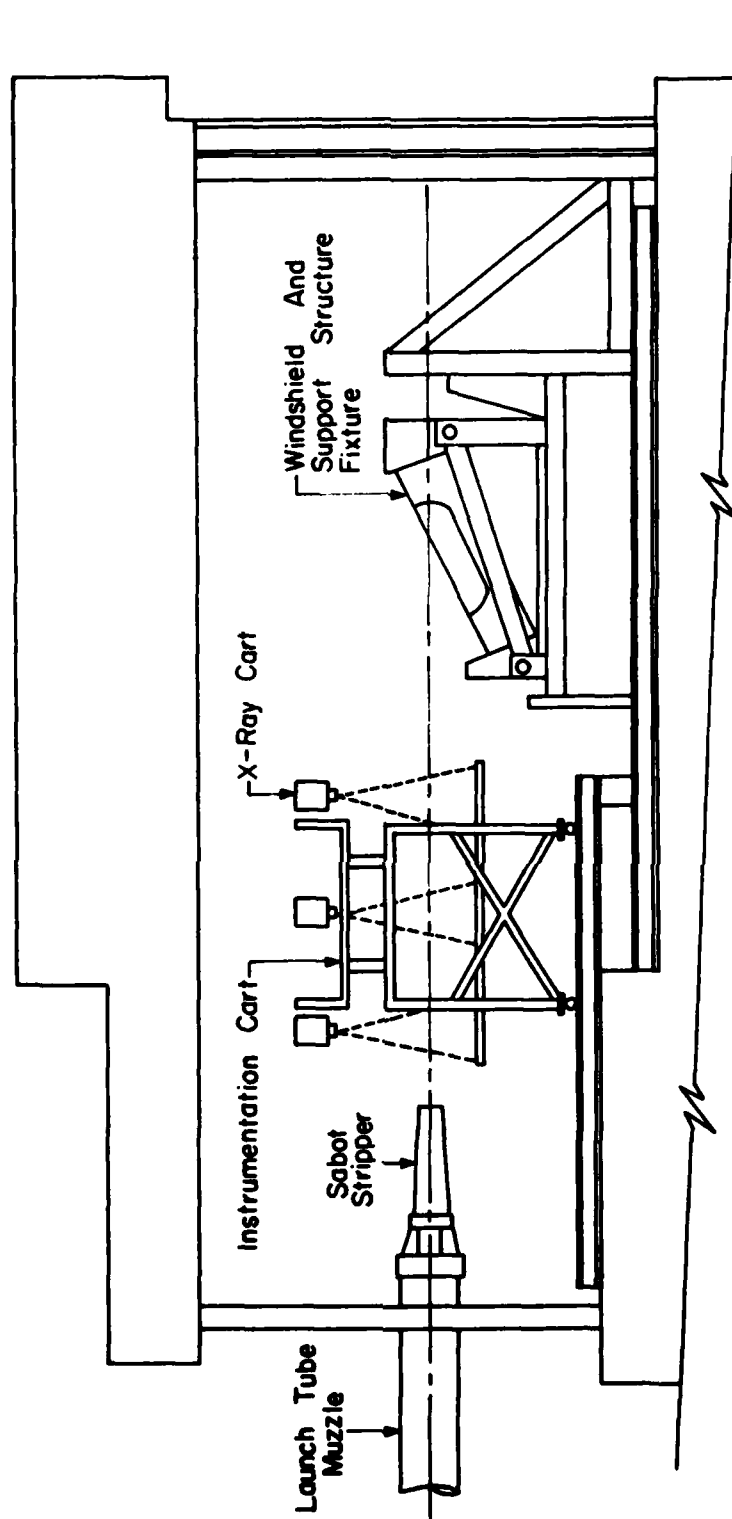


Figure 2. Simulated B-1 Windshield Test Setup.

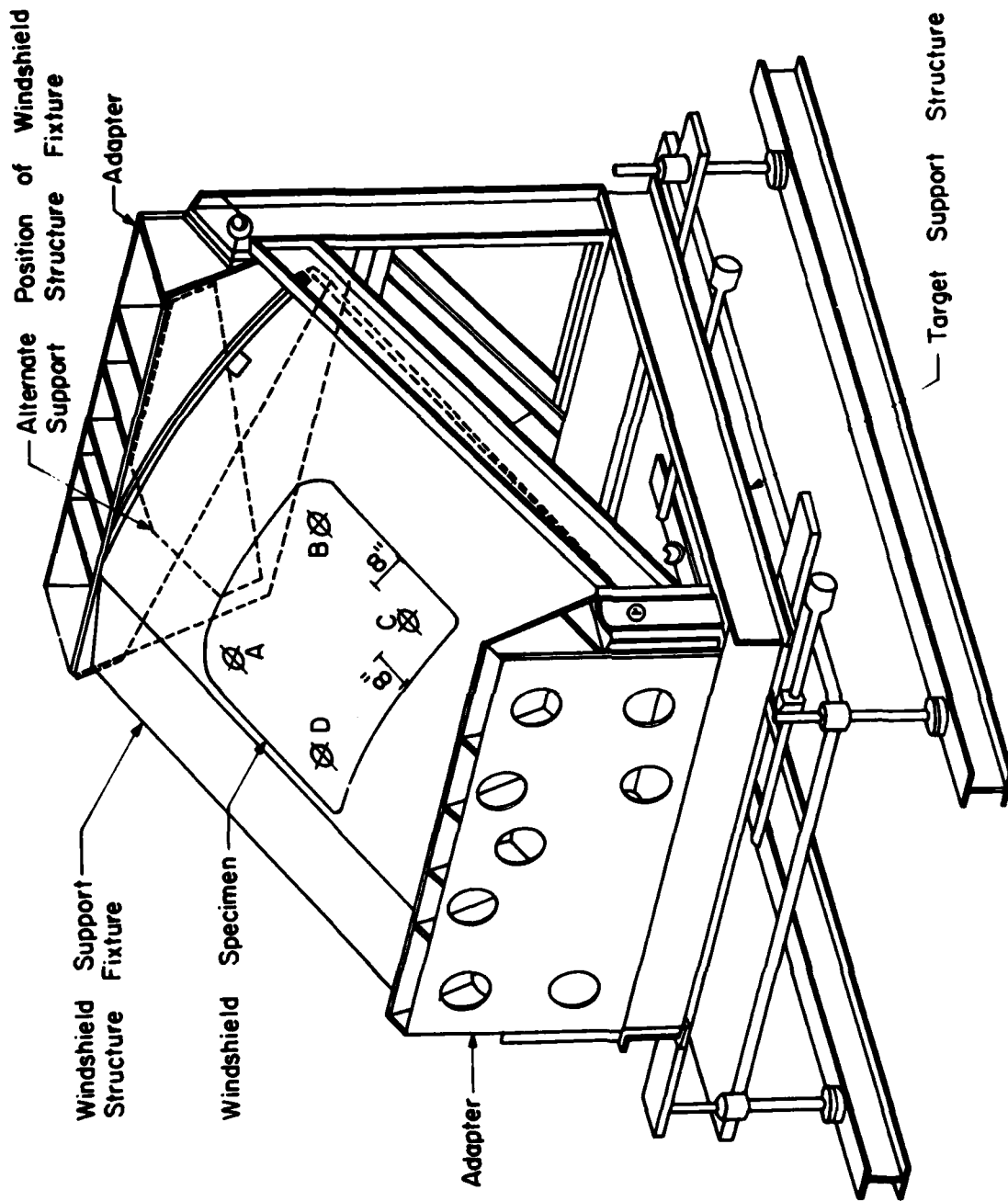


Figure 3. Simulated B-1 Windshield Test Fixture.



Figure 4. Simulated B-1 Windshield Test Fixture Photo.

High-speed 16mm film records of the impact event and target response were taken during each test.

A hood and ducting were used to enclose the test fixture whenever heating or cooling of the test panel was required. Propane was burned to heat the windshield and liquid nitrogen provided cooling for high and low temperature tests, respectively. The test panel temperatures required for each test were verified by making thermocouple measurements (Table 1).

2. B-1 X-5 MODULE TESTS

During February and March 1976, six bird impact tests were conducted on an actual B-1 crew escape module (Figures 5, 6, 7, and 8). Two windshield panels of an early production design were tested, one being shot twice, and the other four times (Table 2).

Twenty-two channels of strain gage data were recorded during each test, sixteen gages being mounted on the interior surface of the windshield and six being mounted at various points on the crew escape module structure (Reference 9).

All tests were conducted with the crew module and test windshield at the ambient temperature of the test facility.

Both the Simulated B-1 Windshield Tests and the B-1 X-5 Module Tests were accomplished on the S-3 Range of the Von Karman Gas Dynamics Facility at AEDC (Reference 20).

(9) E. J. Sanders, Results of Further Tests to Evaluate the Bird Impact Resistance of Windshields for the B-1 Aircraft, AEDC-DR-76-43, Arnold Engineering Development Center, Arnold Air Force Station, Tennessee 37389.

(20) E. J. Sanders, The Von Karman Gas Dynamics Facility Range S-3- Description and Capabilities, Arnold Engineering Development Center, Arnold Air Force Station, Tennessee 37389, AEDC-TR-76-9, January 1976.

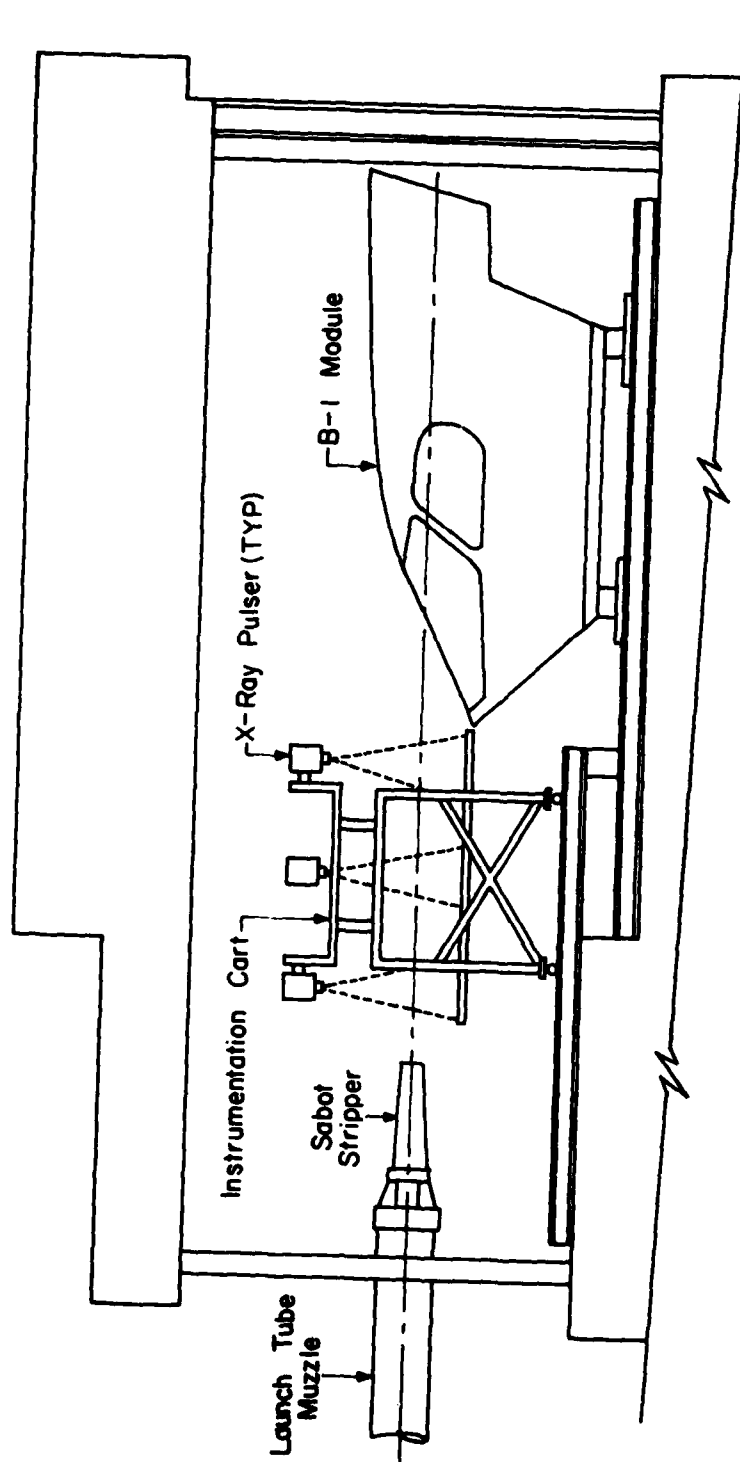


Figure 5. B-1 X-5 Module Test Setup.

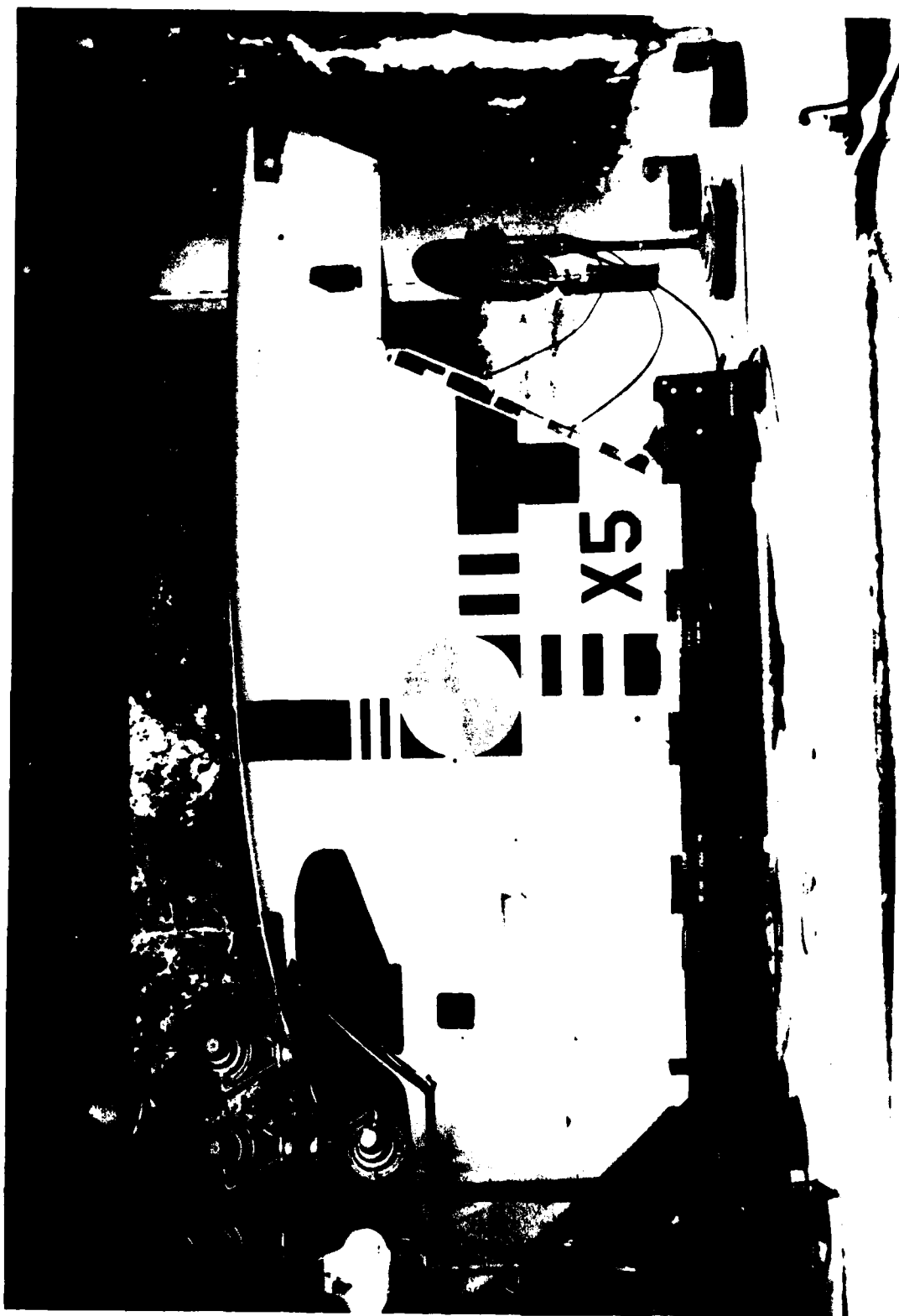


Figure 6. B-1 X-5 Module Test Setup Photo.

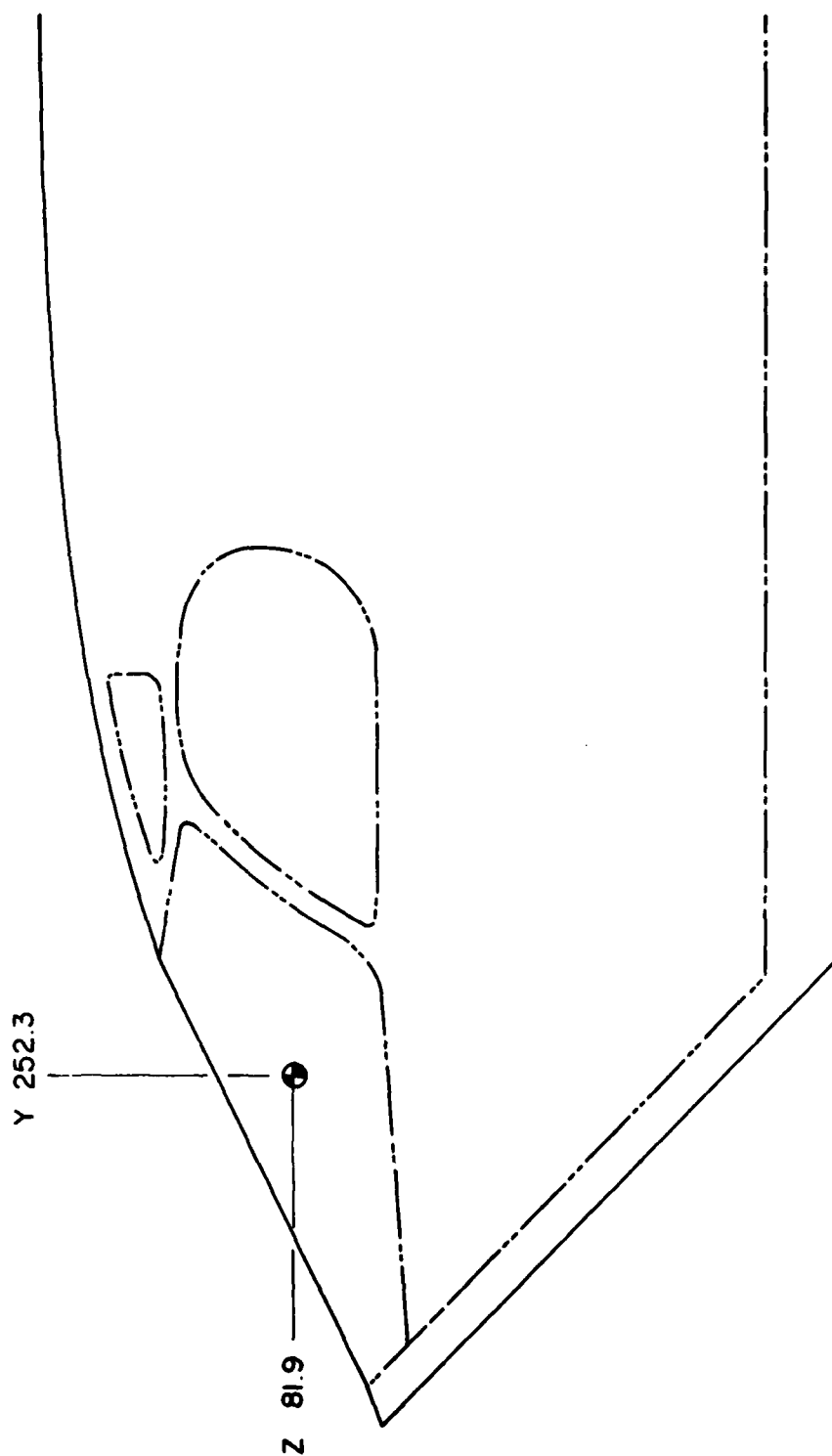


Figure 7. Elevation View of Impact Location.

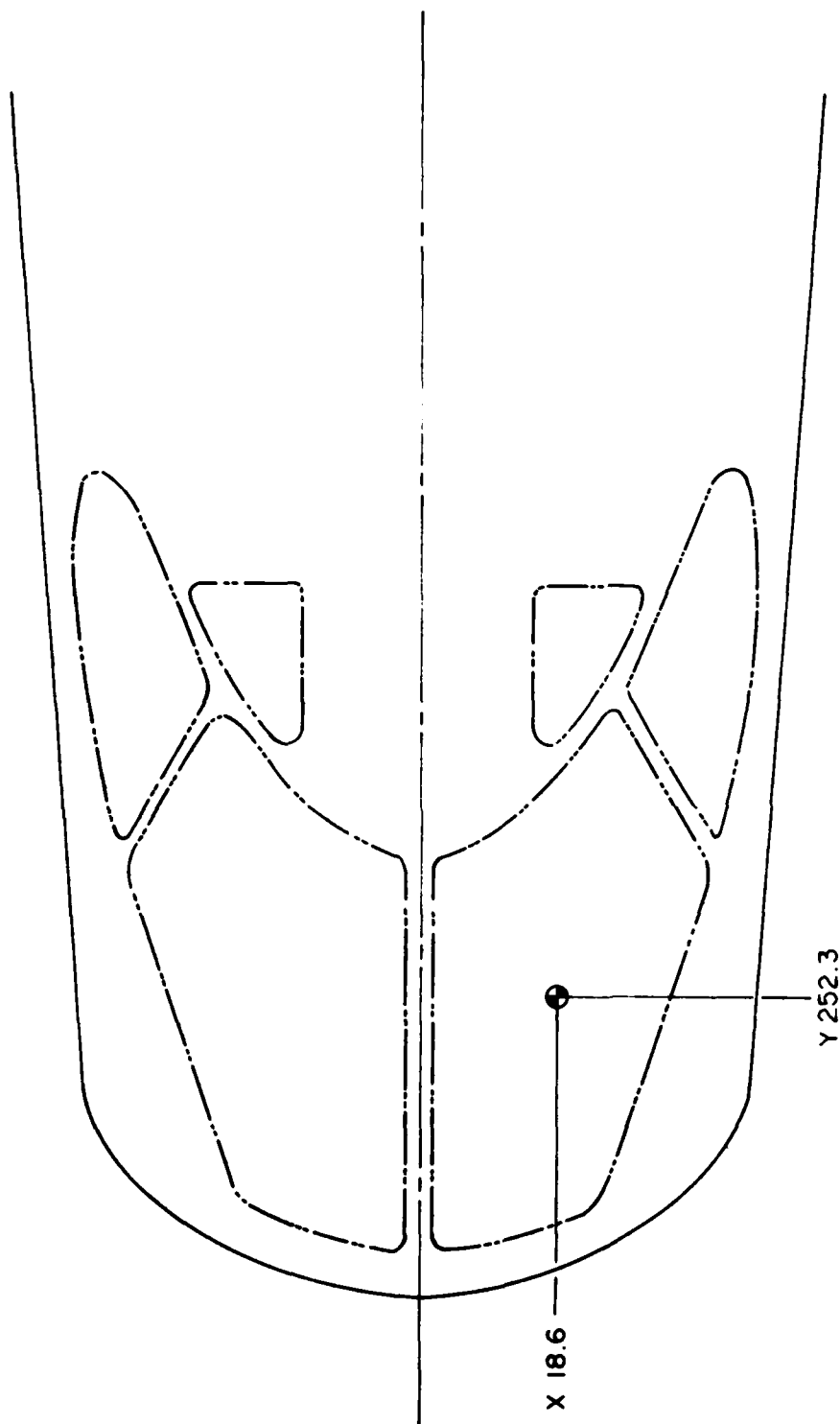


Figure 8. Plan View of Impact Location.

TABLE 2. B-1 X-5 MODULE TESTS

<u>SHOT NO.</u>	<u>BIRD WEIGHT, lbs</u>	<u>BIRD VELOCITY, ft/sec</u>	<u>AMBIENT TEMPERATURE DEG. F</u>
BM004	4.00	957	76
BM005	4.07	951	40
BM006	4.02	967	58
BM007	4.00	936	54
BM008	4.02	930	68
BM009	6.15	952	69

SECTION IV

STRUCTURAL MODELING

1. TEST CASE SELECTION

The experimental data available from the Simulated B-1 Windshield Tests and the B-1 X-5 Module Tests was reviewed to determine which of all the tests performed could be simulated with IMPACT (Reference 9 and 10). Repeat tests on the same test article were considered unacceptable for simulation due to the unknown nature of the residual mechanical properties of the materials. Tests for which strain gage data was missing or showed evidence of gage damage were also thrown out. Tests for which high-speed film records could not be used to verify the location of bird impact were considered unacceptable. Tests for which the films showed bird attitude differing substantially from end-on or axial at impact time were also considered unacceptable because impact forces could be theoretically calculated only for the axial case (Reference 6 and 18).

Since the approach taken in this work was to use only the finite element models already prepared under an earlier

(9) E. J. Sanders, Results of Further Tests to Evaluate the Bird Impact Resistance of Windshields for the B-1 Aircraft, AEDC-DR-76-43, Arnold Engineering Development Center, Arnold Air Force Station, Tennessee 37389.

(10) E. J. Sanders, Results of Bird Impact Testing of Prototype B-1 Windshields and Supporting Structure Design, AEDC-DR-76-100, Arnold Engineering Development Center, Arnold Air Force Station, Tennessee 37389.

(6) G. R. Eide, Aircraft Windshield Bird Impact Math Model--Part 2 - User's Manual, Air Force Flight Dynamics Laboratory, Wright-Patterson Air Force Base, Ohio 45433, AFFDL-TR-77-99, Part 2, December 1977.

(18) J. P. Barber, J. S. Wilbeck, and H. R. Taylor, Bird Impact Forces and Pressures on Rigid and Compliant Targets, Air Force Flight Dynamics Laboratory, Wright-Patterson Air Force Base, Ohio 45433, AFFDL-TR-77-60, May 1978.

contractual work effort (Section I.2), and since the only available model for the Simulated B-1 Windshield Tests was for shot location C (Figure 3), all tests in that series (Table 1) for shot locations other than C were not considered.

The only tests remaining as candidates for IMPACT simulation after this data review were the following: from the Simulated B-1 Windshield Tests, BM14, BM18, and BM19; from the B-1 X-5 Module Tests, BM004 and BM006 (Tables 1 and 2).

The remainder of this section will discuss in some detail the finite element models used for these test cases.

2. TEST BM14

Test BM14 was one of the bird impact tests against simulated B-1 windshields. A 4.04 lb chicken was impacted at location C at 939 fps. The ambient temperature for the entire test fixture was 90°F.

The test fixture (Figure 9) comprised the windshield specimen itself (Figure 10); four beams supporting the sides of the windshield and representing the aircraft center beam, side post, forward longeron, and aft longeron (Figures 11, 12, 13, and 14, respectively); a partial windshield panel on the side of the center beam opposite the full windshield test panel (Figure 15); and aluminum skin over the remainder of the structure (Reference 21). The windshield specimen was a laminated design with two plies of fully-tempered soda lime glass and was fabricated by PPG Industries, Inc. The windshield part number PPG-002 (Reference 8), was 36 in by 36 in and was centered in the 72 in by 72 in support fixture. The area of the fixture spanned by the windshield specimen was a

(21) Drawing Numbers Z5942639-501, Z5942642-1, Z5942694-1, Z5942643-2, Z5942643-1, and Z5942638-1, Douglas Aircraft Company, Long Beach California.

(8) R. H. Magnusson, High Speed Bird Impact Testing of Aircraft Transparencies, Air Force Flight Dynamics Laboratory, Wright-Patterson Air Force Base, Ohio 45433, AFFDL-TR-77-98, February 1978.

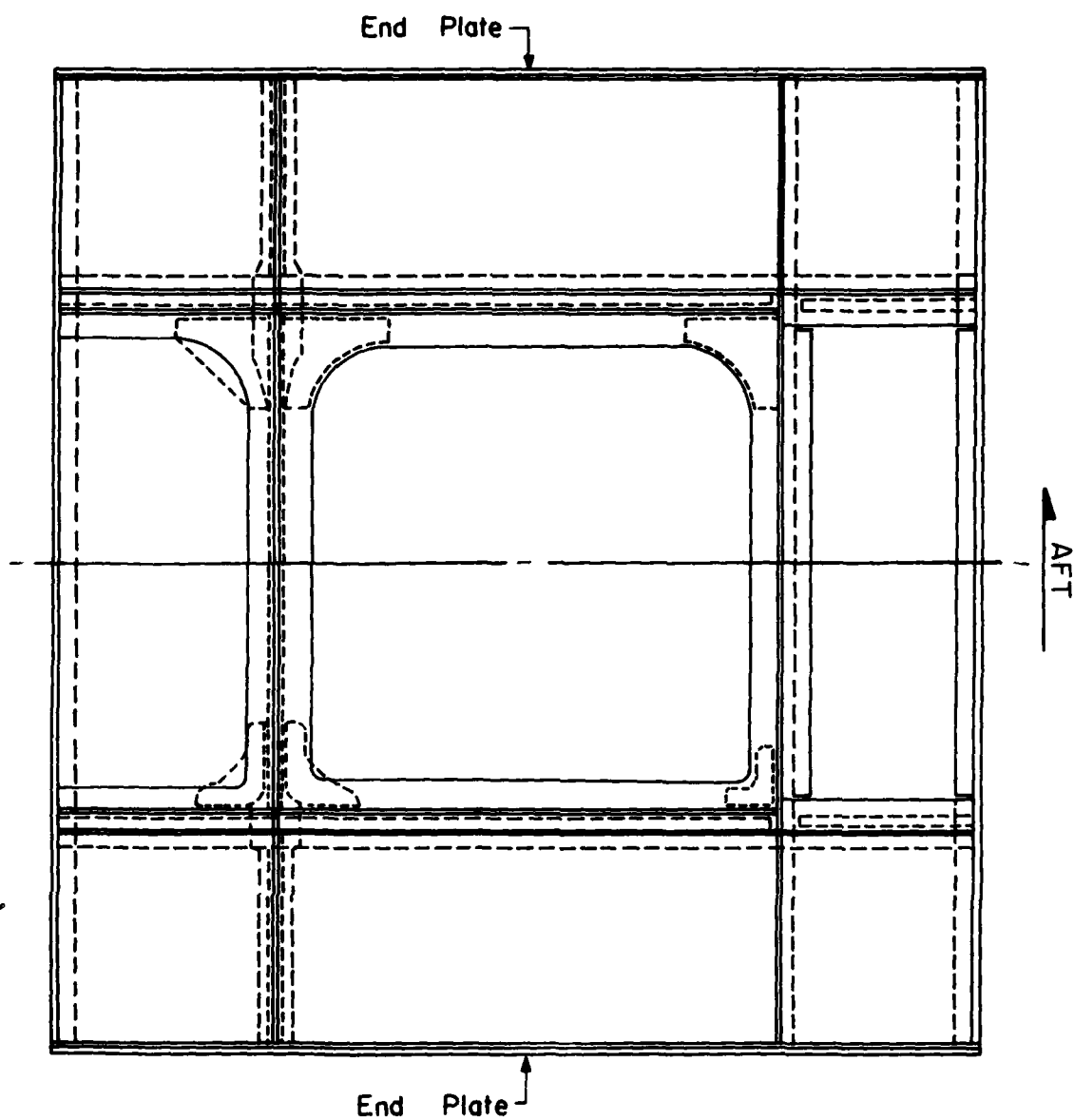


Figure 9. Simulated Windshield Support Structure.

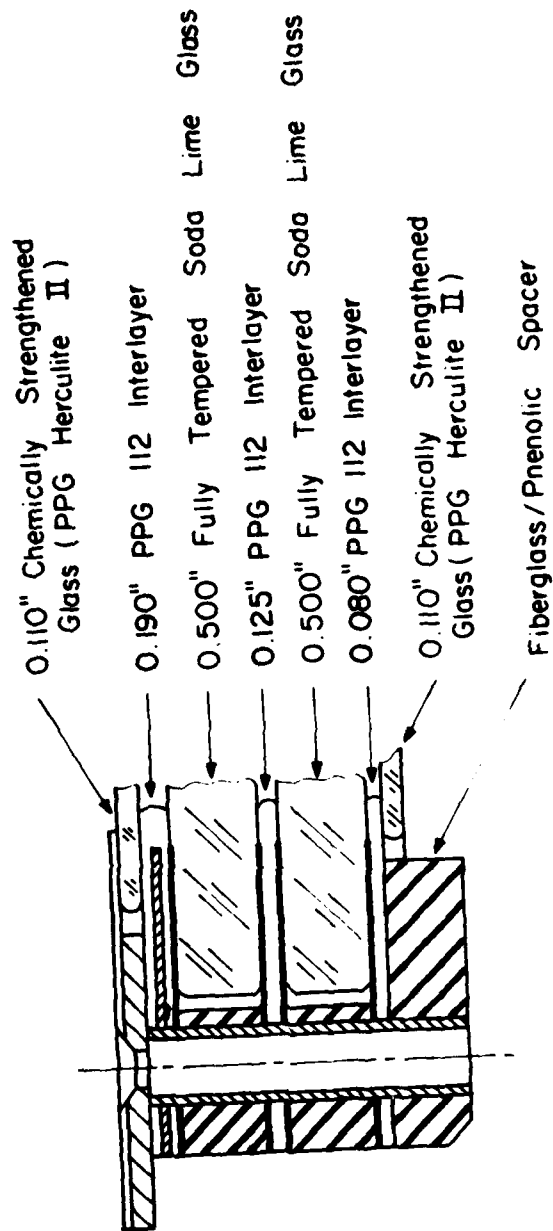


Figure 10. Test BM14/BM19 Simulated B-1 Windshield.

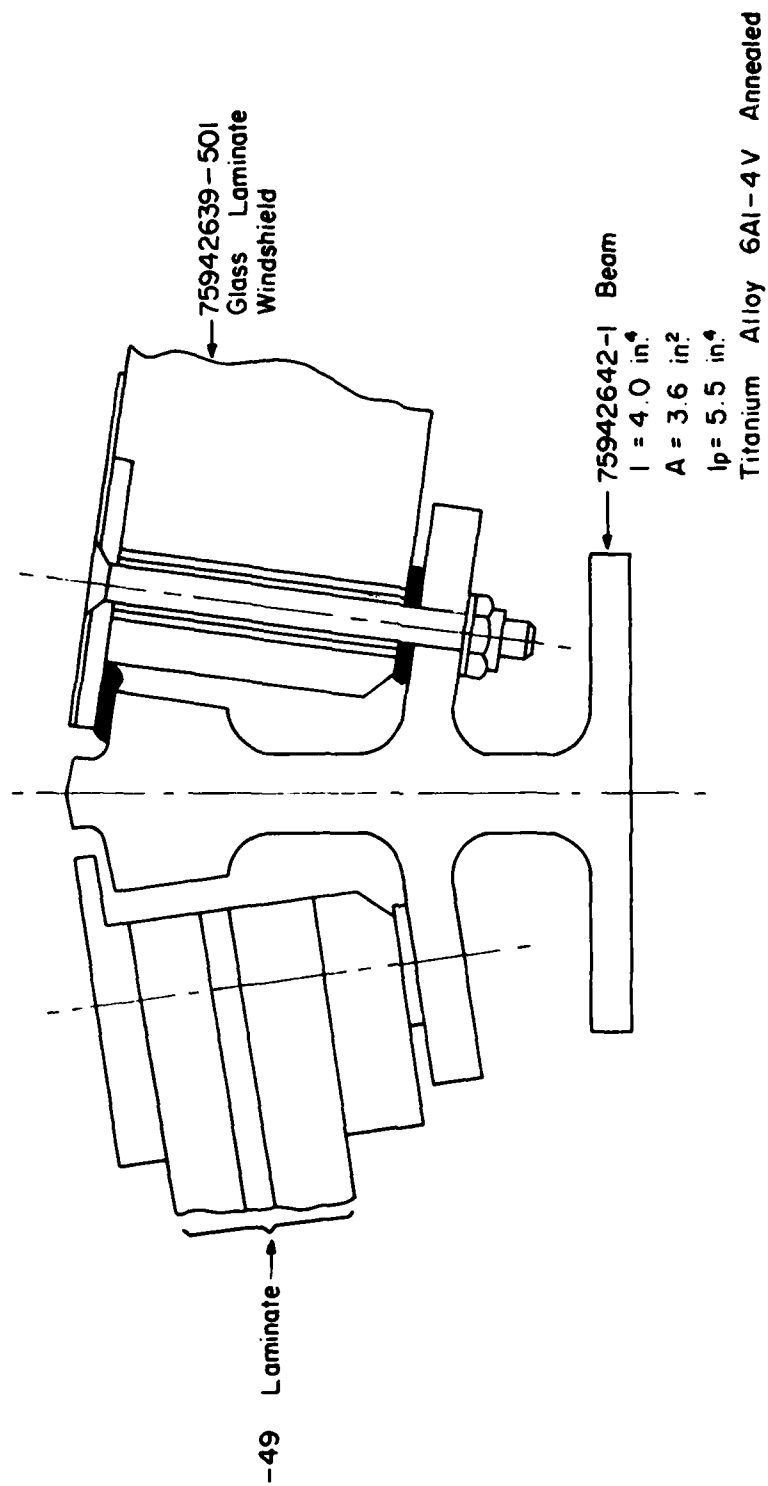


Figure 11. Test BM14/BM19 Center Member Support Structure.

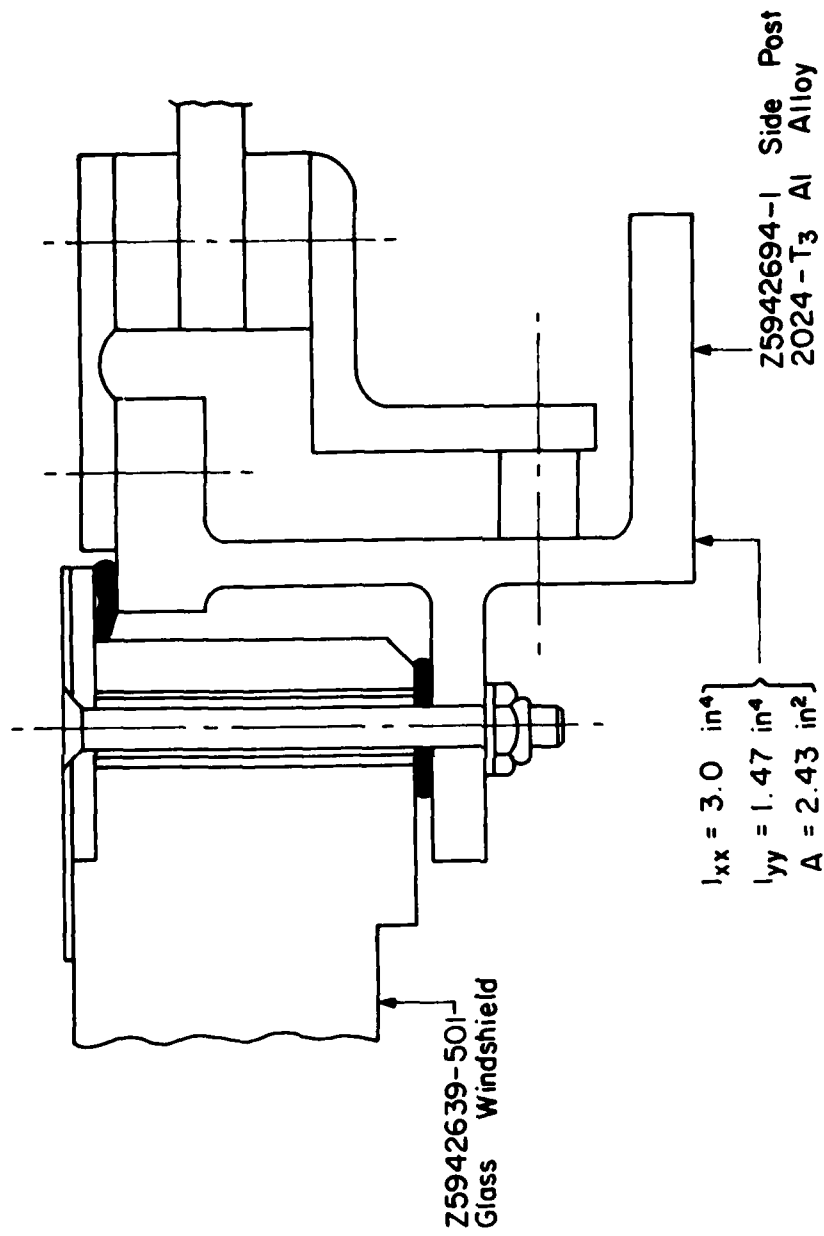


Figure 12. Test BM14/BM19 Side Post Support Structure.

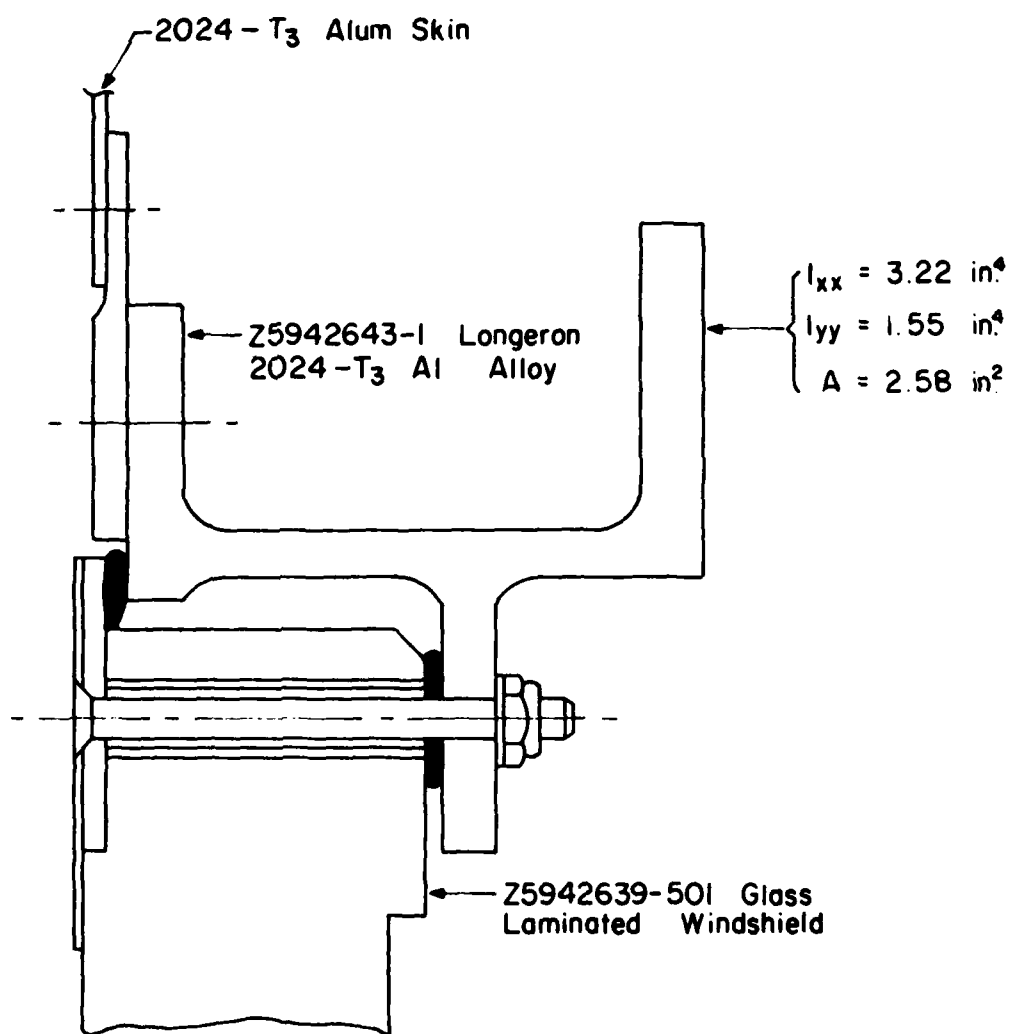


Figure 13. Test BM14/BM19 Forward Longeron Support Structure.

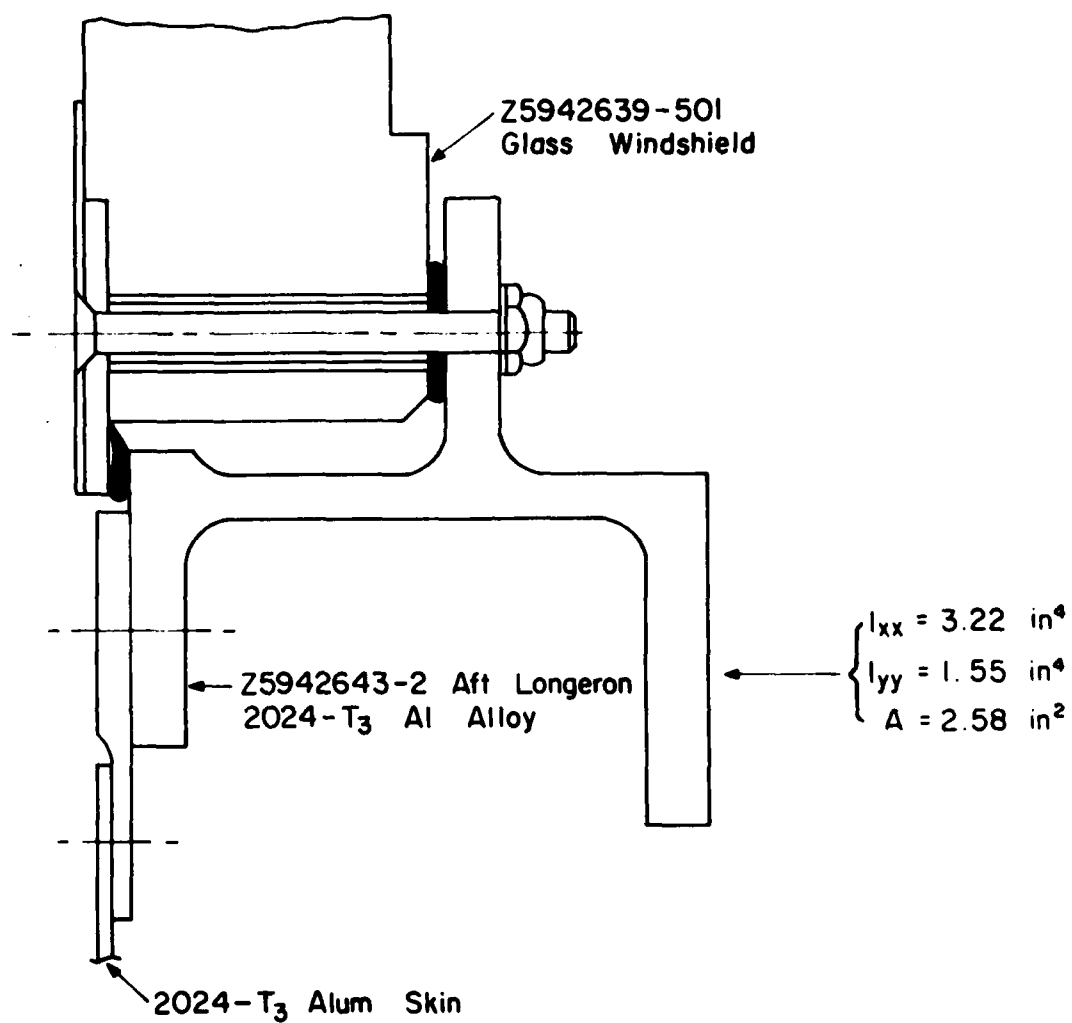


Figure 14. Test BM14/BM19 Aft Longeron Support Structure.

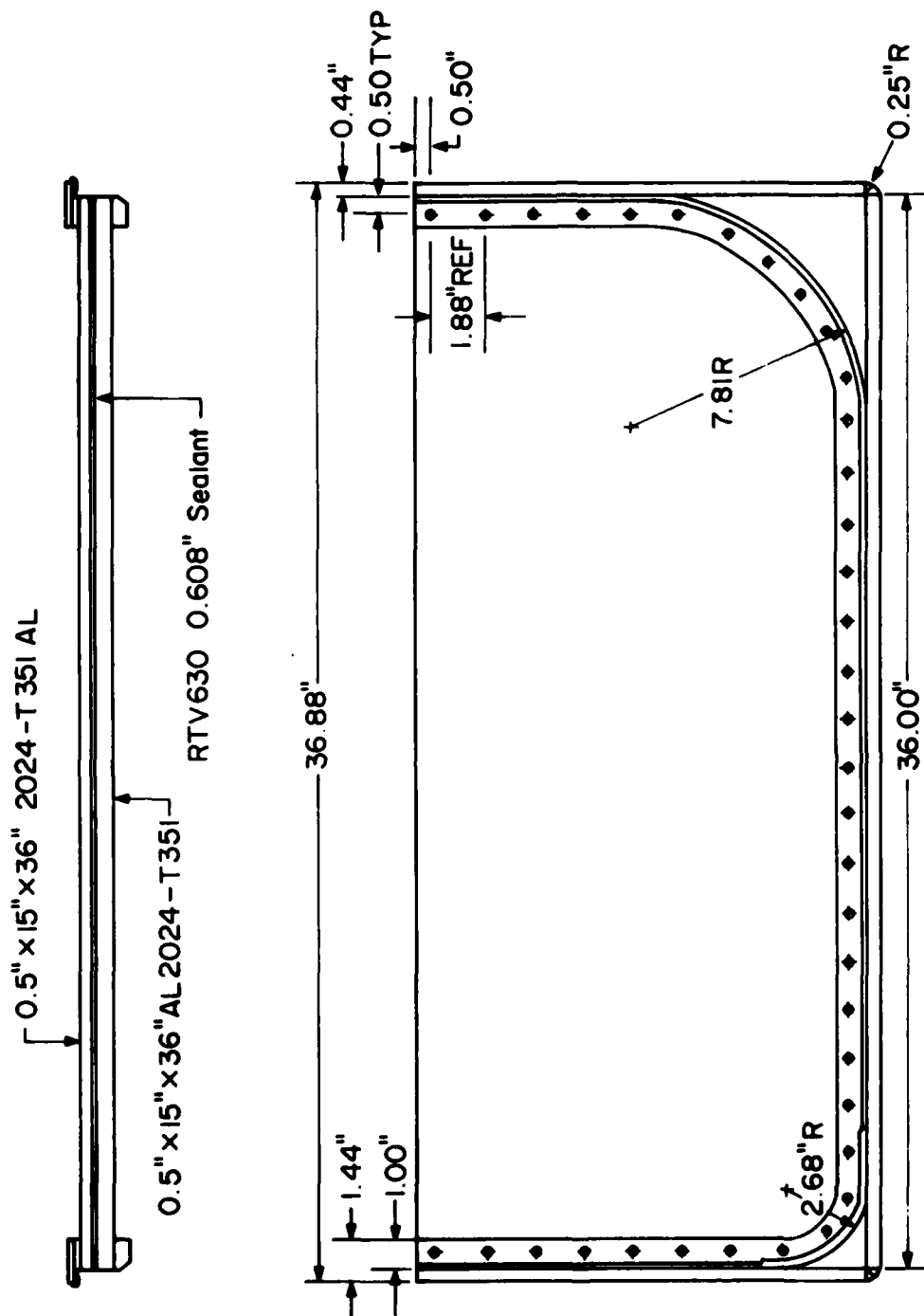


Figure 15. -49 Laminate Partial Windshield Panel in Support Fixture.

portion of a right circular cylinder 60 in in radius. The areas of the fixture outboard of the windshield were flat (Figure 4). The periphery of the support fixture was rigidly attached to heavy channels and plates of the adaptor, all resting on the target support structure (Figure 3).

The entire test fixture was modeled for IMPACT birdstrike simulation as illustrated in Figure 16. The finite element model is not symmetrical. The same finite element is used throughout the model; it is called a cell element and its theoretical development and capabilities are discussed thoroughly in Reference 5. It is a three-dimensional solid element which is 'built up' from one- and two-dimensional elements. The cell element has been fully validated for three-dimensional, linear analysis (Reference 5).

All the joints on the periphery of the model (Figure 16) were rigidly constrained to simulate the way in which the actual test fixture had been supported for bird impact testing (Figure 3).

Each of the layers in the windshield specimen (Figure 10) was modeled with a separate layer of cell elements. The beams supporting the windshield were modeled as having rectangular cross sections. The cross-sectional areas and moments of inertia for bending of the actual cross sections (Figures 11 through 14) were matched as nearly as possible in the model. Polar moments of inertia for torsion of the beams were not matched, the assumption being made that the beams would respond primarily in bending, not in torsion, when subjected to bird impact (Reference 22).

(5) P. H. Denke, Aircraft Windshield Bird Impact Math Model, Part 1 Theory and Application, Air Force Flight Dynamics Laboratory, Wright-Patterson Air Force Base, Ohio 45433, AFFDL-TR-77-99, Part 1, December 1977.

(22) S. H. Crandall and N. C. Dahl, An Introduction to the Mechanics of Solids, McGraw Hill, 1959.

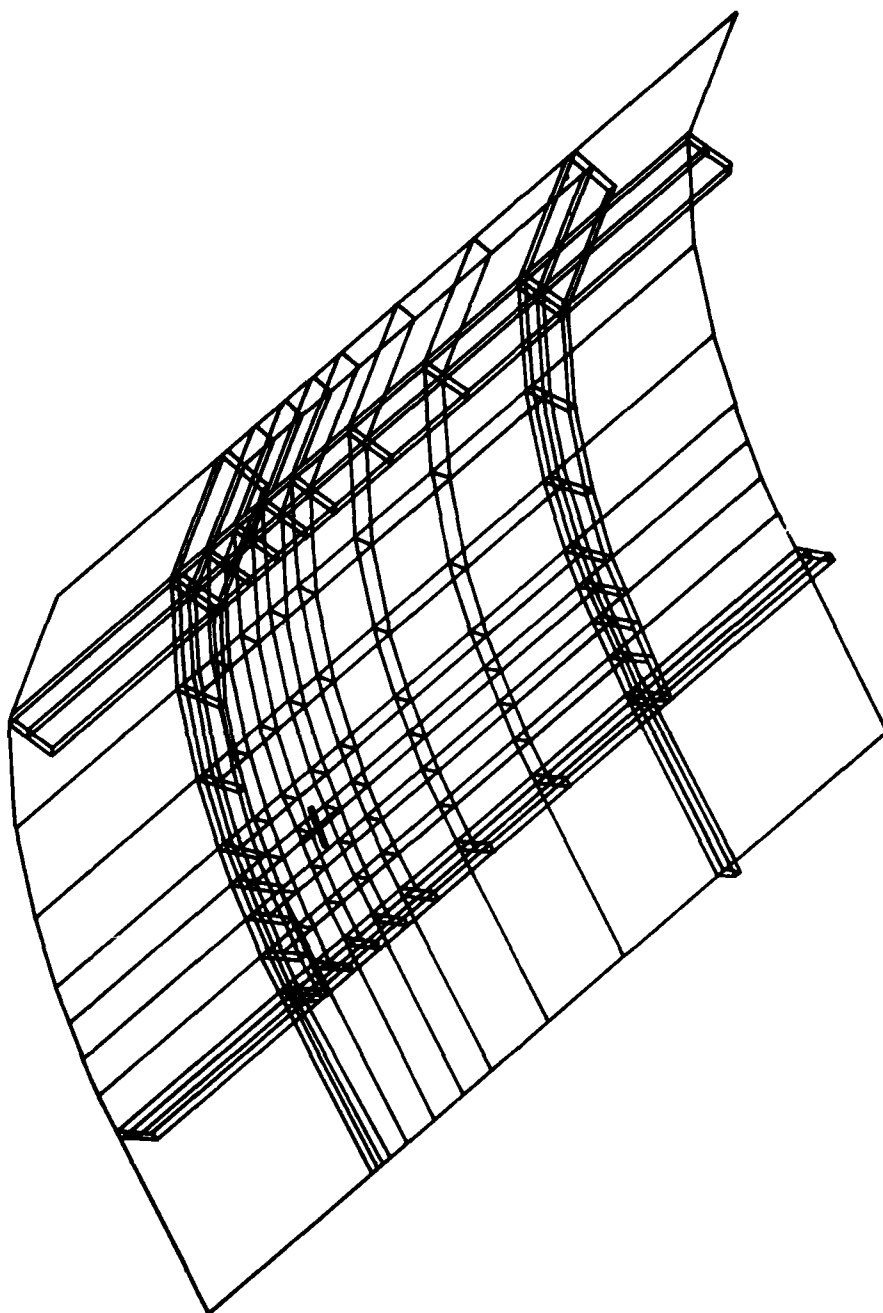


Figure 16. Test BM14/BM19 Finite Element Model.

The bending stiffness of 80 aircraft bolts used around the periphery of the windshield was not accounted for in the model. The attachment of the windshield to its support fixture was modeled with frictionless three-dimensional hinges at each joint lying on the interior edge of the windshield. The attachment of aluminum skin panels to the beams was modeled in the same way.

The various materials used in the test article are shown in Figures 10 through 14. Each was modeled as being linearly elastic with the respective mechanical properties given in Table 3. Four properties in addition to those six shown in Table 3 are included for each material in the model because they are required as input by IMPACT. These were the secant modulus, yield stress, rupture strain, and specific heat. None of the four are actually utilized by the edition of IMPACT used for this analysis, however, so they have not been included in Table 3. Since the only modulus reported for PPG-112 interlayer in Reference 13 was the Shear Modulus, Young's Modulus was calculated using the following identity for linear elastic materials (Reference 22).

$$E = 2G(1 + \nu) \quad (1)$$

E - Young's Modulus

G - Shear Modulus

ν - Poisson's Ratio

The value of Poisson's ratio reported for PPG-112 interlayer in Reference 23 was 0.50. This was not used in Equation (1)

(13) F. E. Greene, Testing for Mechanical Properties of Monolithic and Laminated Polycarbonate Materials, Air Force Flight Dynamics Laboratory, Wright-Patterson Air Force Base, Ohio 45433, AFFDL-TR-77-96, October 1977.

(22) S. H. Crandall and N. C. Dahl, An Introduction to the Mechanics of Solids, McGraw Hill, 1959.

(23) G. F. Rhodes, Damping, Static, Dynamic and Impact Characteristics of Laminated Beams Typical of Windshield Construction, Air Force Flight Dynamics Laboratory, Wright-Patterson Air Force Base, Ohio 45433, AFFDL-TR-76-156, December 1977.

TABLE 3
MECHANICAL PROPERTIES OF MATERIALS
BM14/BM19 FINITE ELEMENT MODELS

Material	Young's Modulus psi	Rupture Stress psi	Poisson's Ratio	Coeff. of Thermal Expansion per deg. F	Mass Density lb sec ² /in ⁴	Damping to Stiffness Ratio	Reference for Data
Glass- Fully Tempered Soda Lime	10.6x10 ⁶	22x10 ³	0.22	51x10 ⁻⁷	23.5x10 ⁻⁵	1.0x10 ⁻¹⁰	12
PPG-112 Interlayer	2044./400.	5542./440.	0.40	17x10 ⁻⁵	10.4x10 ⁻⁵	83x10 ⁻⁵	13, 23
Aluminium 2024-T3	10.5x10 ⁶	47x10 ³	0.33	12.6x10 ⁻⁶	25.9x10 ⁻⁵	1.0x10 ⁻¹⁰	11
Titanium 6 Al-4V Annealed	16.0x10 ⁶	12x10 ⁴	0.31	58x10 ⁻⁷	41.4x10 ⁻⁵	1.0x10 ⁻¹⁰	11
-49 Laminate	35x10 ⁵	22.9x10 ³	0.33	12.9x10 ⁻⁶	18.2x10 ⁻⁵	1.0x10 ⁻¹⁰	--
Glass- Chemically Strengthened -Herculite	11.0x10 ⁶	37x10 ³	0.22	51x10 ⁻⁷	23.5x10 ⁻⁵	1.0x10 ⁻¹⁰	12

because the value 0.50 results in a singularity in the linear elastic isotropic stress-strain law incorporated in IMPACT, shown in the following equation (Reference 24).

$$\sigma_{ij} = \frac{E}{1+\nu} \epsilon_{ij} + \frac{\nu E}{(1+\nu)(1-2\nu)} \delta_{ij} \epsilon_{kk} \quad (2)$$

σ_{ij} - stress tensor

ϵ_{ij} - strain tensor

ϵ_{kk} - $(\epsilon_{11} + \epsilon_{22} + \epsilon_{33})$, the dilatation

E - Young's Modulus

ν - Poisson's Ratio

δ_{ij} - 1 when $i=j$ (the Kronecker Delta)
0 when $i \neq j$

Note that the dilatation term is undefined when Poisson's ratio is 0.50. A value of 0.40 was assumed for Poisson's ratio as a result and was used in Equation (1) to calculate Young's modulus for the interlayer.

The temperature of all cell elements in the model was set at 90 deg F, the same as the ambient temperature for the test.

The finite element model for test BM14 can be summarized as follows:

Number of joints	828
Number of constraints	324
Number of materials	6
Number of cell elements	453
Number of unconstrained degrees of freedom	4230

(24) A. S. Saada, Elasticity: Theory and Applications, Pergamon Press, 1974.

3. TEST BM19

Test BM19 was another simulated B-1 windshield test. A 4.02 lb chicken was impacted at location C at 971 fps. For location C, the test panel had been rotated to make point C correspond to the aft outboard corner of the right windshield (Figure 3). This time the test article had been heated to an outer surface temperature of 220 deg F, measured via thermocouples before the test. The inboard surface of the outer soda lime glass ply was measured to be at 190 deg F at test time and the inner surface of the windshield was measured to be at 160 deg F (Figure 10).

The design of the test windshield, part number PPG-003, and its support structure were the same as for test BM14. As a result, the finite element model for BM19 was the same as that for BM14 with the exception of cell element temperatures.

A linear temperature distribution was assumed through the windshield panel based on the three thermocouple measurements mentioned earlier (Figure 17). The temperature for all of the supporting metal structure was assumed to be a uniform 160 deg F based on additional thermocouple data (Reference 25).

4. TEST BM18

Test BM18 was another one of the simulated B-1 windshield tests. A 4.09 lb chicken was impacted at location C at 847 fps (Table 1). The outer surface of the windshield was heated to 230 deg F for the test. The windshield panel involved was a four-ply laminated polycarbonate design manufactured by the Sierracin Corporation, part number SK-001 (Reference 8).

(25) Personal Communication, 24 May 1978, Merle J. Coker, Douglas Aircraft Company, Cl-253, 3855 Lakewood Boulevard, Long Beach, California 90846.

(8) R. H. Magnusson, High Speed Bird Impact Testing of Aircraft Transparencies, Air Force Flight Dynamics Laboratory, Wright-Patterson Air Force Base, Ohio 45433, AFFDL-TR-77-98, February 1978.

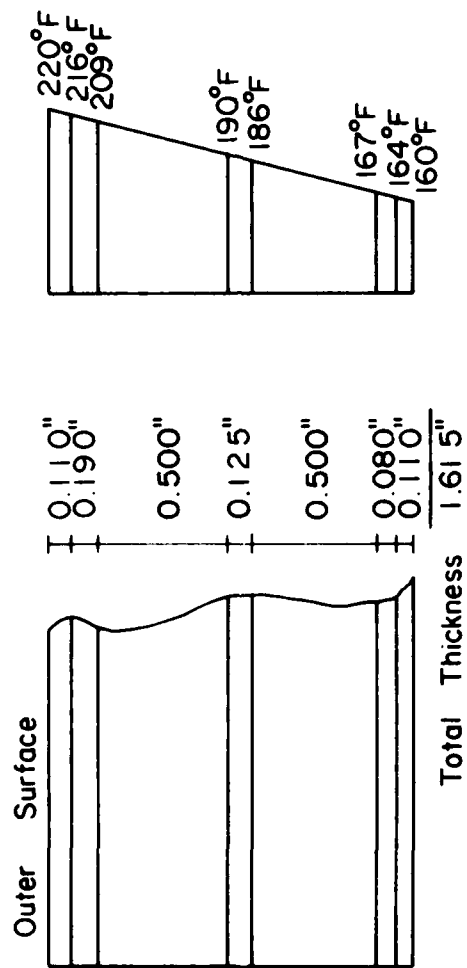


Figure 17. BM19 Windshield Temperature Distribution Assumed.

Modification of the BM14/BM19 finite element model was considered as a method of developing a BM18 model since BM18 had not been modeled earlier. This would have entailed changing the mechanical properties of the materials in the windshield as well as the number and thickness of the layers (Figures 10 and 18). It would also have required changing the mechanical and cross-sectional properties of the beams supporting the windshield (Figures 11 and 19). The way in which windshield attachment to supporting structure was modeled would have required changing also. The model for BM18 would have had to model attachment at joints along both inboard and outboard edges of the windshield (Figure 19).

Since the preprocessor for IMPACT provided no capability for interactive editing of finite element models, the modifications just discussed would have had to be done by hand and hence would have required a considerable investment of in-house manpower for their accomplishment. Because manpower for this work effort was limited, plans to generate a BM18 model were scrapped. This would not have been necessary had a capable preprocessor for IMPACT been available.

5. TEST BM006

Test BM006 was one of the B-1 X-5 module tests. The specific windshield panel tested was a laminated conceptual design, part number SWU-107, manufactured by Swedlow, Inc. (Reference 8). A 4.02 lb chicken was impacted at the location shown in Figures 7 and 8 at 967 fps. The test was performed at an ambient temperature of 58 deg F (Table 2).

The test article comprised the windshield panel (Figure 20) mounted in the B-1 aircraft X-5 crew module which rested on test support structure as shown in Figure 5.

(8) R. H. Magnusson, High Speed Bird Impact Testing of Aircraft Transparencies, Air Force Flight Dynamics Laboratory, Wright-Patterson Air Force Base, Ohio 45433, AFFDL-TR-77-98, February 1978.

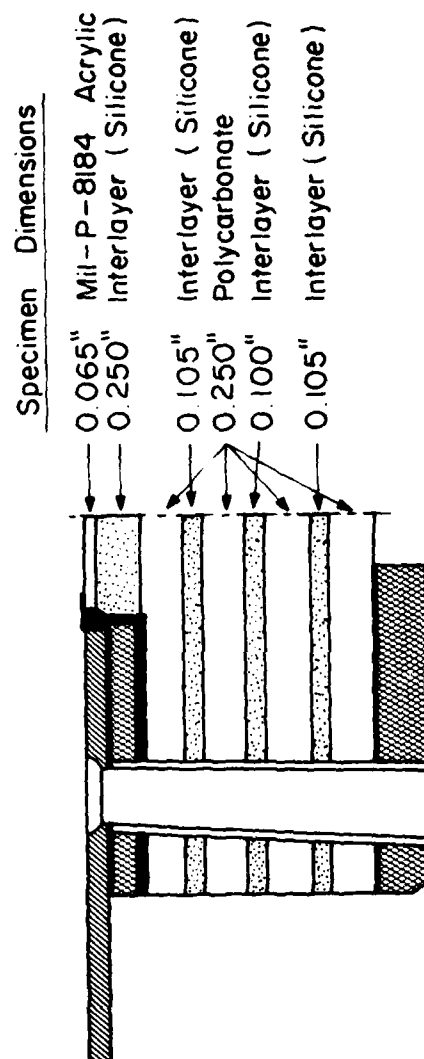


Figure 18. Test BM18 Simulated B-1 Windshield.

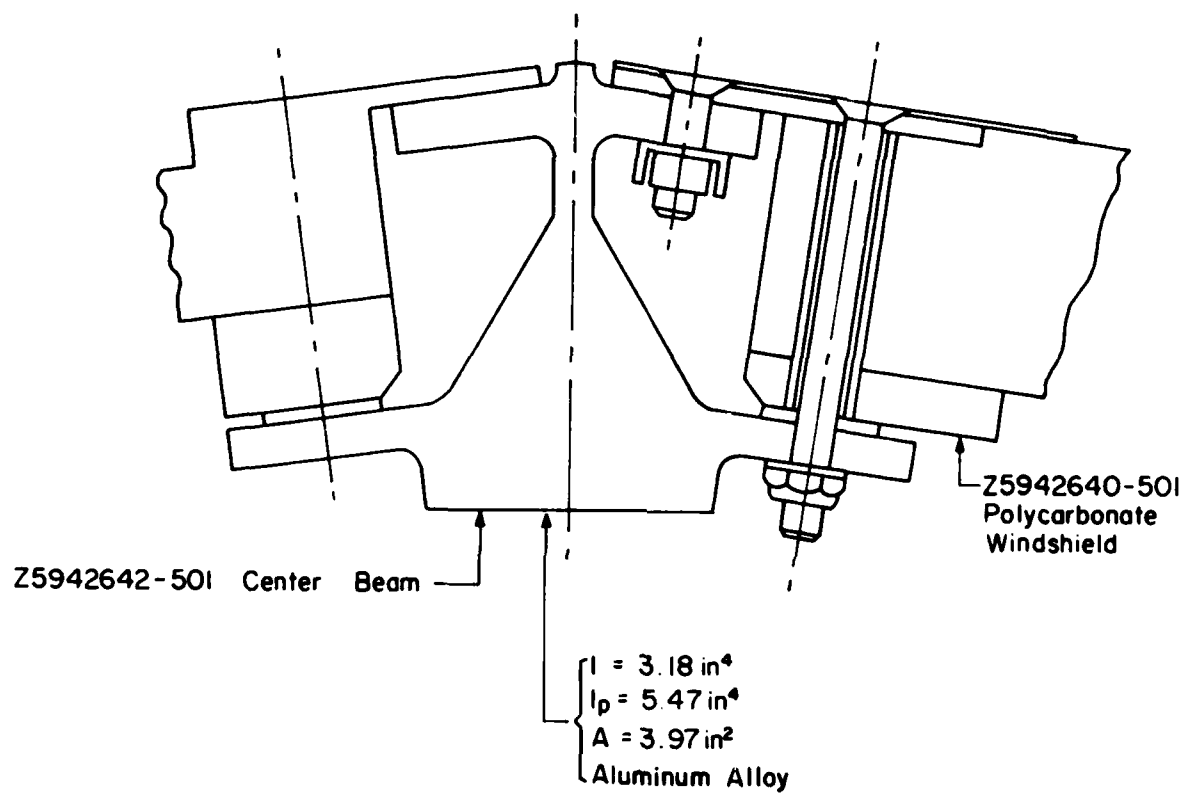


Figure 19. Test BM18 Center Member Support Structure.

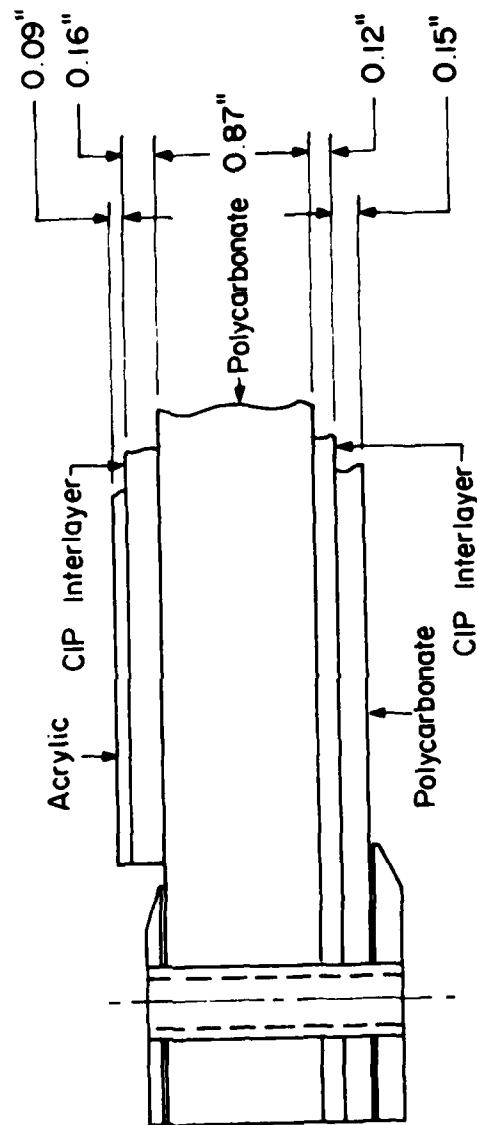


Figure 20. Test BM006 B-1 X-5 Module Windshield.

The finite element model prepared for BM006 analysis with IMPACT is shown in Figure 21. The model is not symmetrical. Less structure was modeled on the right side of the aircraft than on the left side. The left or target windshield is modeled with five separate layers of cell elements, each representing one layer of material in one laminate. The other transparencies included in the model are all represented by one layer of cell elements having effective properties for the total cross-section involved. The remainder of the structure was modeled with the cell element already discussed, plus bar and membrane elements. The latter two are simply the components from which the cell element is "built up." Both can be used individually as for BM006 and have been validated for linear elastic applications (Reference 5).

As for the BM14 and BM19 models, all joints on the periphery of the test module model are rigidly constrained. The bending stiffness of aircraft bolts around the periphery of the windshield was ignored, and attachment of the windshield to the aircraft structure was again modeled with frictionless three-dimensional hinges at each joint lying on the interior edge of the windshield.

Materials were assumed to be linearly elastic with the mechanical properties given in Table 4. The temperature of all finite elements was assumed to be 58 deg F, the ambient temperature during the test.

The finite element model may be summarized as follows:

Number of joints	863
Number of constraints	306
Number of materials	11

(5) P. H. Denke, Aircraft Windshield Impact Math Model, Part 1 Theory and Application, Air Force Flight Dynamics Laboratory, Wright-Patterson Air Force Base, Ohio 45433, AFFDL-TR-77-99, Part 1, December 1977.

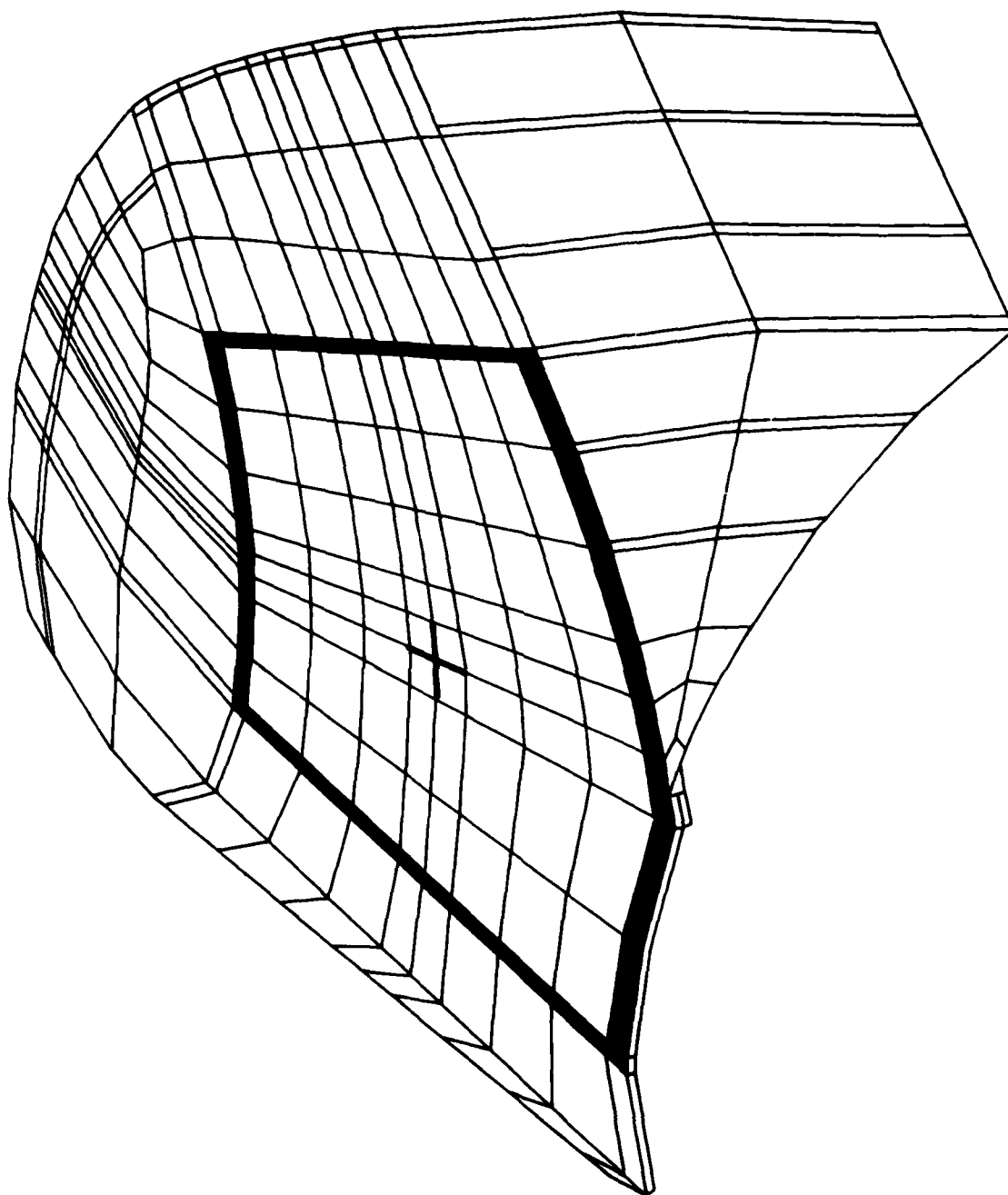


Figure 21. Test AM006 Finite Element Model.

TABLE 4
MECHANICAL PROPERTIES OF MATERIALS
BM006 FINITE ELEMENT MODEL

Material	Young's Modulus psi	Rupture Stress psi	Poisson's Ratio	Coeff. of Thermal Expansion per deg. F	Mass Density lb sec ² /in ⁴	Damping to Stiffness Ratio	Reference for Data
Polycarbonate .875 in. thick	30x10 ⁴	9.5x10 ³	0.35	34.7x10 ⁻⁶	11.1x10 ⁻⁵	36x10 ⁻⁶	13, 23
Polycarbonate .155 in. thick	33.3x10 ⁴	9.5x10 ³	0.35	34.7x10 ⁻⁶	11.1x10 ⁻⁵	36x10 ⁻⁶	13, 23
As Cast Acrylic	45.0x10 ⁴	7.4x10 ³	0.35	41.0x10 ⁻⁶	11.1x10 ⁻⁵	47x10 ⁻⁵	12, 23
Swedlow SS-5272Y(HT) interlayer	435	679	0.45	21.2x10 ⁻⁵	9.6x10 ⁻⁵	12.7x10 ⁻⁴	13, 23
Aluminum Bar 2024-T81	10.8x10 ⁶	58.x10 ³	0.33	12.6x10 ⁻⁶	25.9x10 ⁻⁵	1.0x10 ⁻¹⁰	11
Aluminum Sheet 2024-T81	10.5x10 ⁶	59.x10 ³	0.33	12.6x10 ⁻⁶	25.9x10 ⁻⁵	1.0x10 ⁻¹⁰	11

TABLE 4
CONTINUED

Material	Young's Modulus psi	Rupture Stress psi	Poisson's Ratio	Coeff. of Thermal Expansion per deg. F	Mass Density lb sec ² /in ⁴	Damping to Stiffness Ratio	Reference for Data
Aluminum Sheet 2024-T62	10.5x10 ⁶	49.0x10 ³	0.33	12.6x10 ⁻⁶	25.9x10 ⁻⁵	1.0x10 ⁻¹⁰	11
Aluminum Plate 2124-T851	10.4x10 ⁶	60.0x10 ³	0.33	12.6x10 ⁻⁶	25.9x10 ⁻⁵	1.0x10 ⁻¹⁰	11
Effective Right Windshield	31.7x10 ⁴	9.5x10 ³	0.35	34.7x10 ⁻⁶	11.1x10 ⁻⁵	36x10 ⁻⁶	-
Effective Side Window	11.8x10 ⁴	9.5x10 ³	0.35	34.7x10 ⁻⁶	11.1x10 ⁻⁵	36x10 ⁻⁶	-
Effective Eyebrow Window	34.0x10 ⁴	9.5x10 ³	0.35	34.7x10 ⁻⁶	11.1x10 ⁻⁵	36x10 ⁻⁶	-

Number of cell elements	453
Number of bar elements	15
Number of membrane elements	18
Number of unconstrained degrees of freedom	4450

6. TEST BM004

Test BM004 was another B-1 X-5 module test. The panel tested was a laminated polycarbonate left windshield manufactured by Swedlow, Inc., part number SWU-108 (Reference 8). It was made according to the same drawing as part number SWU-107 which was used in test BM006. Other than slightly different bird impact conditions and ambient temperatures, no differences existed between tests BM004 and BM006. For this reason the decision was made to use the same finite element model for both test BM004 and test BM006.

The finite element models discussed in this section represent the major portion of input data required by IMPACT for the purpose of bird impact analyses. The remaining portion of input data required relates to description of the transient forces which are felt by the windshield during the bird impact event. Development of this force data is the subject matter of the following section.

(8) R. H. Magnusson, High Speed Bird Impact Testing of Aircraft Transparencies, Air Force Flight Dynamics Laboratory, Wright-Patterson Air Force Base, Ohio 45433, AFFDL-TR-77-98, February 1978.

SECTION V
BIRDSTRIKE LOADS

1. THEORY

A considerable body of experimental and analytical work has been accomplished to investigate the forces and pressures on targets subject to soft body or bird impacts (References 15 through 19, 26, and 27). This work has progressed to the point where it is now possible to theoretically predict the spatial and temporal distribution of bird impact pressures over the face of an inclined flat, rigid target. This capability has been validated for bird masses up to 8 lb, for target obliquities from 90 to 25 deg, and for velocities of nearly 1000 fps (Reference 26).

(15) J. P. Barber and J. S. Wilbeck, Characterization of Bird Impacts on a Rigid Plate: Part I, Air Force Flight Dynamics Laboratory, Wright-Patterson Air Force Base, Ohio 45433, AFFDL-TR-75-5, January 1975.

(16) R. L. Peterson and J. P. Barber, Bird Impact Forces in Aircraft Windshield Designs, Air Force Flight Dynamics Laboratory, Wright-Patterson Air Force Base, Ohio 45433, AFFDL-TR-75-150, March 1976.

(17) Y. M. Ito, G. E. Carpenter, and F. W. Perry, Bird Impact Loading Model for Aircraft Windshield Design, CRT 3090-2, California Research & Technology, Inc., Woodland Hills, California 91364, July 1977.

(18) J. P. Barber, J. S. Wilbeck, and H. R. Taylor, Bird Impact Forces and Pressures on Rigid and Compliant Targets, Air Force Flight Dynamics Laboratory, Wright-Patterson Air Force Base, Ohio 45433, AFFDL-TR-77-60, May 1978.

(19) J. S. Wilbeck, Impact Behavior of Low Strength Projectiles, Air Force Materials Laboratory, Wright-Patterson Air Force Base Ohio 45433, AFML-TR-77-134, July 1978.

(26) A. Challita and J. P. Barber, The Scaling of Bird Impact Loads, Air Force Flight Dynamics Laboratory, Wright-Patterson Air Force Base, Ohio 45433, AFFDL-TR-79-3042, March 1979.

(27) J. Y. Parker, Measurement of Impact Bird Pressure on a Flat Plate, Arnold Engineering Development Center, Arnold Air Force Station, Tennessee 37389, AEDC-TR-79-14.

Something less than this current capability to predict bird impact pressures was incorporated into IMPACT during its development. For the purpose of this report, only that level of development which was actually included in IMPACT will be reviewed.

It was found by all the investigators in this field of interest that the assumption of a fluid bird is fully warranted in considering the forces and pressures resulting from bird impact. The linear momentum of the bird along its trajectory before impact is mv , mass times velocity. If the bird acts as a fluid during normal impact on a rigid target, its linear momentum after impact is zero because the only motion remaining is in a radial direction (Figure 22). The momentum transfer to the target in this case becomes just mv . When the target is inclined with respect to the bird trajectory, the momentum transfer or impulse is given by the component of mv normal to the target surface as shown in Equation (3).

$$I = mv \sin \theta \quad (3)$$

I - impulse

m - mass

v - velocity

θ - angle between target surface and bird trajectory

If the bird did not behave as a fluid during impact but rather as a deformable body with some elasticity, it would rebound from the target and impart a higher impulse than that defined in Equation (3) to the target.

For normal impact, the duration of the impact event can be written as shown in Equation (4).

$$T = L/v \quad (4)$$

T = impact period

L = bird length

v = bird velocity

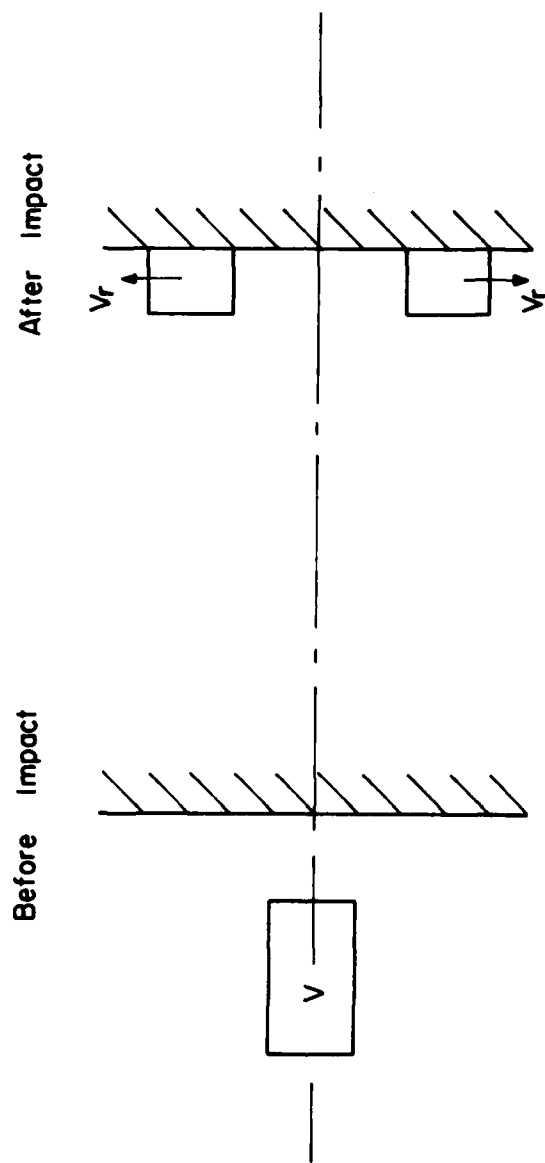


Figure 22. Motion of a Bird Before and After Impact.

For oblique impact, if the bird is represented as a right circular cylinder, an effective length can be defined as shown by Figure 23 and Equation (5).

$$L_{\text{eff}} = L + (d/\tan \theta) \quad (5)$$

L_{eff} - effective length of bird

L - bird length

d - bird diameter

θ - angle between target surface and bird trajectory

The duration of the impact event can be written more generally then as shown in Equation (6).

$$T = L_{\text{eff}}/v \quad (6)$$

T - impact period

L_{eff} - effective length of bird

v - bird velocity

Having written expressions for the impulse and the period of fluid bird impact on rigid targets, an expression for the average force on the target surface can be written as in Equation (7).

$$F_{\text{avg}} = \frac{I}{T} = \frac{mv^2 \sin \theta}{L_{\text{eff}}} \quad (7)$$

F_{avg} - average force

m - bird mass

v - velocity

L_{eff} - effective length of bird

θ - angle between target surface and bird trajectory

A broad base of experimental data has confirmed the applicability of Equations (3) and (6) to bird impact of rigid

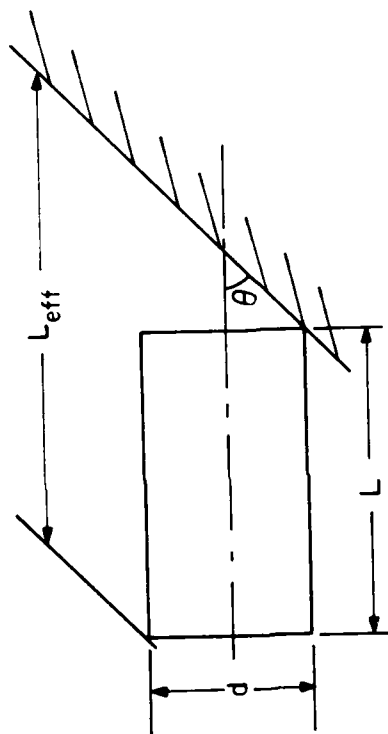


Figure 23. Oblique Impact Effective Bird Length.

targets (Reference 18). This same experimental data has also demonstrated that the peak force exerted on the target during impact is about twice the average force defined by Equation (7). The rise time from the beginning of impact to peak force was found to be about 0.2 times the period defined by Equation (6) (Reference 18). This information made it possible to generalize the force-time history for bird impact on inclined rigid targets as illustrated in Figure 24.

This force-time model of bird impact was the one considered by the developers of IMPACT. The IMPACT user is not restricted to the triangular force-time history illustrated in Figure 24, however, but may arbitrarily choose the nondimensional force history. IMPACT also allows the user to specify, at several times during the impact event, the joints on the surface of the finite element model over which he wishes to distribute the instantaneous bird impact force acting on the structure. This distribution of joint forces is accomplished for the user by the Loads Generator Module of IMPACT (Section II. 2). This calculation of joint forces does not, however, take advantage of what is known about the spatial distribution of pressures during bird impact (Reference 18). Instead, the force distribution to an arbitrary set of joints on the surface of the model is based on the Lagrangian Multiplier Method (Reference 30). Equilibrium equations relating joint forces to the resultant impact force are solved to obtain the joint forces (Appendix G of Reference 5).

(18) J. P. Barber, J. S. Wilbeck, and H. R. Taylor, Bird Impact Forces and Pressures on Rigid and Compliant Targets, Air Force Flight Dynamics Laboratory, Wright-Patterson Air Force Base, Ohio 45433, AFFDL-TR-77-60, May 1978.

(30) R. L. Ketter and S. P. Prawel, Jr., Modern Methods of Engineering Computation, McGraw-Hill, 1969.

(5) P. H. Denke, Aircraft Windshield Bird Impact Math Model, Part 1 Theory and Application, Air Force Flight Dynamics Laboratory, Wright-Patterson Air Force Base, Ohio 45433, AFFDL-TR-77-99, Part 1, December 1977.

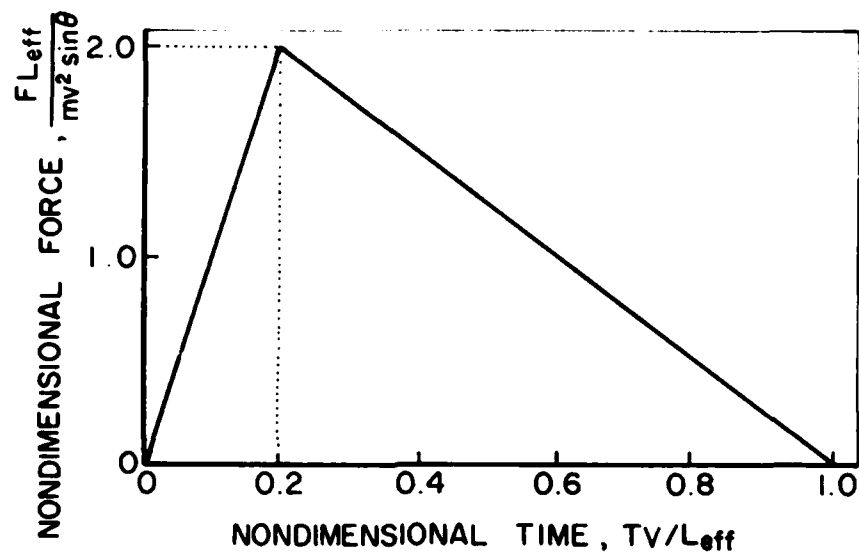


Figure 24. Generalized Bird Impact Force-Time Profile.

The remainder of this section will review the steps which were taken to specify bird impact force data for those bird-strike tests simulated with IMPACT. The data required and the methods by which to develop it are described in detail in Reference 6. Since attempts to simulate both tests BM006 and BM004 were ultimately unsuccessful, no discussion of force data for these tests will be presented even though it was prepared.

2. BIRDSTRIKE LOADS DATA— TEST BM14

Two angles relating the bird trajectory to the windshield panel and two linear dimensions of the bird were required in order to be able to define all the bird impact force data for IMPACT. One of these angles was that between the target surface and the bird trajectory, θ , which has already been discussed in Section V.1. The second angle was that between the bird trajectory and the aircraft plane of symmetry measured in the plane tangent to the windshield at the point of impact. This angle will be referred to as gamma, γ . Neither θ nor γ were determined directly but rather were calculated as functions of two more angles, alpha, α , and beta, β , which were easier to measure directly for a particular test setup. Figure 32 illustrates each of these four angles. The two bird dimensions also required were the length and diameter, L and d , as already discussed in Section V.1. The remainder of this section will discuss how values for each of these six quantities were determined for test BM14 and how these values were used in developing bird impact force data for input to IMPACT.

The bird which was launched against windshield part number PPG-002 for test BM14 was a chicken of mass 4.04 lb. The bird velocity just before impact was measured to be 939 fps. Figure 25 shows the locations of the 16mm high-speed cameras used to record the test.

(6) G. R. Eide, Aircraft Windshield Bird Impact Math Model - Part 2 - User's Manual, Air Force Flight Dynamics Laboratory, Wright-Patterson Air Force Base, Ohio 45433, AFFDL-TR-77-99, Part 2, December 1977.

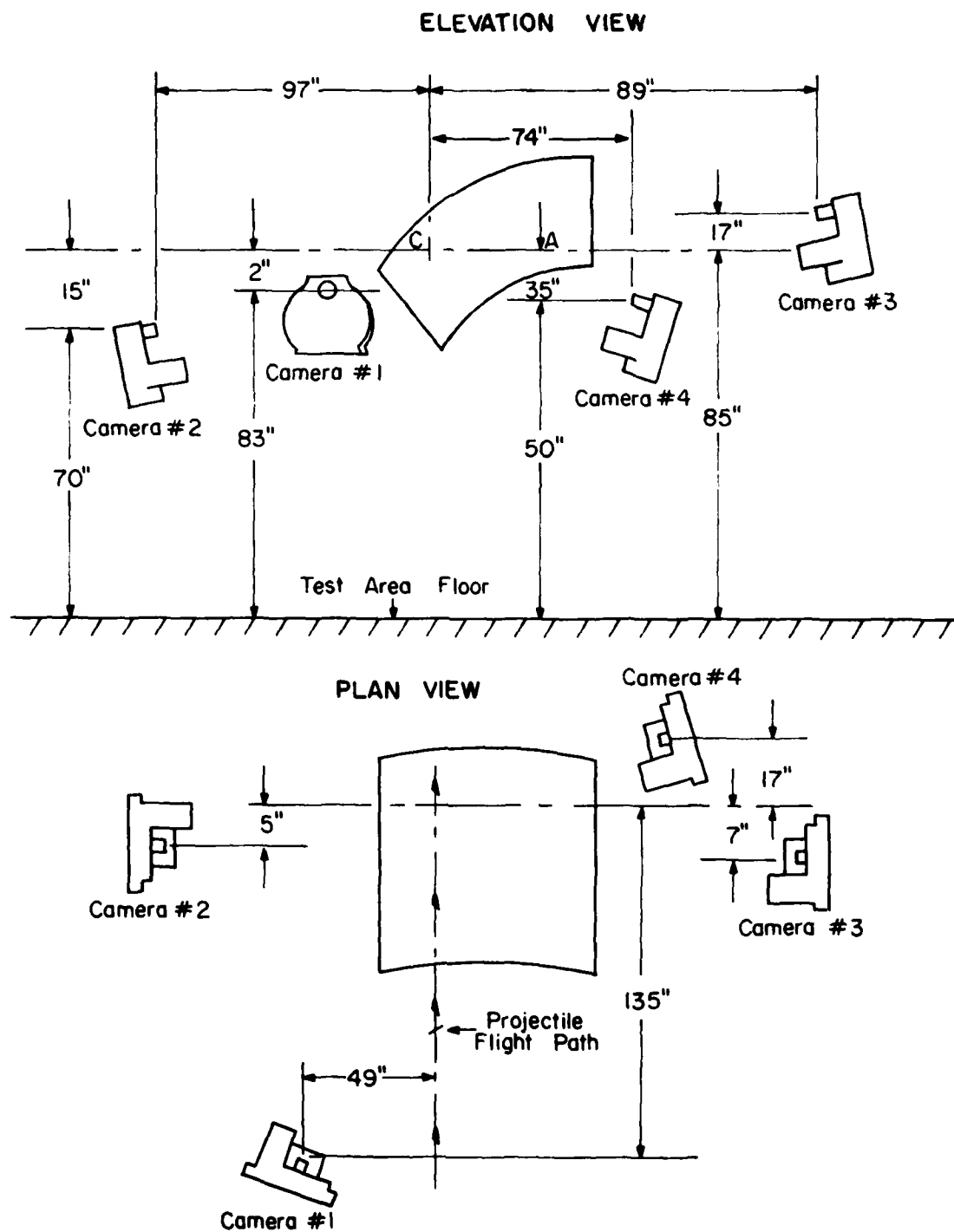


Figure 25. Camera Locations for Shots BM-14 through BM-19.

Figure 26 is a tracing made from three frames of the camera number 2 film. Several pieces of information were drawn from Figure 26. It was seen that the bird was traveling in its axial direction at impact with no measurable yaw or pitch. The dimensions of the bird were obtained by comparing measurements of the bird image to the length of the windshield centerline which is known to be 36-in (Section IV.2). All birds were enclosed in nylon sacks before launching to prevent disintegration before impact. The dimensions of the bird were taken to be somewhat less than the dimensions of the image seen in Figure 26 because some of the image was judged to be loose nylon, not bird material. The angle between the windshield centerline and the bird trajectory measured in the aircraft plane of symmetry, α , was 25 deg. The geometry of the bird was seen to be close to a right circular cylinder during its flight.

Because of the shallow viewing angle of camera number 2, the location of the initial impact point was difficult to determine from Figure 26. Camera number 4, however, was placed to view the interior surface of the windshield during the test and Figure 27 shows a tracing made from that film. The initial impact point was determined to be forward and inboard of the target point on the windshield panel by the distances shown on the figure. Scaling was accomplished again by comparing measurements to a line of known length drawn through the target point parallel to the windshield centerline.

Figure 28 is an axial view of the test windshield panel showing the location of the target point (C in Figure 3) and the normal to the surface at this point. The angle between the surface normal at point C and the aircraft right-hand direction measured in the plane normal to the windshield centerline, β , was found to be 55.9 deg.

To determine the magnitude of the bird impact force on the windshield panel it was necessary to know the angle between the bird trajectory and the surface measured in the plane of

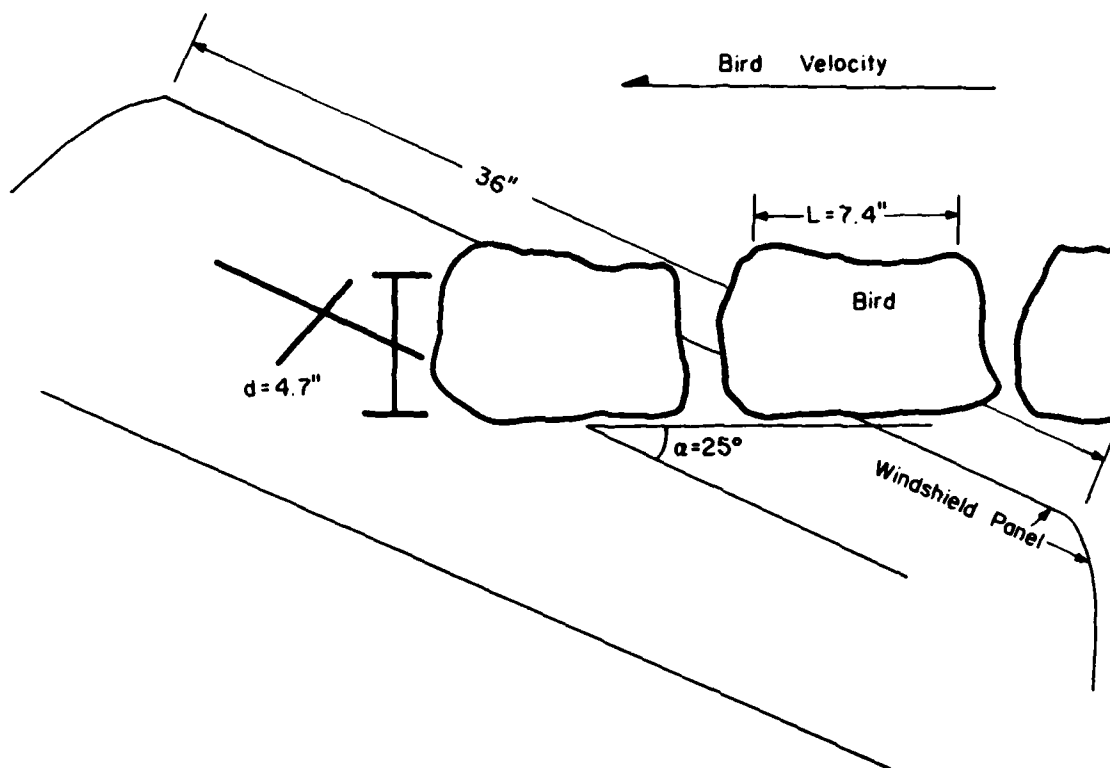


Figure 26. Camera Number 2 Record of Test BM14.

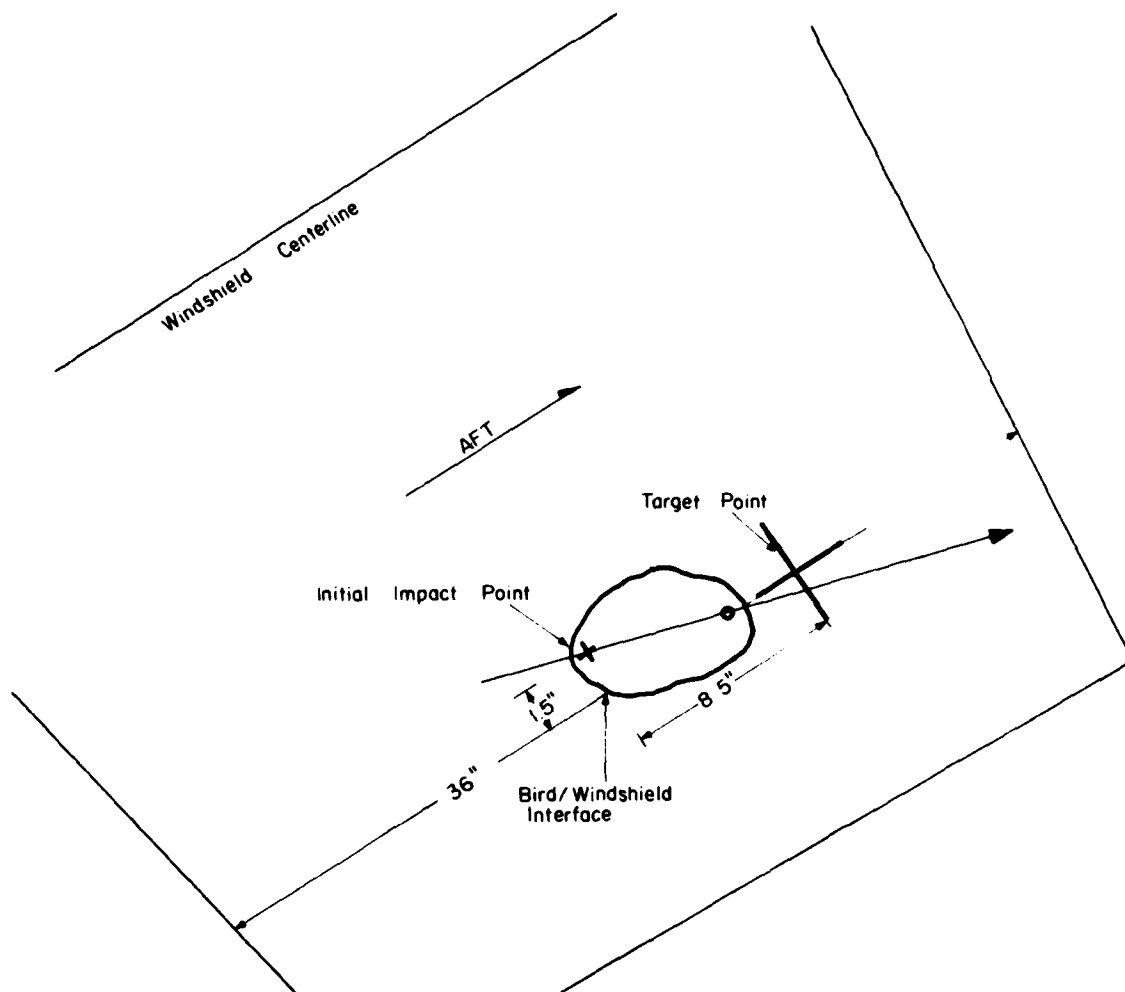


Figure 27. Camera Number 4 Record of Test BM14.

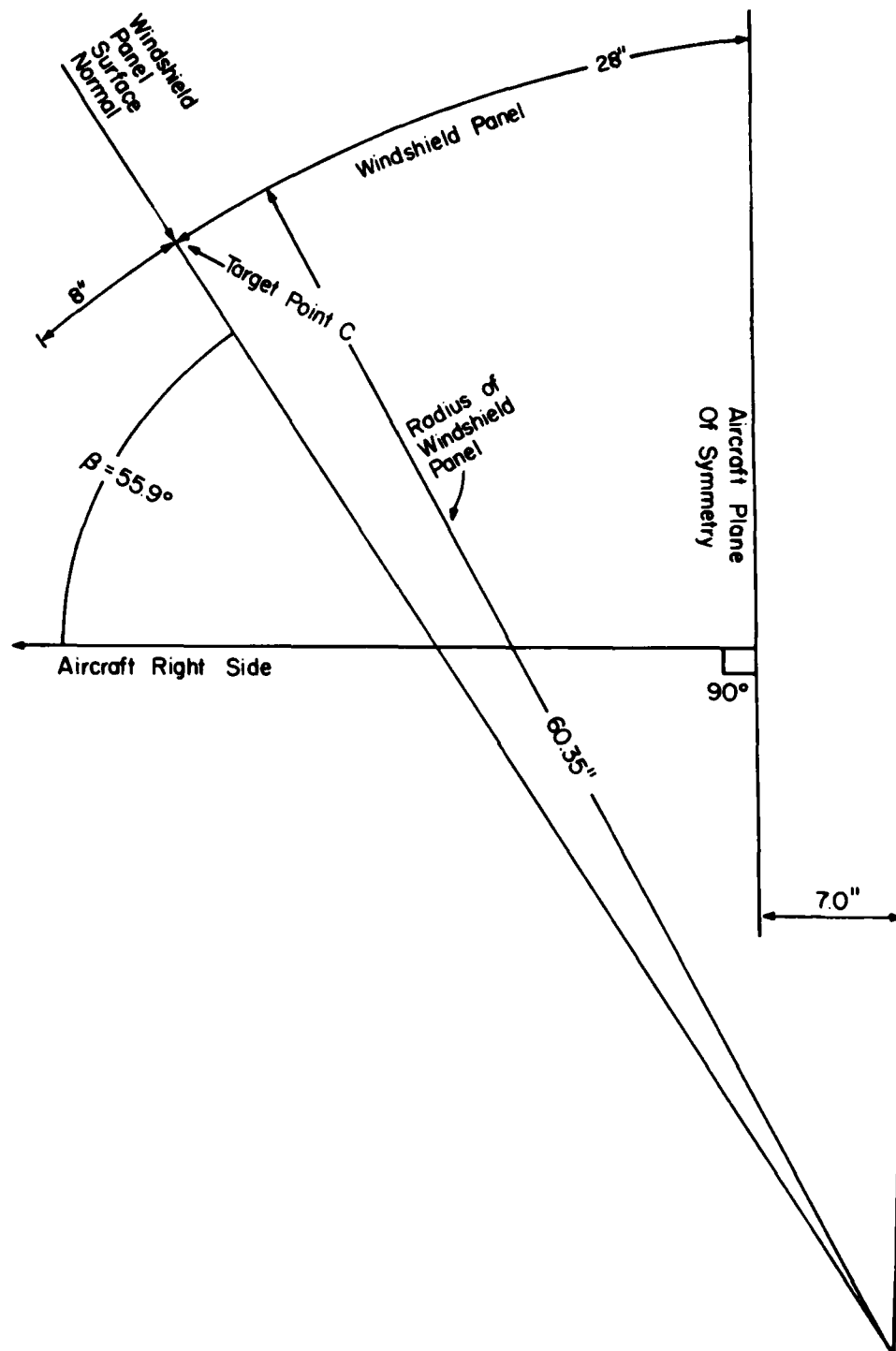


Figure 28. Axial View of BM14 Test Fixture.

of the surface normal at the impact point and the bird trajectory [Equation (7)]. This angle has already been referred to as θ and was determined directly from α and β as illustrated in Figure 29. Angle α lies in the plane BCE; angle β in plane ABN; angle δ , in plane DEN; and angle θ is the complement of δ . The length of side N is 1 since it is taken to be a unit vector normal to the surface at the target point. The equalities listed below follow by observation from Figure 29.

$$A = N \cos \beta = \cos \beta \quad (8)$$

$$B = N \sin \beta = \sin \beta \quad (9)$$

$$C = B \cot \alpha = \sin \beta \cot \alpha \quad (10)$$

$$\begin{aligned} D &= (A^2 + C^2)^{1/2} \\ &= (\cos^2 \beta + \sin^2 \beta \cot^2 \alpha) \end{aligned} \quad (11)$$

$$\begin{aligned} E &= (B^2 + C^2)^{1/2} \\ &= (\sin^2 \beta + \sin^2 \beta \cot^2 \alpha)^{1/2} \end{aligned} \quad (12)$$

The following expression may be obtained from the Law of Cosines (Reference 28).

$$D^2 = N^2 + E^2 - 2 NE \cos \delta \quad (13)$$

Upon substitution and simplification, Equation (13) reduces to Equation (14).

$$\theta = \text{Arc Sin} (\sin \alpha \sin \beta) \quad (14)$$

The value of θ for test BM14 was found to be 20.5 deg from Equation (14).

The effective length of the bird was determined from Equation (5) to be 1.67 ft and the impact period from Equation (6) was then 0.00177 sec. The average impact force from Equation (7) was 23,245 lb. The bird impact force-time history

(28) G. B. Thomas, Calculus and Analytic Geometry, Addison-Wesley, 1965.

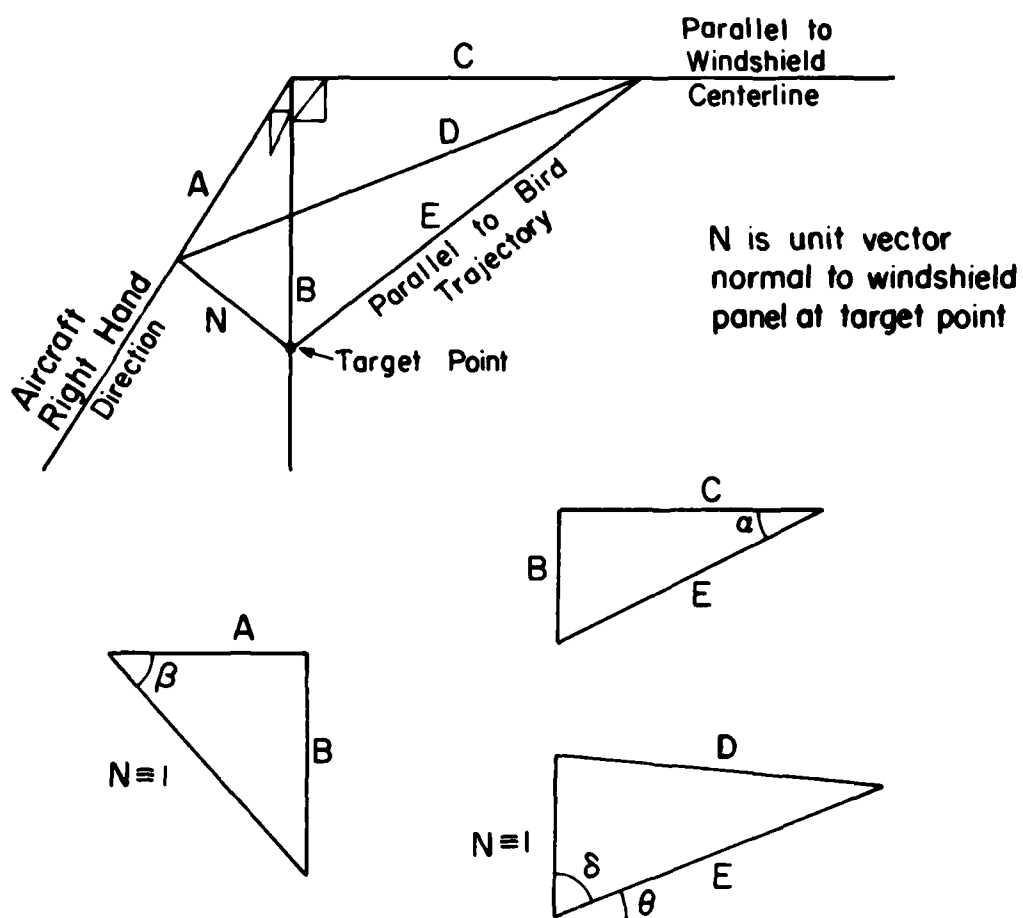
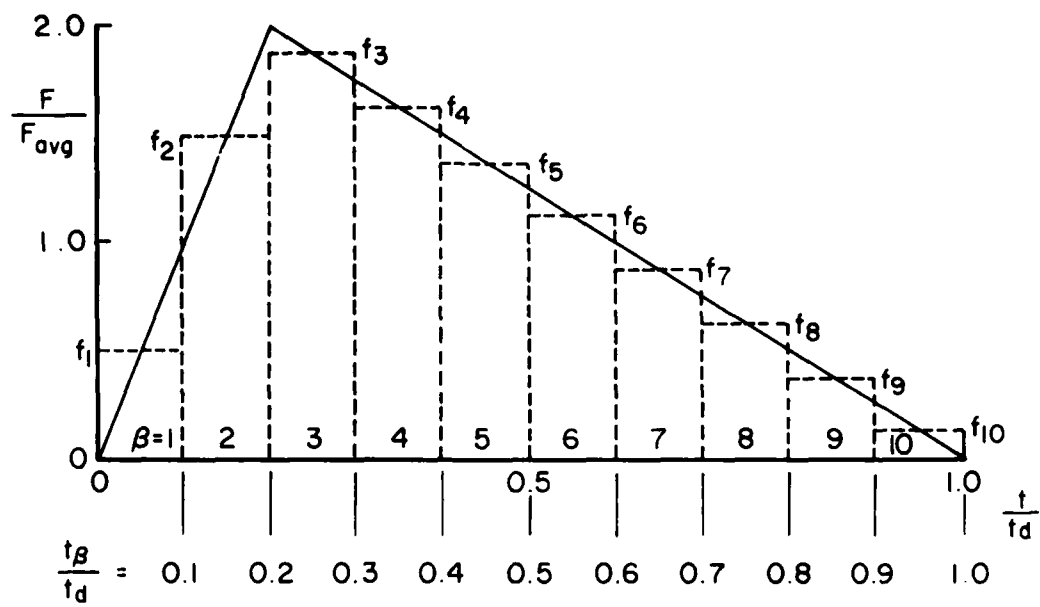


Figure 29. Determination of Angle Theta, θ .

for test BM14 as modeled on the basis of these calculations is shown in Figure 30. The impact event was divided into ten uniform time increments and the theoretically developed triangular force history (Figure 24) was then approximated with ten rectangular force-time segments. The area under both the triangular and the rectangular paths, hence the impulse, was the same. The ten times corresponding to the end of a rectangular segment also correspond exactly to times at which IMPACT performed a linear solution for the response of the structure; i.e., constant applied forces are assumed by IMPACT within each time increment of the linear solution so the time increments in the force-time input data were made to correspond to those time increments at which linear solutions would be requested from IMPACT.

The next task in preparing force input data for test BM14 was the determination, at each of the ten time increments, of the sets of joints on the surface of the finite element model over which the impact force for that time increment would be distributed. This required making layout drawings of the bird impact footprint on the surface of the structure. To accomplish this, the bird was assumed to be a right circular cylinder and the windshield panel was assumed to be flat in the region near the impact site. With these assumptions, the bird footprint or intersection with the windshield became an ellipse. The centroid of this ellipse was taken as the actual impact point. The forward end of the ellipse corresponded to the initial point of impact which had already been located on the surface of the windshield from film analysis (Figure 27). The orientation of the ellipse on the surface had not yet been determined, however. The angle between the major axis of the ellipse and the center-line of the windshield measured in the plane tangent to the surface at the impact point was called gamma, γ . This angle, when determined, together with the other data already calculated would suffice to allow the layouts mentioned to be drawn. The angle γ was obtained from the three angles α , β , and θ determined earlier. Figure 31 illustrates the relationship used.



$F_{avg} = 23245 \text{ lb}$

$t_d = 0.00177 \text{ sec}$

β	t_β	f_β
1	$0.1 t_d$	0.5
2	$0.2 \uparrow$	1.5
3	0.3	1.875
4	0.4	1.625
5	0.5	1.375
6	0.6	1.125
7	0.7	0.875
8	0.8	0.625
9	$0.9 \downarrow$	0.375
10	$1.0 t_d$	0.125

Figure 30. Bird Impact Force-Time Distribution for Test BM14.

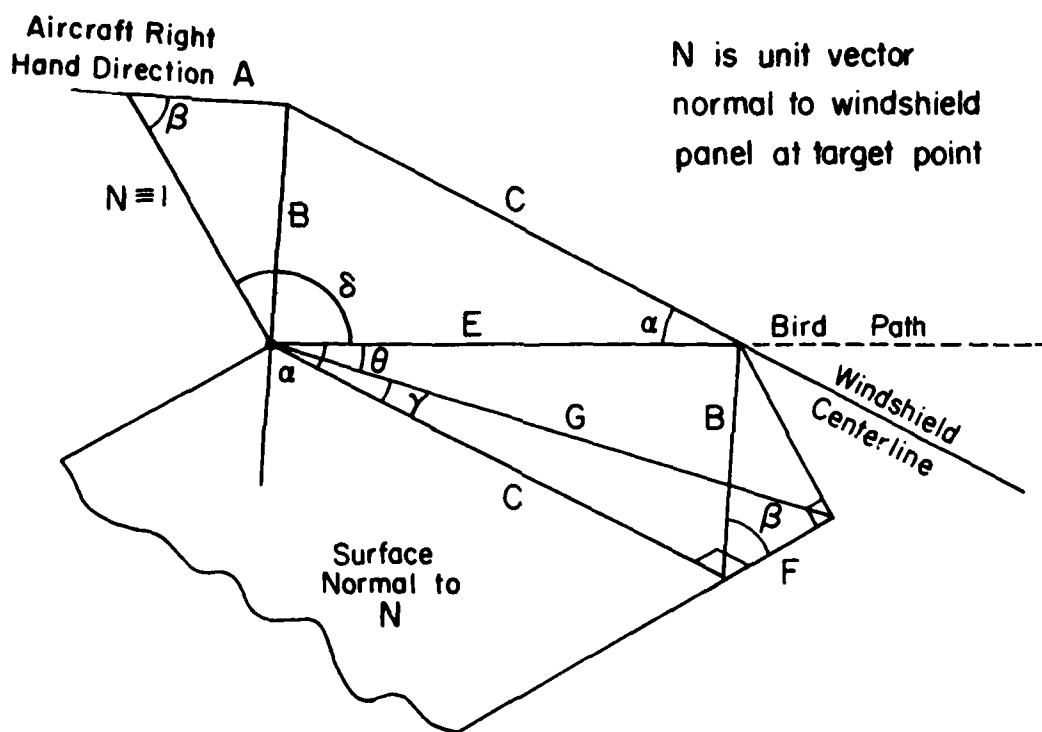


Figure 31. Determination of Angle Gamma, γ .

The following expressions can be written by observation from Figure 31.

$$B = \sin \beta \quad (9)$$

$$C = \sin \beta \operatorname{Ctn} \alpha \quad (10)$$

$$E = (\sin^2 \beta + \sin^2 \beta \operatorname{Ctn}^2 \alpha)^{1/2} \quad (12)$$

$$F = B \cos \beta = \sin \beta \cos \beta \quad (15)$$

$$G = E \cos \theta = \cos \theta (\sin^2 \beta + \sin^2 \beta \operatorname{Ctn}^2 \alpha)^{1/2} \quad (16)$$

$$\gamma = \operatorname{Arc} \sin (F/G)$$

$$\text{or } \gamma = \operatorname{Arc} \sin (\cos \beta \sin \alpha / \cos \theta) \quad (17)$$

The value of γ for test BM 14 was found from Equation (17) to be 14.7 deg. The values of both θ and γ calculated from Equations (14) and (17), respectively, were double checked by the graphic method illustrated in Figure 32 (Reference 29). The graphical results confirmed the calculated values.

Determination of the value of γ permitted the layout of the bird impact footprint on the surface of the finite element model as illustrated in Figure 33. The line intersections are joints on the surface of the finite element model. The forward end of the footprint is located at the initial impact point (Figure 27). The footprint is canted at the angle γ from the direction of the windshield centerline. The length of the minor axis of the footprint ellipse is d , the diameter of the bird (Figure 26). The length of the major axis is $d/\sin \theta$ (Figure 23).

Knowing the velocity of the bird and the geometry of the impact, ten drawings were prepared from Figure 33 to illustrate the area of the windshield covered by bird material at each of the ten time increments shown in Figure 30. The ten drawings are shown in Figures 34 through 43.

(29) R. H. Hammond, C. P. Buck, W. B. Rogers, G. W. Walsh, Jr., and H. P. Ackert, Engineering Graphics for Design and Analysis, The Ronald Press Company, 1964.

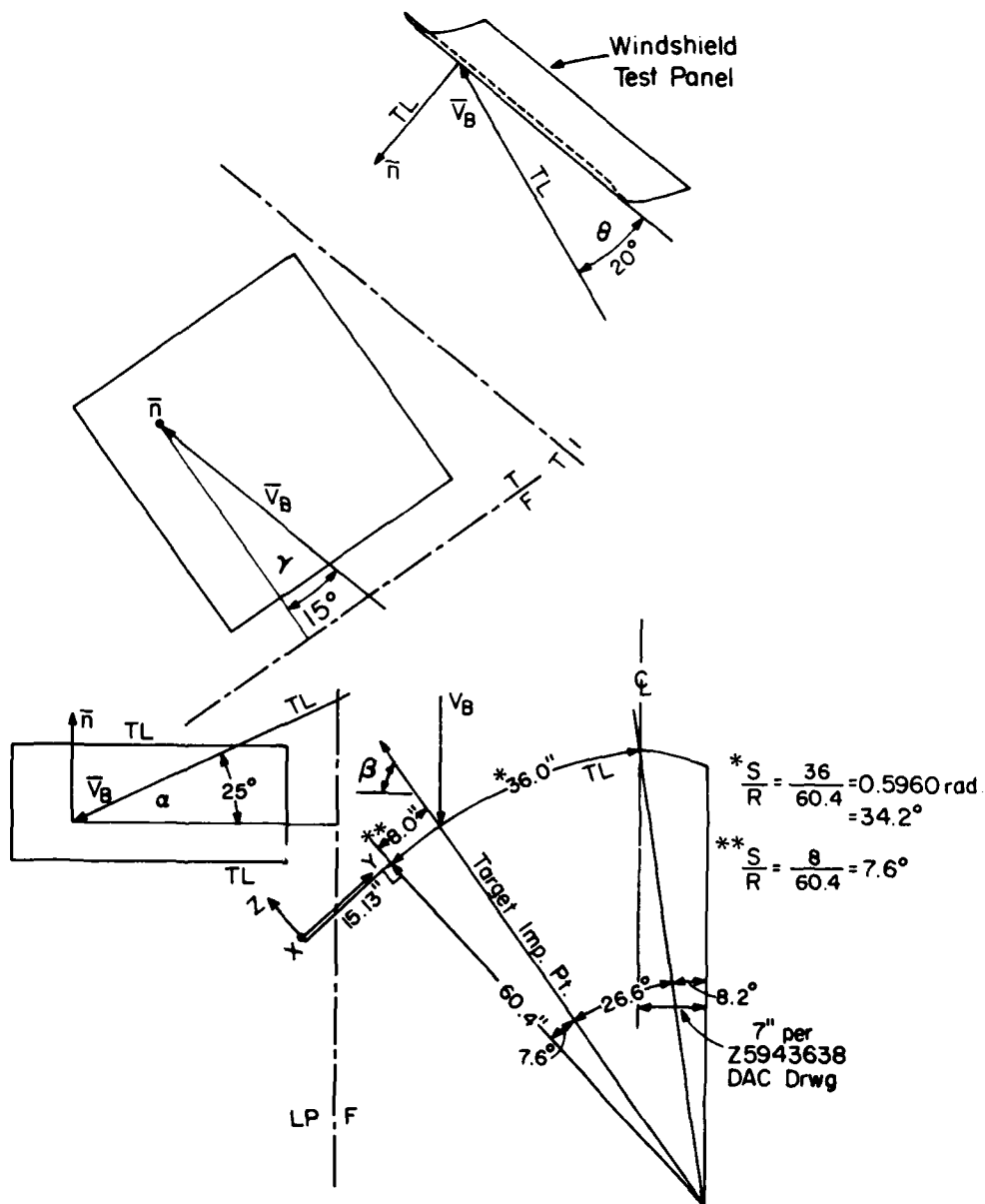


Figure 32. Layout for Bird Impact Loads, BM14.

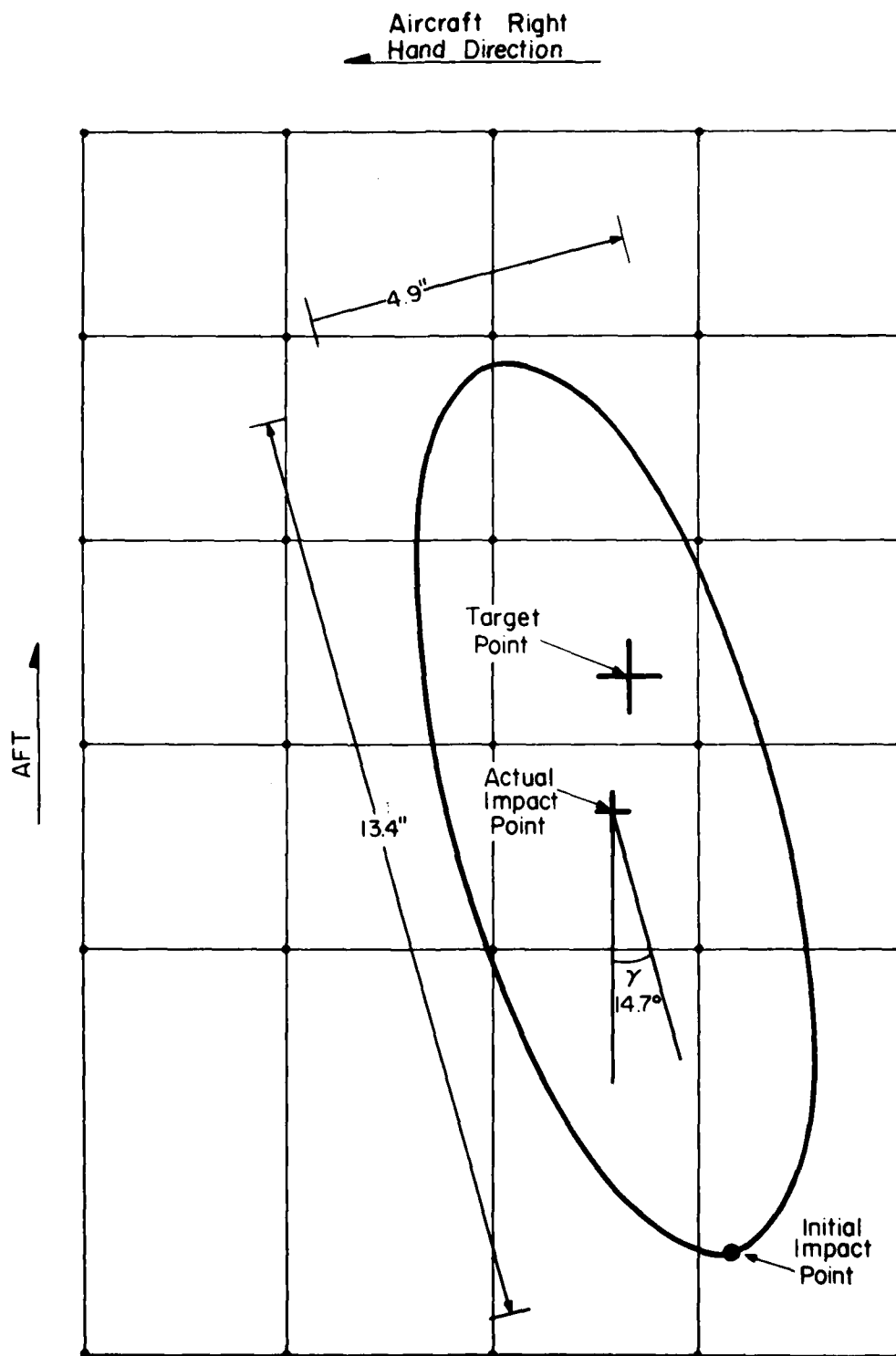


Figure 33. Bird Impact Footprint for Test BM14.

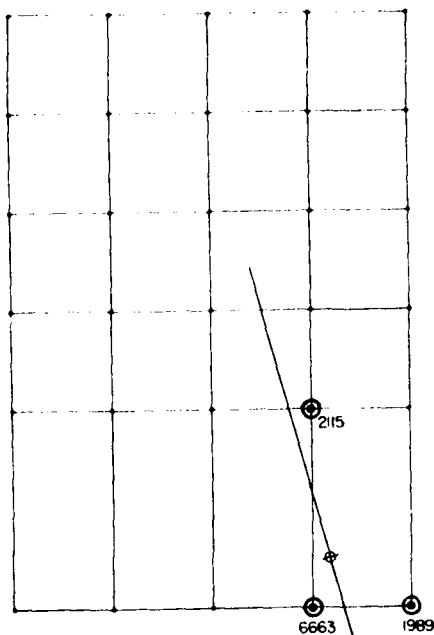


Figure 34. BM14 Bird Footprint
at Time Increment 1.

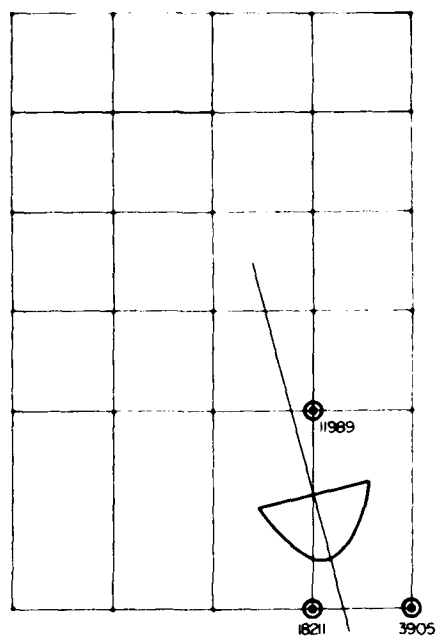


Figure 35. BM14 Bird Footprint
at Time Increment 2.

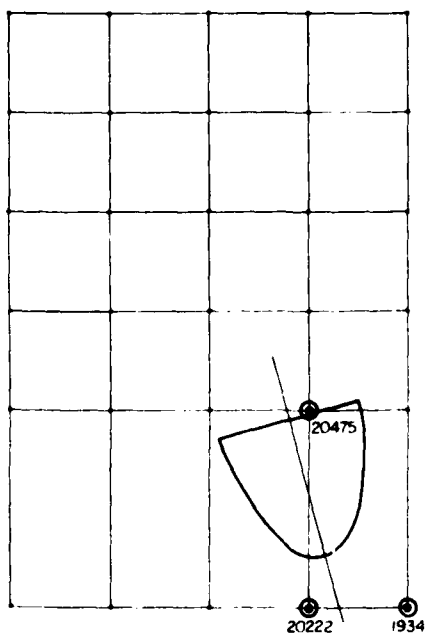


Figure 36. BM14 Bird Footprint
at Time Increment 3.

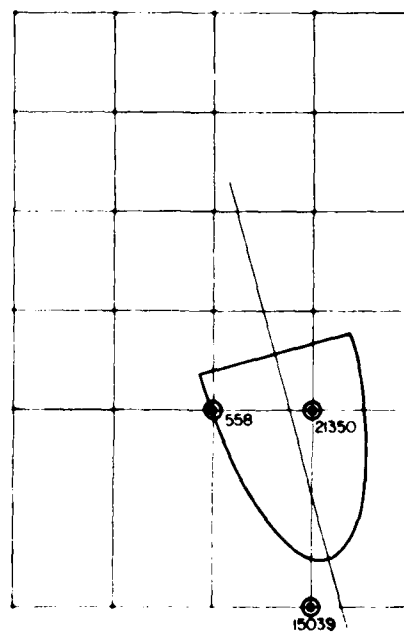


Figure 37. BM14 Bird Footprint
at Time Increment 4.

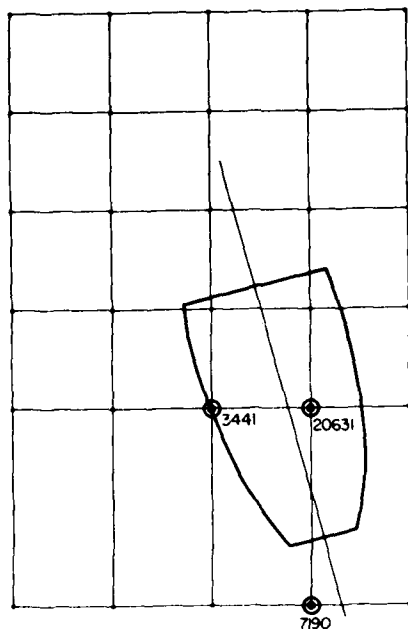


Figure 38. BM14 Bird Footprint at Time Increment 5.

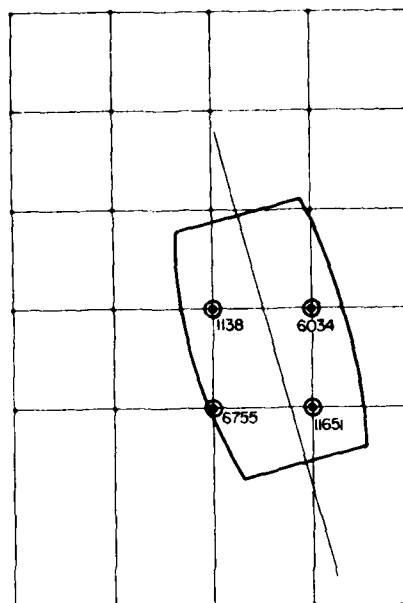


Figure 39. BM14 Bird Footprint at Time Increment 6.

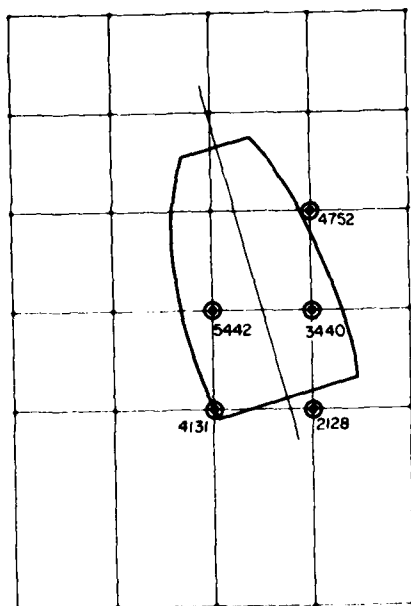


Figure 40. BM14 Bird Footprint at Time Increment 7.

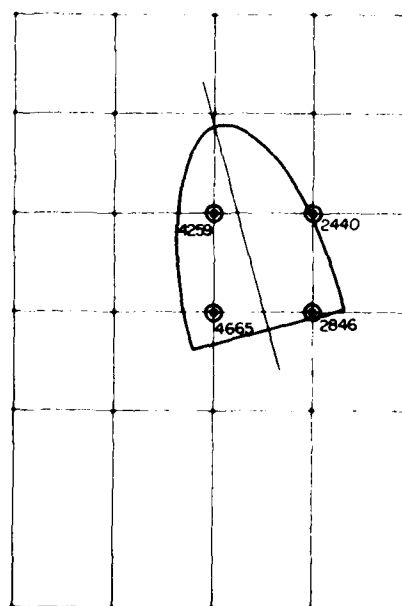


Figure 41. BM14 Bird Footprint at Time Increment 8.

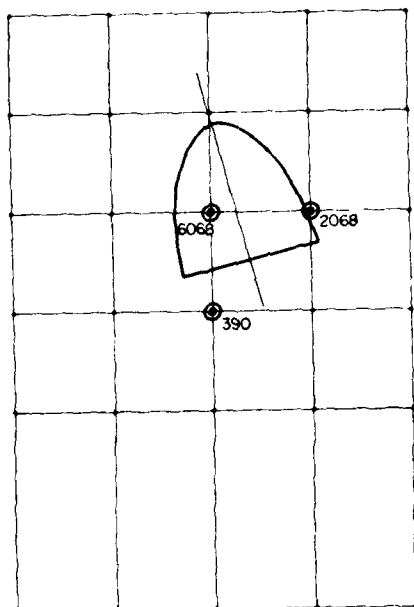


Figure 42. BM14 Bird Footprint
at Time Increment 9.

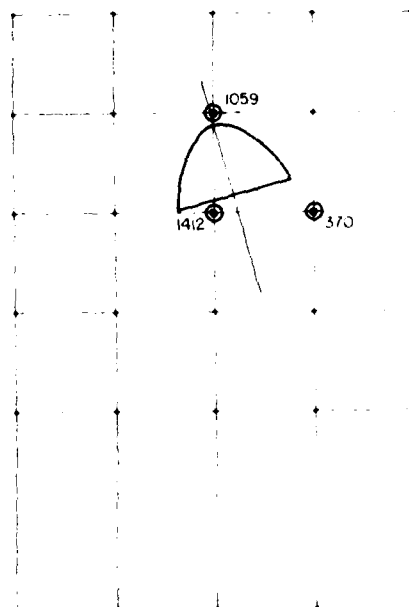


Figure 43. BM14 Bird Footprint
at Time Increment 10.

The centroid of each of the areas shown in Figures 34 through 43 was estimated, and then the coordinates on the windshield surface of these ten centroids and the force history per Figure 30 were input to the Loads Generator Module of IMPACT (Section II.2). Also input were the components of the unit inward normal to the windshield surface at the actual impact point along with ten sets of joints on the surface of the finite element model. Each joint set corresponded to one of the Figures 34 through 43 and represented the joints loaded by bird material during the respective time increment.

The joints so chosen have been circled on Figures 34 through 43. The Loads Generator Module of IMPACT was executed to calculate joint forces at each time increment. The magnitudes of the forces calculated are shown in lb just below the circled joints in Figures 34 through 43. All joint forces are oriented parallel to an inward normal to the windshield surface at the actual impact point. The resultant of each set of joint forces acted at the centroid of the area of intersection for the respective time increment. As can be seen from the figures, the individual joint force levels are quite large, some in excess of 20,000 lb.

The output of the Loads Generator Module for test BM14 was stored on magnetic tape until required for later IMPACT runs.

3. BIRDSTRIKE LOADS DATA—TEST BM19

The same methods were used to develop the bird impact force data for test BM19 as for test BM14. Since the camera locations and test fixture geometry were the same for both tests, the only differences were in parameters defining the impact event itself.

For test BM19 the chicken had mass 4.02 lb and the impact velocity was 971 fps. Figure 44 shows the obliquity of the impact and the dimensions of the bird as taken from high-speed film records of the test. Figure 45 shows a tracing made

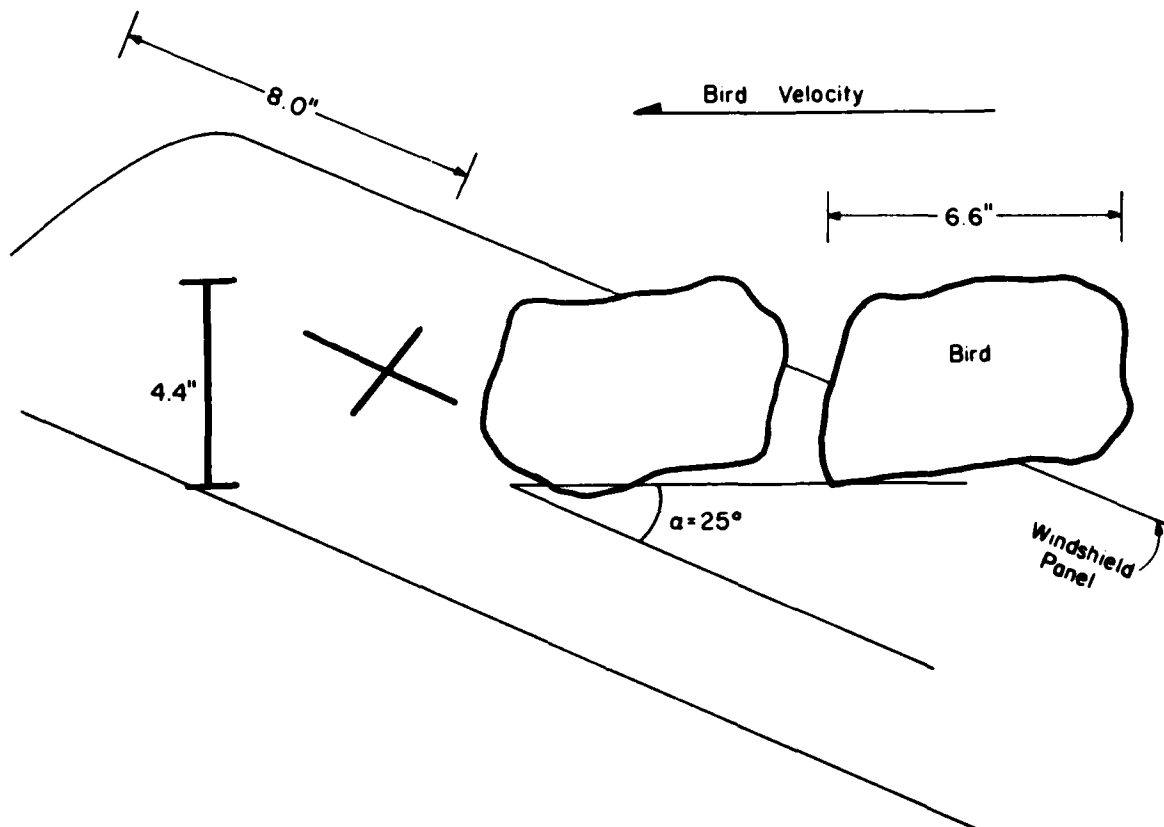


Figure 44. Camera Number 2 Record of Test BM19.

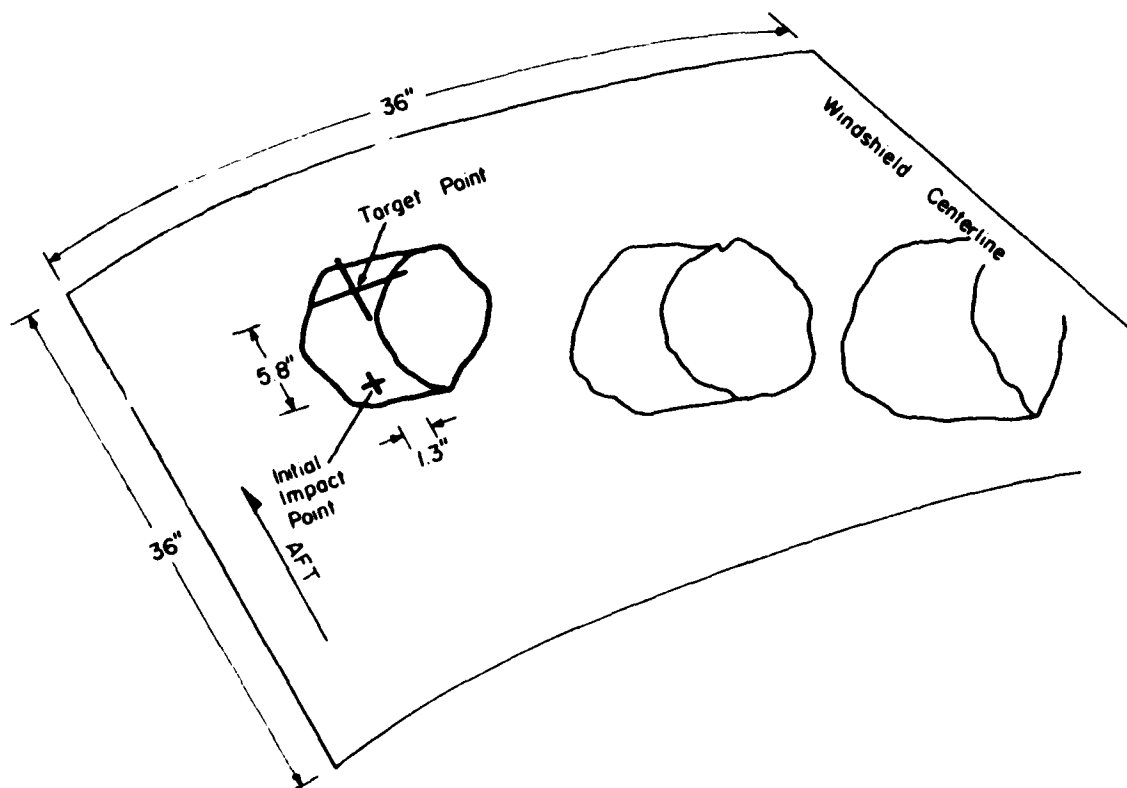


Figure 45. Camera Number 1 Record of Test BM10.

from the camera number 1 film for test BM19. This is an exterior view of the windshield panel and was used to determine the initial impact point of the bird on the windshield.

For test BM19, the angle θ was determined to be 19.6 deg, less than for test BM14 due to the slightly more outboard location of impact. Angle γ was determined to be 15.8 deg, slightly more than for test BM14 again due to the slightly more outboard location of impact. The effective length of the bird was found to be 1.58 ft and the period of the impact event, 0.00163 sec. Both were slightly less than for test BM14. The average impact force was 24,991 lb, greater than for test BM14 due primarily to the higher impact velocity. The graphic method of verifying angles θ and γ was not repeated for test BM19.

A surface layout of the bird impact footprint for test BM19 is shown in Figure 46. Joint loads as computed by the Loads Generator Module of IMPACT at ten time intervals are shown in Figures 47 through 56. As for test BM14, each joint which is loaded over a particular time increment has been circled and the joint force is shown in lb directly below the joint.

The output of the Loads Generator Module run for test BM19 was stored on magnetic tape for later use as was that for test BM14.

The finite element models discussed in Section IV and the bird impact force data discussed in this section both served as input data for IMPACT analyses of the birdstrike testing. The next section will discuss these analyses in some detail.

AIRCRAFT RIGHT HAND DIRECTION

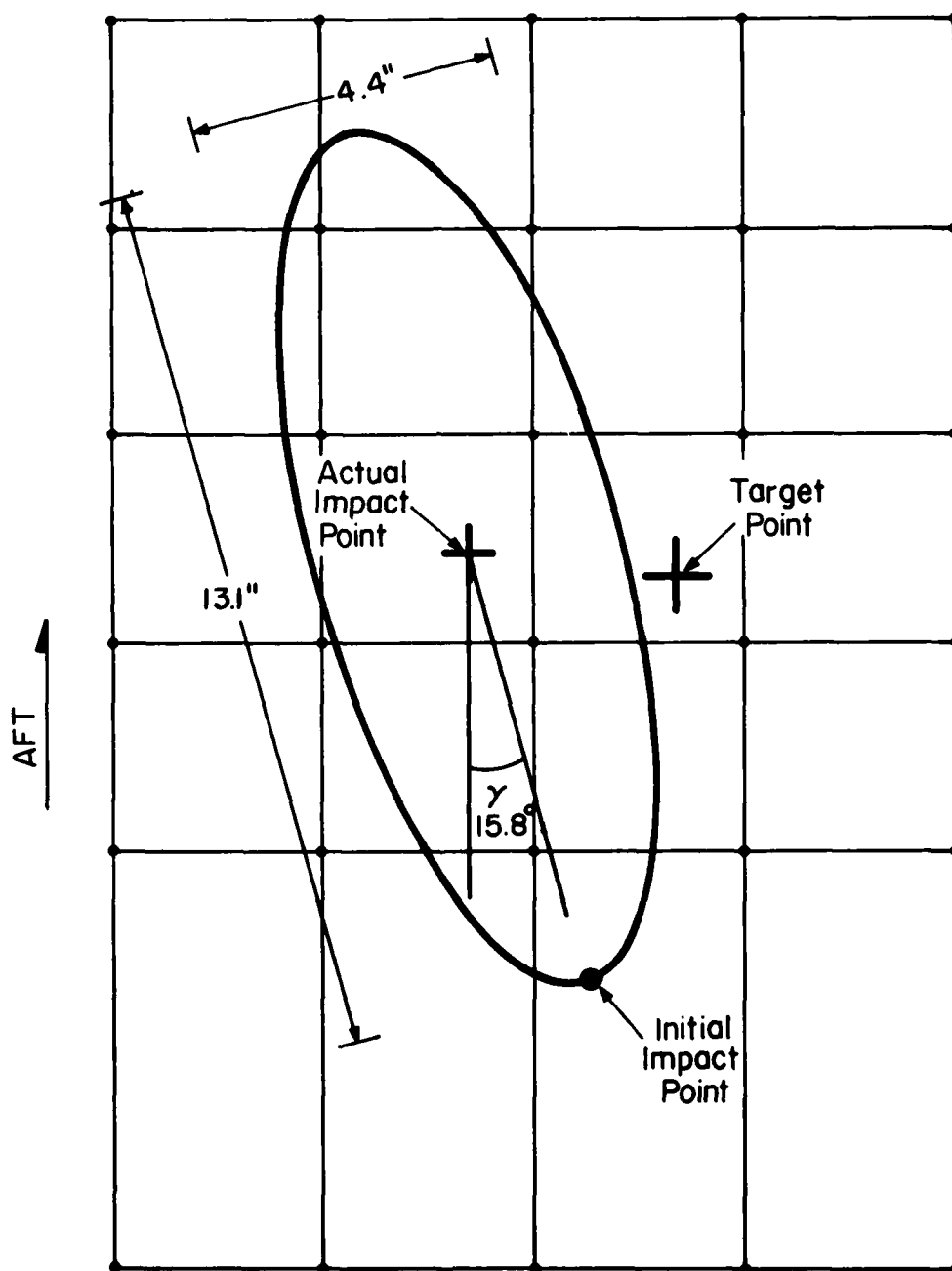


Figure 46. Bird Impact Footprint for Test BM19.

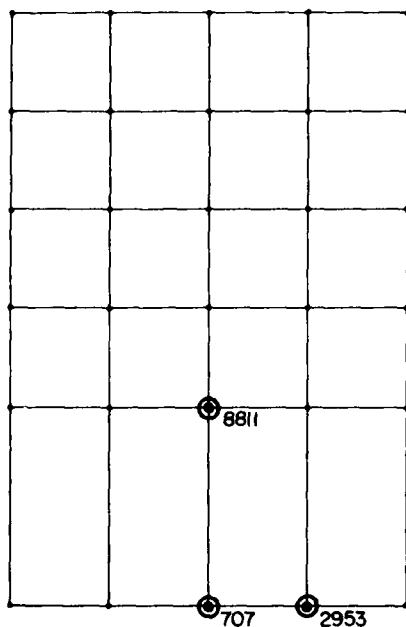


Figure 47. BM19 Bird Footprint
at Time Increment 1.

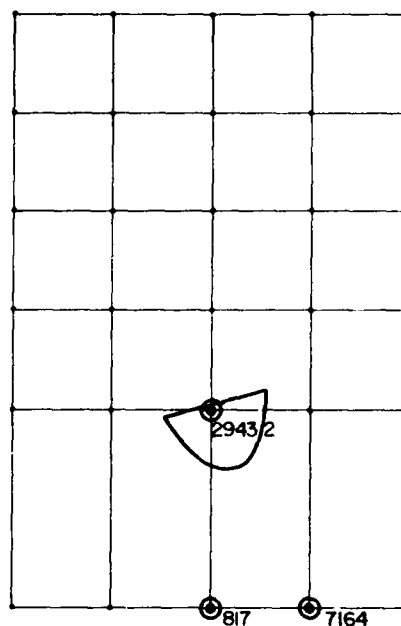


Figure 48. BM19 Bird Footprint
at Time Increment 2.

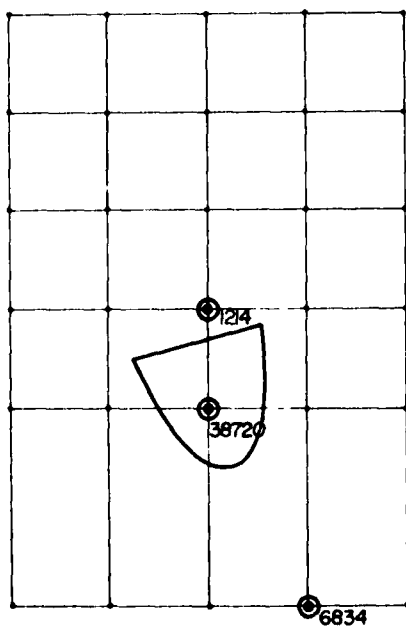


Figure 49. BM19 Bird Footprint
at Time Increment 3.

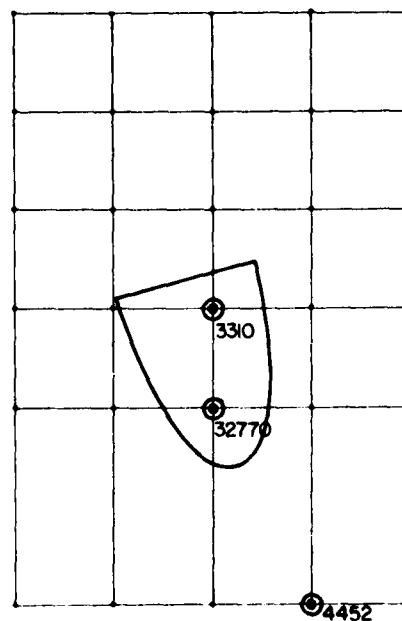


Figure 50. BM19 Bird Footprint
at Time Increment 4.

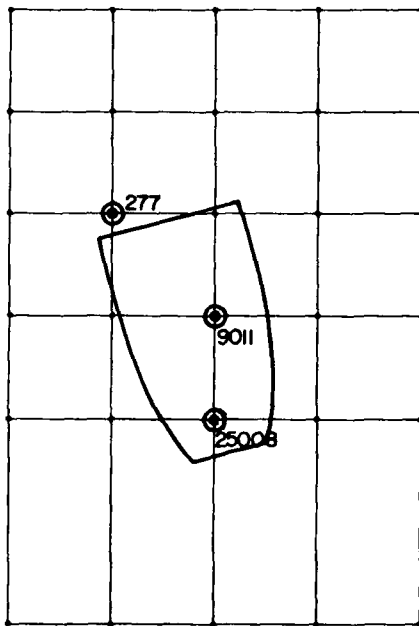


Figure 51. BM19 Bird Footprint
at Time Increment 5.

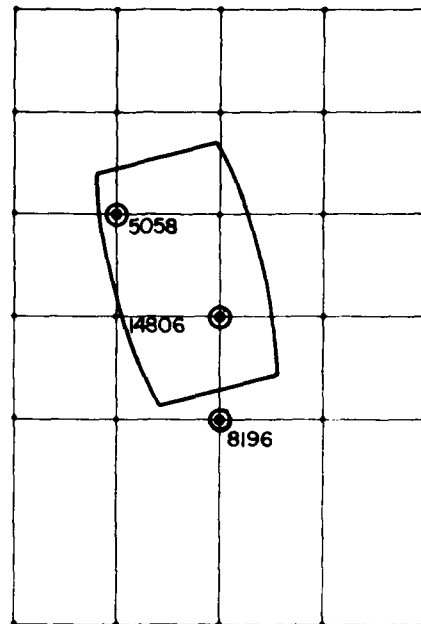


Figure 52. BM19 Bird Footprint
at Time Increment 6.

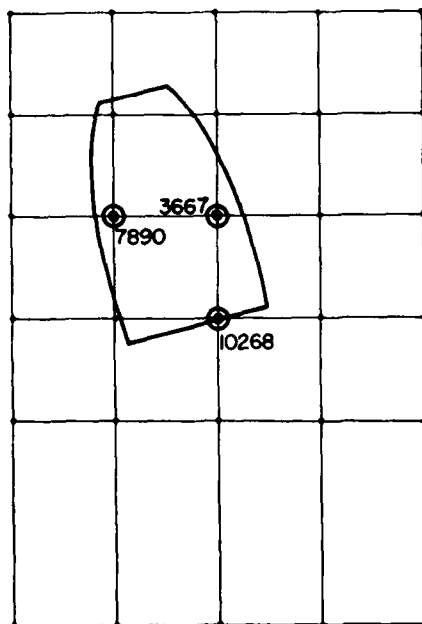


Figure 53. BM19 Bird Footprint
at Time Increment 7.

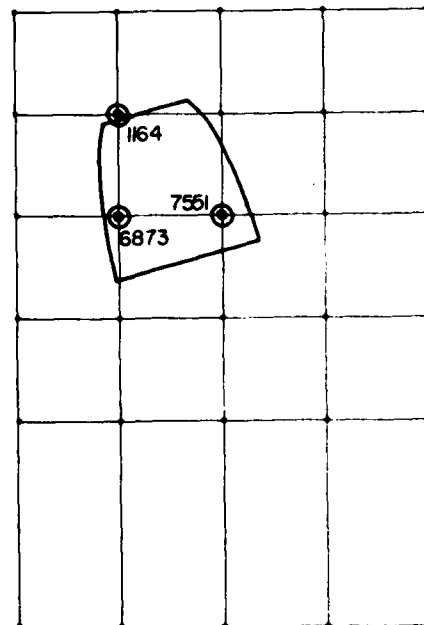


Figure 54. BM19 Bird Footprint
at Time Increment 8.

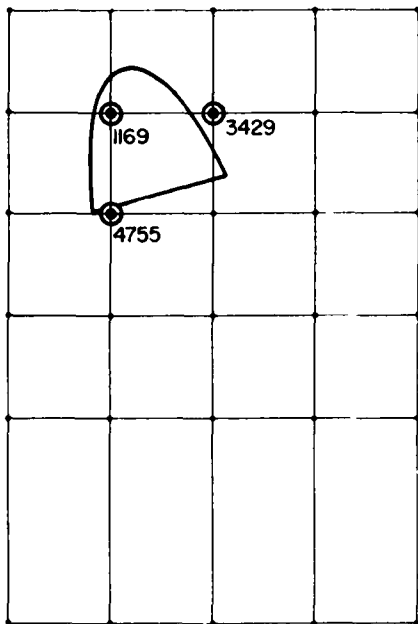


Figure 55. BM19 Bird Footprint
at Time Increment 9.

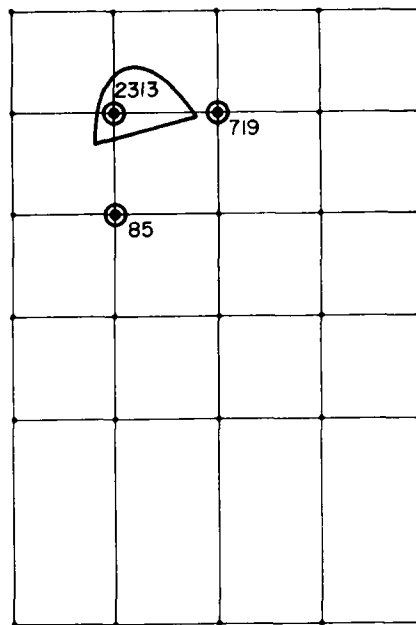


Figure 56. BM19 Bird Footprint
at Time Increment 10.

SECTION VI

COMPUTER ANALYSES

1. ASSUMPTIONS

Even though the assumptions which were made in using IMPACT have already been mentioned at various points in earlier sections of this report, it will be useful to review them all again here.

Section I.2 stated that all IMPACT analyses would be fully linear since the nonlinear version which was planned was unsuccessful. This means that neither the effects of geometric nonlinearities nor of material nonlinearities were accounted for in the IMPACT studies.

The assumption of material linearity was reasonable for a number of the materials used in the test structures, namely the glasses and the aluminum and titanium alloys used. The assumption was reasonable for the glasses because they do indeed behave in a linearly elastic fashion and exhibit brittle failure (in tension). It was also reasonable for the metal alloys involved because none of the metallic support structures in the test articles incurred any plastic deformation during the tests which were simulated (Reference 8). All the metallic structures, hence, must have experienced only stresses below their respective yield stresses. The assumption of material linearity is a bad one for polycarbonate, acrylic, and the Swedlow, Inc. high-temperature interlayer because these materials are in fact strongly nonlinear (Reference 13). The only other material considered was the PPG 112 interlayer. Data shown in Figure 57 illustrates that the linear elastic assumption was not unreasonable for this material (Reference 13).

(8) R. H. Magnusson, High Speed Bird Impact Testing of Aircraft Transparencies, Air Force Flight Dynamics Laboratory, Wright-Patterson Air Force Base, Ohio 45433, AFFDL-TR-77-98, February 1978.

(13) F. E. Greene, Testing for Mechanical Properties of Monolithic and Laminated Polycarbonate Materials, Air Force Flight Dynamics Laboratory, Wright-Patterson Air Force Base, Ohio 45433, AFFDL-TR-77-96, October 1977.

AD-A091 051

AIR FORCE FLIGHT DYNAMICS LAB WRIGHT-PATTERSON AFB OH F/G 1/3
EVALUATION OF THE IMPACT COMPUTER PROGRAM AS A LINEAR DESIGN TO--ETC(U)
MAR 80 R E MCCARTY

UNCLASSIFIED AFFDL-TR-79-3103

NL

2 1 2

11 11 11



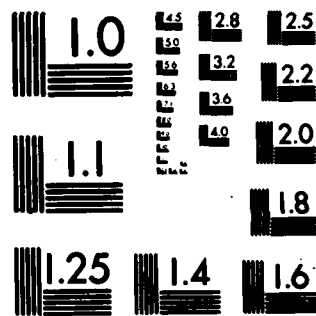
END

DATE

FILED

12-80

DTIC



MICROCOPY RESOLUTION TEST CHART
NATIONAL BUREAU OF STANDARDS-1963-A

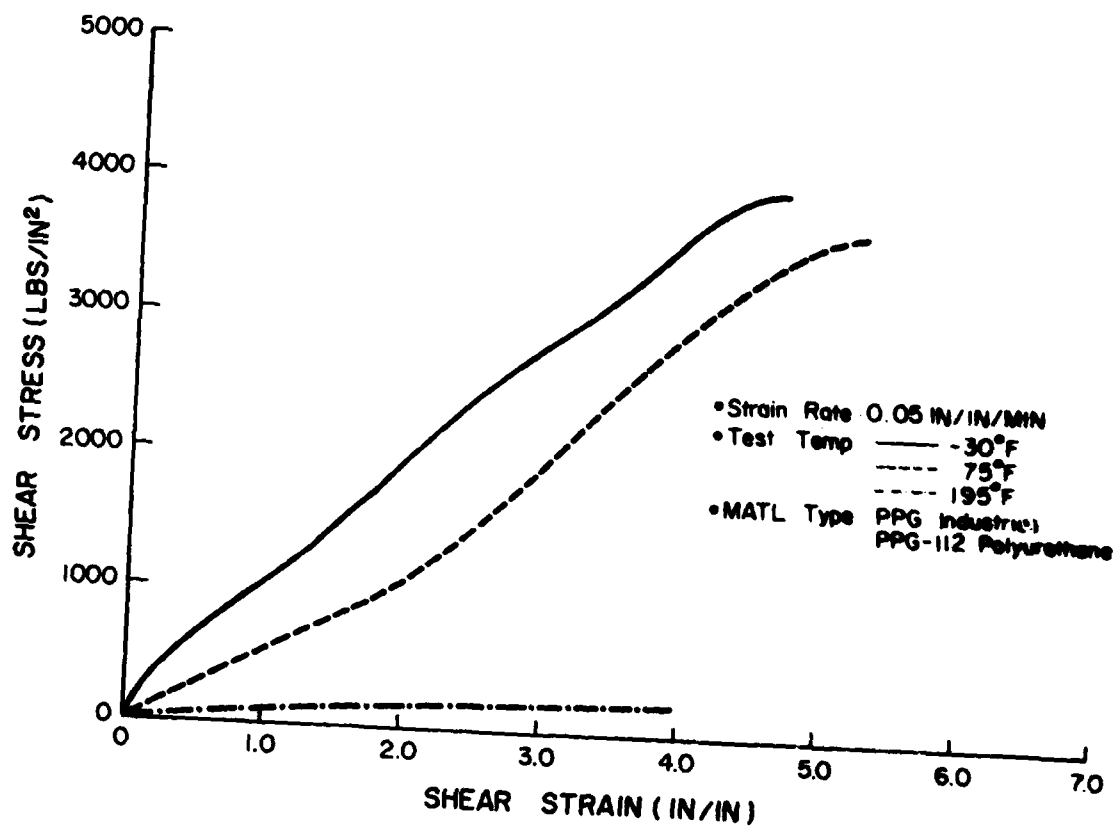


Figure 57. Shear Stress-Strain Characteristics for PPG 112 Interlayer.

In contrast to the material linearity assumption, the validity of the geometric linearity assumption could not be evaluated a priori. In fact, one of the goals of this work effort as pointed out in Section I.2 was to determine whether or not the assumption of geometric linearity was warranted for the B-1 windshield class of structures.

Section I.2 also stated that only existing finite element models would be utilized in IMPACT analyses. No refinement of existing models or generation of new models would be accomplished. This constitutes an assumption that the fineness of the finite element mesh or grid present in existing models was adequate for obtaining an accurate solution. No parametric studies of mesh fineness were planned or accomplished. The only modification of finite element models which did occur was the updating of data for mechanical properties of plastic materials and interlayers with the latest available information (Reference 13). Temperature and strain rate effects upon mechanical properties of materials were accounted for in a manner external to IMPACT by selecting data acquired at temperatures or strain rates of interest.

Section II.1 stated that the forces on the structure resulting from bird impact were assumed to be uncoupled from the resulting deformation of the structure. In fact, the bird impact forces applied to the structure in the IMPACT analyses performed were derived from data obtained in bird strike tests against pressure transducers mounted in rigid steel targets (References 15,

(13) F. E. Greene, Testing for Mechanical Properties of Monolithic and Laminated Polycarbonate Materials, Air Force Flight Dynamics Laboratory, Wright-Patterson Air Force Base, Ohio 45433, AFFDL-TR-77-96, October 1977.

(15) J. P. Barber and J. S. Wilbeck, Characterization of Bird Impacts on a Rigid Plate: Part I, Air Force Flight Dynamics Laboratory, Wright-Patterson Air Force Base, Ohio 45433, AFFDL-TR-75-5, January 1975.

16, 17, 18, and 19). The assumption of uncoupled loading would be valid for cases when structural deflections remained small as was the case for tests BM14 and BM19. The assumptions made regarding the force-time history for the bird impact event and the distributions of the net instantaneous force to joints on the surface of the finite element model are discussed in Section V.1 of this report.

Section II.2 alludes to the fact that the only type of dynamic solution available from IMPACT involves a modal approach. In this method, an arbitrary number of free vibration modes for the structure are determined and are subsequently used to transform structural and loads matrices thereby reducing the size of the numerical problem. The modal approach has long been an accepted method in linear structural analysis so its adoption in these studies should not represent any inherent penalty. The assumption was made for all IMPACT analyses conducted that the first 30 free vibration modes would suffice to provide a solution of acceptable accuracy. This number of modes is suggested by the developers of IMPACT in Reference 6.

(16) R. L. Peterson and J. P. Barber, Bird Impact Forces in Aircraft Windshield Designs, Air Force Flight Dynamics Laboratory, Wright-Patterson Air Force Base, Ohio 45433, AFFDL-TR-75-150, March 1976.

(17) Y. M. Ito, G. B. Carpenter, and F. W. Perry, Bird Impact Loading Model for Aircraft Windshield Design, CRT 3090-2, California Research & Technology, Inc., Woodland Hills, California 91364, July 1977.

(18) J. P. Barber, J. S. Wilbeck, and H. R. Taylor, Bird Impact Forces and Pressures on Rigid and Compliant Targets, Air Force Flight Dynamics Laboratory, Wright-Patterson Air Force Base, Ohio 45433, AFFDL-TR-77-60, May 1978.

(19) J. S. Wilbeck, Impact Behavior of Low Strength Projectiles, Air Force Materials Laboratory, Wright-Patterson Air Force Base, Ohio 45433, AFML-TR-77-134, July 1978.

(6) G. R. Eide, Aircraft Windshield Bird Impact Math Model - Part 2 - User's Manual, Air Force Flight Dynamics Laboratory, Wright-Patterson Air Force Base, Ohio 45433, AFFDL-TR-77-99, Part 2, December 1977.

Section II.2 points out that the IMPACT user is free to choose the size and number of time increments to be used in the solution. Since IMPACT performs a linear analysis, these choices do not affect the accuracy of the solution. In general this is not the case in nonlinear analysis, for which numerical stability must be considered.

Section IV of this report discusses the fact that the attachment of windshield specimens to supporting structures was modeled in a manner which ignored the fixity in bending around the periphery and the relative shear stiffness between plies in the panel produced by bolts running through the panel. In the models, the panel is attached to the structure with frictionless hinges along the inner edge so no bending stiffness whatsoever exists at attachment points. Shear is transferred from one structural ply to the next only through the action of the interlayer materials in the models.

The effects of the assumptions listed above upon results of the IMPACT analyses performed will be discussed in the next section. The remainder of this section will be used to describe, step by step, the computer program analyses which were accomplished.

2. TEST BM14

The first step taken in simulation of test BM14 was preparation of the finite element model which has been discussed in Section IV.2 of this report.

Computer resources which were required for the IMPACT analysis of test BM14 are listed in Table 5. The first IMPACT analysis accomplished was the execution of the Initial Generator for test BM14 (see Section II.2). Job control language required to run the IMPACT Initial Generator on the Wright-Patterson Air Force Base ASD CDC CYBER 74 computer was developed according to instructions in the IMPACT user's manual (Reference 6).

(6) G. R. Eide, Aircraft Windshield Bird Impact Math Model - Part 2 - User's Manual, Air Force Flight Dynamics Laboratory, Wright-Patterson Air Force Base, Ohio 45433, AFFDL-TR-77-99, Part 2, December 1977.

TABLE 5
COMPUTER RESOURCES REQUIRED FOR IMPACT ANALYSIS OF TEST BM14

<u>IMPACT Module</u>	<u>CP Seconds</u>	<u>I/O Seconds</u>	<u>Cost</u>	<u>Date</u>
Initial Generator	426	1,043	\$ 65	7 April 1978
Loads Generator	17	21	1	20 April 1978
FORMAT Setup 1	2,546	7,120	635	12 May 1978
FORMAT Setup 2	3,650	7,020	696	24 May 1978
FORMAT Setup 3	231	891	57	2 June 1978
Incremental Solution	873	2,412	175	6 June 1978
Postprocessor	<u>25</u>	<u>159</u>	<u>7</u>	<u>7 June 1978</u>
	7,768	18,666	\$1,636	61 Days

The CDC operating system under which all jobs described in this section were run was NOS/BE Level 454D, Extended Core Storage (Reference 34). The only input data required by the Initial Generator Module was a file containing the complete finite element model for Test BM14.

The second IMPACT module executed was the Loads Generator (Section II.2). Again, the only input required was the file containing the finite element model. The output of the Loads Generator was a set of joint loads representing the bird impact event as illustrated in Figures 34 through 43.

The next IMPACT module executed was FORMAT Setup 1 (Section II.2). This time three input files were required, the first being the output from the Initial Generator run, the second being the output of the Loads Generator run, and the third being matrix operation instructions in the jobstream which were required to

(34) NOS/BE Version 1 Reference Manual, Publication Number 60493800, Control Data Corporation, Publications and Graphics Division, ARH219, 4201 North Lexington Avenue, Saint Paul, Minnesota, 55112.

direct the execution of FORMAT (Reference 14). The output of this run included an upper triangular structural mass matrix, a decomposed structural stiffness matrix, and static displacements in the reordered unconstrained degrees of freedom resulting from application of the set of static loads representing the first time increment of the bird impact event. The maximum number of active columns encountered during decomposition of the stiffness matrix was 275.

The IMPACT FORMAT Setup 2 module was executed next for BM14. Three input files were required for this run, the first being the output of the Initial Generator run, the second being the output of the FORMAT Setup 1 run, and the third being matrix operation instructions again for FORMAT. Output of this run included a listing of the reciprocals of the squares of the natural frequencies associated with the 30 free vibration modes extracted and a listing of the normalized displacement modes of the structure. A few of the mode shapes were studied in detail and appeared to be reasonable in shape. Natural frequencies for the structure ranged from 736 to 9,315 Hz.

The next IMPACT module executed was FORMAT Setup 3. Again, three input files were required: the Initial Generator output, the FORMAT Setup 2 output, and matrix operating instructions for FORMAT.

The Incremental Solution module of IMPACT was executed next. Three input files were required for the run, two of which were output from the FORMAT Setup 3 run and one which was in the jobstream to define solution parameters such as number of time increments and number of modes. The output of the Incremental

(14) J. Pickard, FORMAT - Fortran Matrix Abstraction Technique--Volume 5. Engineering User and Technical Report, Air Force Flight Dynamics Laboratory, Wright-Patterson Air Force Base, Ohio 45433, AFFDL-TR-66-207, Volume V, October 1968; Volume V Supplement I, June 1970; Volume V Supplement II, April 1973; Volume V Supplement III, December 1977.

Solution included the transient modal response of the structure in terms of element forces, stresses, and strains and joint displacements, velocities, and accelerations at each time increment.

The last module executed for BM14 was the Postprocessor. Data in the jobstream was read as input by the Postprocessor to define the output desired to be listed. The only other input required was the file generated by the Incremental Solution module. The listing printed by the Postprocessor contained the global displacements of all joints on the outer surface of the transparency. Also printed were cell element strains and equivalent stresses for 25 cells of each main ply (soda lime glass) in the target corner of the transparency (50 cells total). This data is discussed in detail in the next section.

3. TEST BM19

The IMPACT analyses were performed for Test BM19 as for BM14. The computer resources required to run each IMPACT module for Test BM19 are listed in Table 6.

TABLE 6
COMPUTER RESOURCES REQUIRED FOR IMPACT ANALYSIS OF TEST BM19

<u>IMPACT Module</u>	<u>CP Seconds</u>	<u>I/O Seconds</u>	<u>Cost</u>	<u>Date</u>
Initial Generator	422	809	\$ 58	25 May 1978
Loads Generator	23	27	2	2 June 1978
FORMAT Setup 1	2,536	7,153	566	3 June 1978
FORMAT Setup 2	3,737	7,010	624	3 June 1978
FORMAT Setup 3	233	890	54	6 June 1978
Incremental Solution	870	2,444	177	6 June 1978
Postprocessor	25	159	7	9 June 1978
Postprocessor	31	179	8	---
Totals	7,877	18,671	\$1,496	15 Days

The joint loads on the surface of the finite element model for BM19 are illustrated in Figures 47 to 56. The maximum number of active columns encountered during decomposition of the stiffness matrix in FORMAT Setup 1 was again 275. The natural frequencies of free vibration for the first 30 modes extracted in the FORMAT Setup 2 run ranged from 702 to 7,672 Hz. These frequencies were lower than those calculated for Test BM14. This had been expected due to the decreased stiffness of inter-layer materials at the BM19 elevated temperatures. The incremental Solution was performed at 30 time increments and for 30 modes as for Test BM14.

Two Postprocessor runs were made for BM19, the first being for the same data printed for Test BM14 and the second being for the deflections along a longitudinal section through the test article including the metal support structure. The second also contained a listing of strain and equivalent stress data for all cell elements in the windshield center beam. This data is discussed in detail in the next section.

4. TESTS BM006 and BM004

Sections I.3 and IV.1 of this report state that IMPACT simulations were planned for five birdstrike tests: BM004, BM006, BM14, BM18, and BM19. Section IV.5 explains circumstances leading to a decision not to simulate BM18. Having run BM14 and BM19 then, only BM004 and BM006 remained to be analyzed. These latter two tests differed only in bird impact parameters and very slightly at that. Since the film records of Test BM006 were better, IMPACT analyses of that test were attempted first. The computer resources which were required are listed in Table 7.

As it turned out, IMPACT simulations of both tests were ultimately unsuccessful. In light of this fact, the discussion will be limited to the cause of the failures and the attempts made to overcome the problem.

The first run for Test BM006 was the Loads Generator module. This job ran normally.

TABLE 7
COMPUTER RESOURCES REQUIRED FOR IMPACT ANALYSIS OF TEST BM006

<u>IMPACT Module</u>	<u>CP Seconds</u>	<u>I/O Seconds</u>	<u>Cost</u>	<u>Date</u>
Loads Generator	18	22	\$ 2	23 May 1978
Initial Generator	485	1,057	70	25 May 1978
FORMAT Setup 1	849	1,492	154	31 May 1978
FORMAT Setup 2	71	499	26	31 May 1978
FORMAT Setup 3	70	555	28	31 May 1978
FORMAT Setup 1	907	1,441	153	3 June 1978
FORMAT Setup 2	72	502	26	3 June 1978
FORMAT Setup 3	69	493	26	3 June 1978
Initial Generator	486	1,059	73	6 June 1978
FORMAT Setup 1	907	1,371	150	10 June 1978
FORMAT Setup 2	78	545	28	10 June 1978
FORMAT Setup 3	<u>69</u>	<u>590</u>	<u>29</u>	<u>10 June 1978</u>
Totals	4,081	9,626	\$ 765	18 Days

The second IMPACT module executed for BM006 was the Initial Generator. This job ran normally, too.

Next, a string of three dependent jobs was run to execute FORMAT Setup 1, Setup 2, and Setup 3 in a series. The first job terminated abnormally causing the second and third jobs to do the same.

The reason for FORMAT Setup 1 failure was determined to be an insufficient length having been assigned to an array named NWORK within the computer program. In setting up FORMAT jobs, the user must make two estimates of space on the computer required to run the job. The first is the number of words of

central memory required for the computer to execute the job; the second is the length or number of words in the array named NWORK. This array is used within FORMAT during decomposition of the structural stiffness matrix. For the first sequence of FORMAT runs, 275,000 octal words of central memory had been requested on the job card and NWORK had been sized to 58,000 words. Studying the IMPACT user's manual (Reference 6) revealed that NWORK could have been sized up to 74,000 words for the same central memory space.

The first failure then was attributed to inadequate space in NWORK, and the second string of FORMAT jobs was submitted with NWORK sized to 74,000 words. But again the FORMAT Setup 1 job failed precipitating failures in the second and third jobs.

At this point, some time was devoted to comparison between the finite element models used for Test BM14 and Test BM006. In terms of unconstrained degrees of freedom, the two models seemed very similar having 4,230 and 4,450, respectively. But the BM14 case had executed with room to spare at 200,000 octal words central memory and NWORK sized to only 40,000 words. The maximum number of active columns during stiffness matrix decomposition had been only 275 for BM14 but was 383 for BM006 at the point of failure. These disparities were attributed to the basic differences in geometry between the two models. The BM14 structure was simply-curved in one area and flat elsewhere, quite regular geometrically. The BM006 structure in contrast included many areas of compound curvature and was quite irregular in shape. These differences resulted in a much higher level of coupling among degrees of freedom in the BM006 model. This level of coupling determines the number of active columns during stiffness matrix decomposition, hence, the much greater number for BM006

(6) G. R. Eide, Aircraft Windshield Bird Impact Math Model - Part 2 - User's Manual, Air Force Flight Dynamics Laboratory, Wright-Patterson Air Force Base, Ohio 45433, AFFDL-TR-77-99, Part 2, December 1977.

than for BM14. The critical area in the BM006 model was the cross section of the model containing the left side of the wind-shield centerbeam; this section contained 86 joints.

The point at which the FORMAT Setup 1 job failed for NWORK sized to 58,000 words was at joint 726 (on the left face of the centerbeam). Increasing the size of NWORK to 74,000 allowed processing to continue only as far as joint 711 on the same section before failure again occurred. Thirty-Three joints still remained to be processed to complete that pass through the model. Something providing a major reduction in the size of the problem was required before any hope of accomplishing the decomposition was possible.

A query to the developers of IMPACT provided one candidate for solving the BM006 size problem (Reference 33). During execution of the Initial Generator, a parameter referred to as the cell stiffness suppression coefficient is specified by the user. The function of this parameter is to test the magnitudes of elements in the structural stiffness matrix assembled by the Initial Generator. The value of any element in the stiffness matrix having a magnitude less than that of the suppression coefficient is automatically set equal to zero. This procedure provides a stiffness matrix as sparse as possible to enhance the efficiency of subsequent matrix operations like decomposition. Specifying a greater suppression coefficient may result in a smaller number of nonzero elements in the stiffness matrix and as a result reduce the size of the decomposition problem. All analyses up to this point had used a value of 10^{-12} for the suppression coefficient, but the IMPACT developers stated that the coefficient could be increased as much as four orders of magnitude without significantly altering the quality of the solution obtained.

(33) Personal Communication, 5 June 1978, R. C. Morris and G. R. Eide, Douglas Aircraft Company, Cl-253, 3855 Lakewood Boulevard, Long Beach, California 90846.

As a result of this information, the Initial Generator was executed once again for BM006, but this time with the cell stiffness suppression coefficient set to 10^{-8} . This generated a new, hopefully more sparse, structural stiffness matrix. A third sequence of three FORMAT jobs was attempted with the new Initial Generator output, only to fail again. The FORMAT Setup 1 execution was arrested at exactly the same degree of freedom for which the earlier failure had occurred, the 2 degree of freedom for joint 711. Apparently, nothing had been gained by increasing the value of the cell stiffness suppression coefficient.

Since the central memory space requested for the BM006 jobs had been the maximum authorized during normal operation of the CDC CYBER 74 computer on which the analyses were performed, it was not possible to reattempt them as even larger jobs. An alternate approach of modifying the BM006 model to reduce its size was considered briefly but rejected as being too costly in terms of manpower. Subsequently, all plans to simulate Tests BM006 or BM004 with IMPACT were dropped. Conclusions drawn from these BM006 simulation attempts are presented in Section VIII of this report.

5. BOUNDARY CONDITIONS STUDY

Some small auxiliary studies were accomplished before the analysis of IMPACT results was initiated. These studies were intended to determine the effects of some of the assumptions made in the IMPACT analyses. It was hoped that knowledge of the probable effects of assumptions made would help to clarify the interpretation of IMPACT results.

One of the effects which was studied was that of assuming zero bending fixity around the edges of the windshield test specimens. A computer program much smaller than IMPACT was used in this study. It had been developed to perform static analyses of laminated beams having either fixed or pinned ends

and being subjected to concentrated central loads (Reference 31). This code could accommodate up to nine layers in the laminate. It solved in closed form according to small displacement theory for the following variables: horizontal and vertical displacements of the structural plies; axial and shear forces in the structural plies; the slope, rate of change of slope, and rate of change of rate of change of slope of the structural plies; and the shear flow in the interlayers.

The code was modified slightly for these studies. Since the output of IMPACT analyses had included strain data, the small code was modified to calculate and print out the normal strains due to bending and axial forces in the structural plies. The relationship added to the code is shown in Equation (18) (Reference 32).

$$\epsilon = \frac{H}{EA} \pm \frac{MXJ}{E} \left(\frac{12}{BB T^3} \right) \left(\frac{T}{2} \right) \quad (18)$$

ϵ - normal strain at top and bottom edges of ply cross section.

H - axial force in ply.

E - Young's modulus for material in ply.

A - cross sectional area of ply.

MXJ - bending moment in ply

BB - width of ply.

T - thickness of ply.

Values of ϵ at the top and bottom edges of all structural plies were printed out by the modified program.

Two cases were analyzed with the modified code. The first was a laminated beam with pinned ends having the same cross

(31) P. H. Denke and J. B. Hoffman, The Determination of Deflection and Stress Distribution for a Laminated Transparent Beam, Air Force Flight Dynamics Laboratory, Wright-Patterson Air Force Base, Ohio 45433, AFFDL-TR-76-114, November 1976.

(32) G. Murphy, Advanced Mechanics of Materials, McGraw-Hill, 1946.

section as the windshield panel in Test BM14. The beam analyzed was 36 in long (same as the BM14 panel dimension), 2 in wide, and was subjected to a 1,000 lb central load as shown in Figure 58. This value of load was chosen because it yielded levels of strain in the structural plies which were approximately equal to the highest levels calculated in the IMPACT analysis of Test BM14. Normal strains were computed at the top and bottom surfaces of all four glass plies in the beam. These strains were printed out for six cross sections of the beam taken 3, 6, 9, 12, 15, and 18 inches from the point of load application. The results obtained are discussed in the next section of this report.

The second case analyzed with the modified beam code was the same as the first but for both ends of the beam being fixed as shown in Figure 59. The idea in analyzing this case was to determine an upper bound for the effect of bending stiffness at the beam boundaries upon the strains. The real BM14 structure represented a boundary condition somewhere between these two extremes. Again, values of strain were computed at the top and bottom surfaces of all four glass plies and at the same six cross sections of the beam. Results obtained are discussed in the following section.

6. INTERLAYER PROPERTIES STUDY

Another of the effects studied with the modified beam code was that of varying the mechanical properties of interlayer materials used in the beam. The effects of interlayer properties upon beam strains and deflections was of interest because the only significant difference between Tests BM14 and BM19 was in the interlayer properties. The interlayer was five times less stiff for BM19 due to the elevated temperature of the test article.

Since a case had already been analyzed for a pinned-pinned beam with mechanical properties of all materials corresponding to ambient temperature, another was run for the same case except

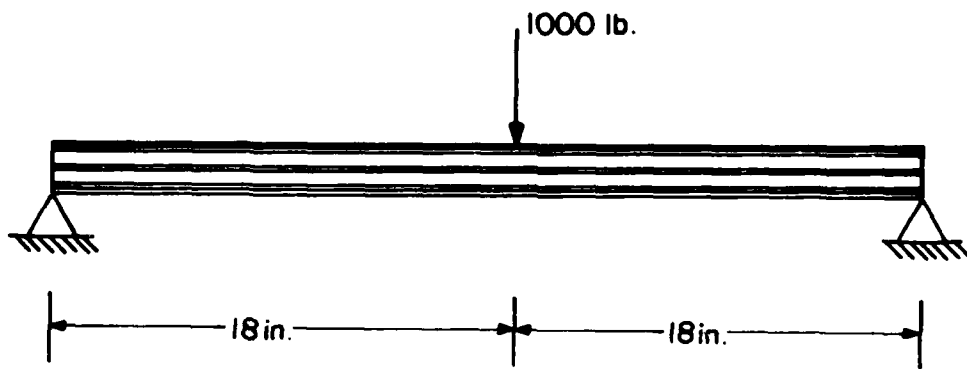


Figure 58. Static Analysis of Pinned-Pinned Laminated Beam.

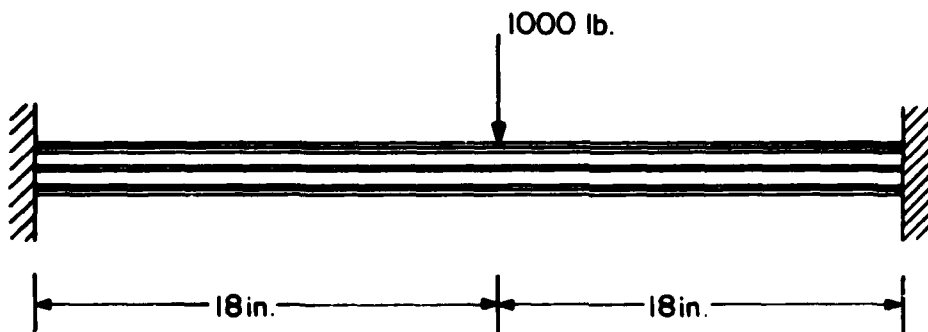


Figure 59. Static Analysis of Fixed-Fixed Laminated Beam.

with the high temperature interlayer properties used in the BM19 model. Values of strain were computed as for the two earlier cases.

The next section reviews and discusses all data calculated in the IMPACT and static beam analyses, and the experimental data available for those cases simulated. It further considers the levels of correlation obtained between test and computed results and studies the factors to which the correlation obtained may be attributed.

SECTION VII

RESULTS

1. ACCURACY OF IMPACT RESULTS

This section begins with a discussion of the experimental data reported for Test BM14. Twenty channels of strain gage data were acquired in the target corner of the test article. Figure 60 illustrates the locations of the strain gages used. Gages 3H, 3V, 4H, 4V, 5H, 5V, 6H, 6V, 7H, 7V, 8H, and 8V were mounted on the outer soda lime glass ply. The remaining eight gages were mounted on the inner soda lime glass ply. The orientation of each gage is also shown in Figure 60. Figures 61 through 80 are copies of the recorded strain data from Reference 10 for all 20 gages. Uncertainty in the data is reported in Reference 10 to be ± 10 percent. Both soda lime glass plies were reported to have failed during the test. Neither chemically strengthened Herculite face ply failed, however. High-speed films of the test were reviewed to determine the period of time during which the main ply failures occurred. The average period obtained from three different camera films was from 0.0012 to 0.0016 sec. Dicing of the soda lime glass plies was first visible at 0.0012 sec in the immediate vicinity of the bird impact site. By 0.0016 sec the dicing had propagated across the panel to the corner opposite the bird impact and the entire panel had become translucent. The period of failure has been indicated on Figures 61 through 80.

All 20 channels of strain data provide a consistent picture of the BM14 windshield panel response. In the V direction (Figure 60), all gages on outer surfaces registered compression up to failure time and all inner gages registered tension. In the H direction, all outer gages showed compression at failure

(10) E. J. Sanders, Results of Bird Impact Testing of Prototype B-1 Windshields and Supporting Structure Design, AEDC-DR-76-100, Arnold Engineering Development Center, Arnold Air Force Station, Tennessee 37389.

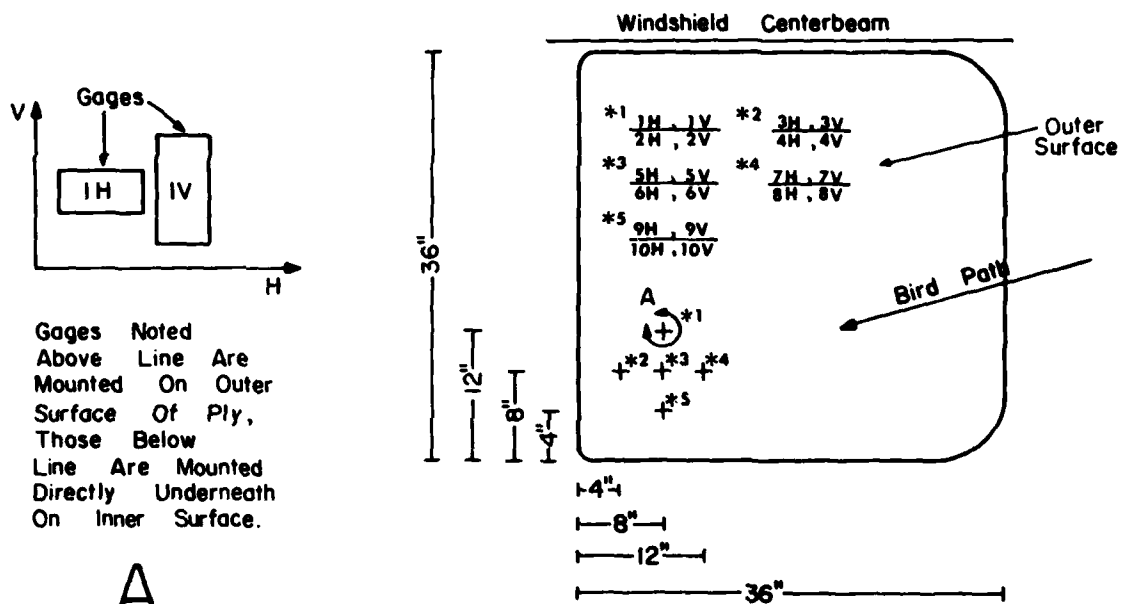


Figure 60. Strain Gage Locations for Tests BM14 and BM19.

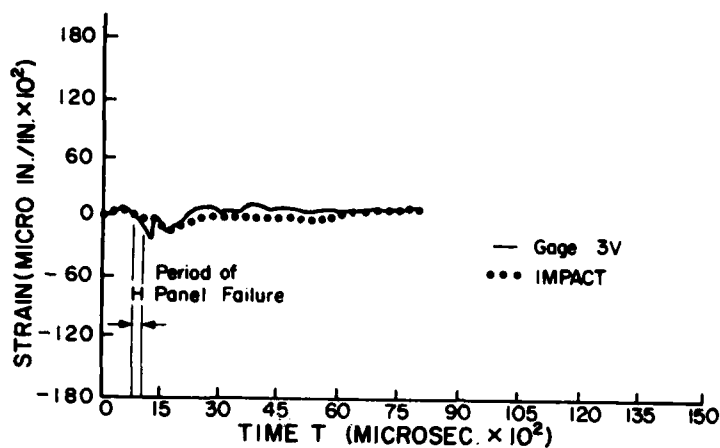


Figure 61. X Strain for the Outer Face of Cell Number 66.

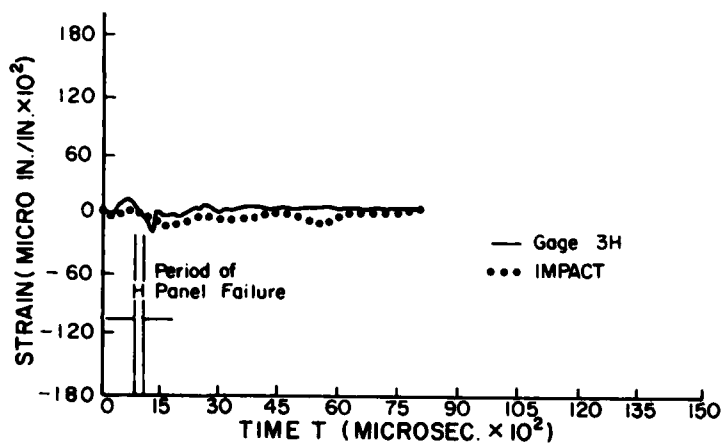


Figure 62. Y Strain for the Outer Face of Cell Number 66.

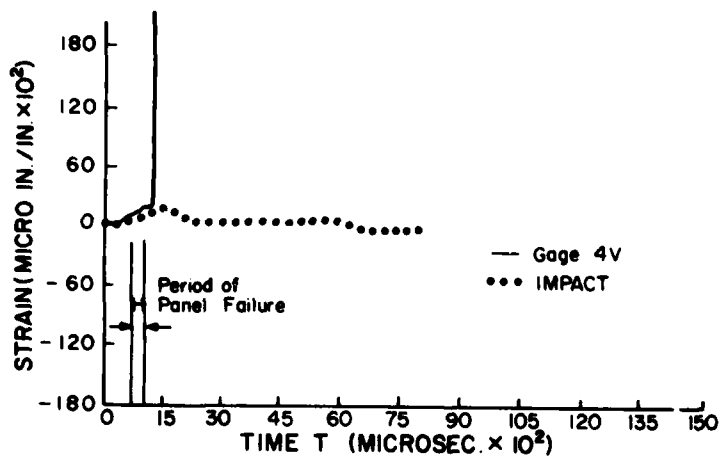


Figure 63. X Strain for the Inner Face of Cell Number 66.

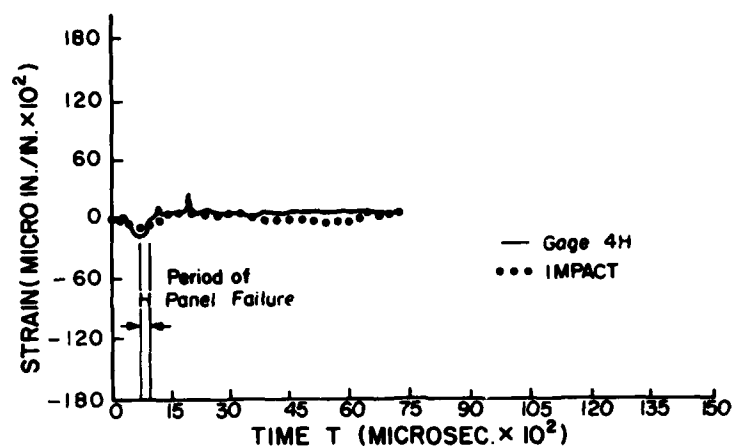


Figure 64. Y Strain for the Inner Face of Cell Number 66.

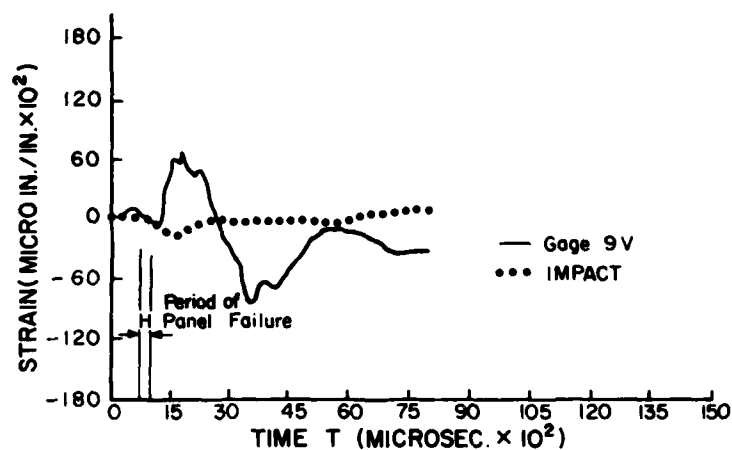


Figure 65. X Strain for the Outer Face of Cell Number 110.

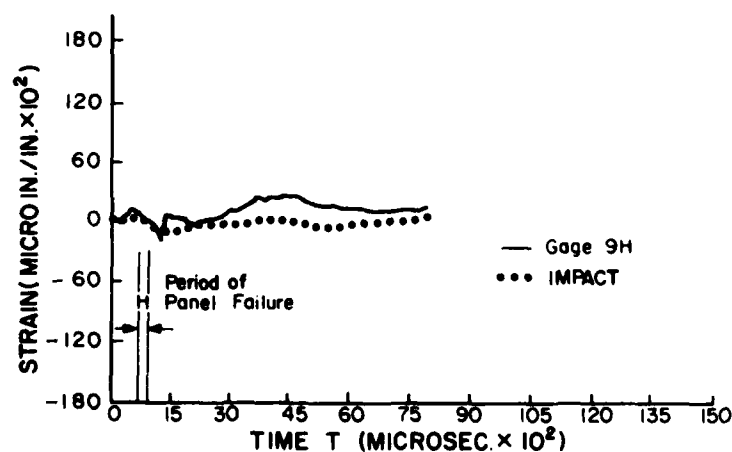


Figure 66. Y Strain for the Outer Face of Cell Number 110.

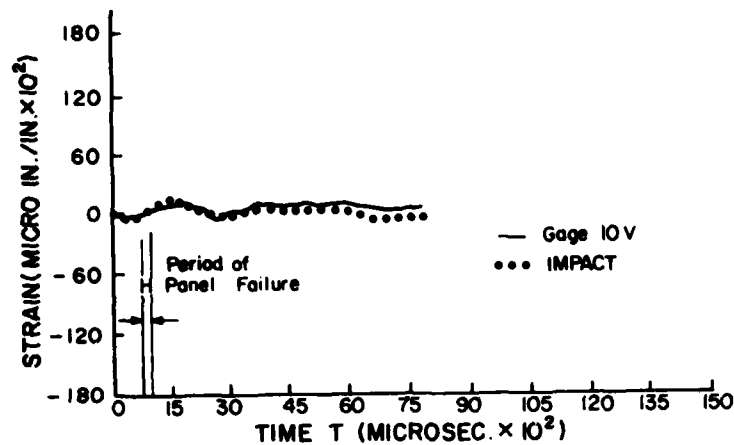


Figure 67. X Strain for the Inner Face of Cell Number 110.

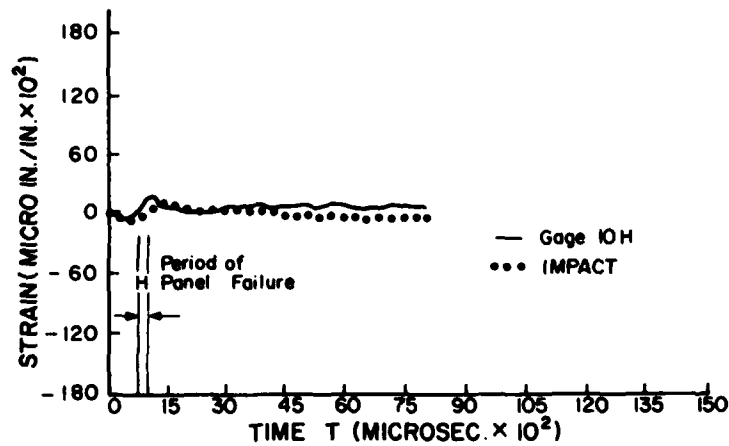


Figure 68. Y Strain for the Inner Face of Cell Number 110.

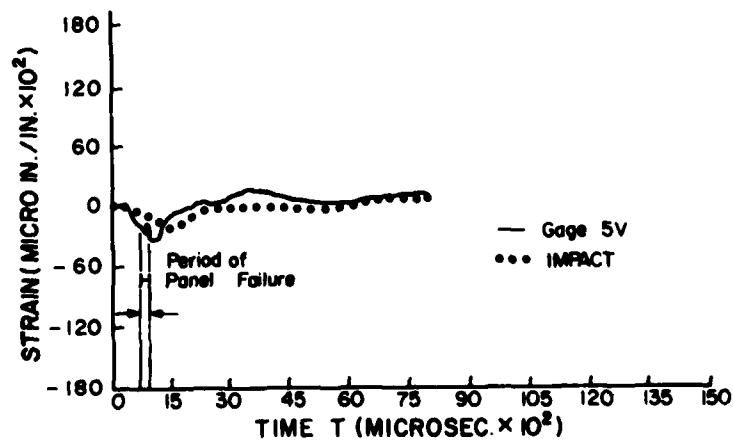


Figure 69. X Strain for the Outer Face of Cell Number 115.

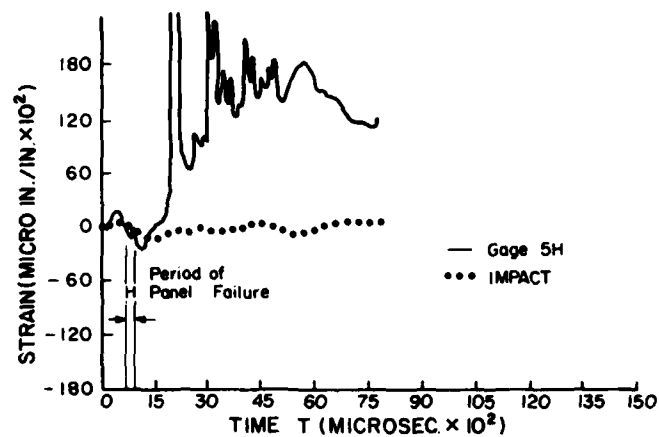


Figure 70. Y Strain for the Outer Face of Cell Number 115.

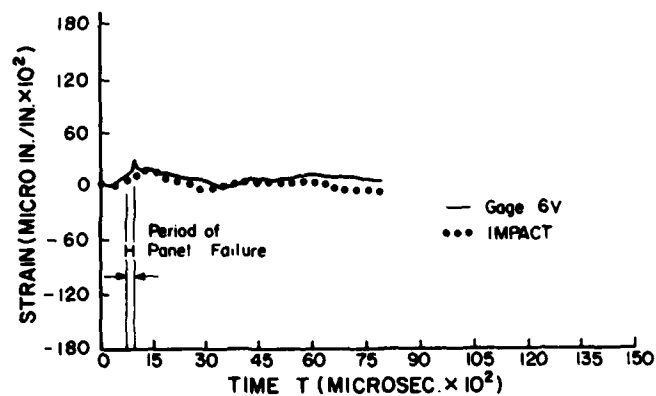


Figure 71. X Strain for the Inner Face of Cell Number 115.

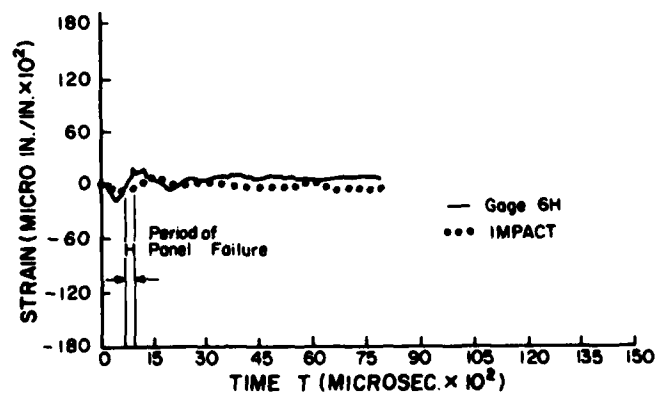


Figure 72. Y Strain for the Inner Face of Cell Number 115.

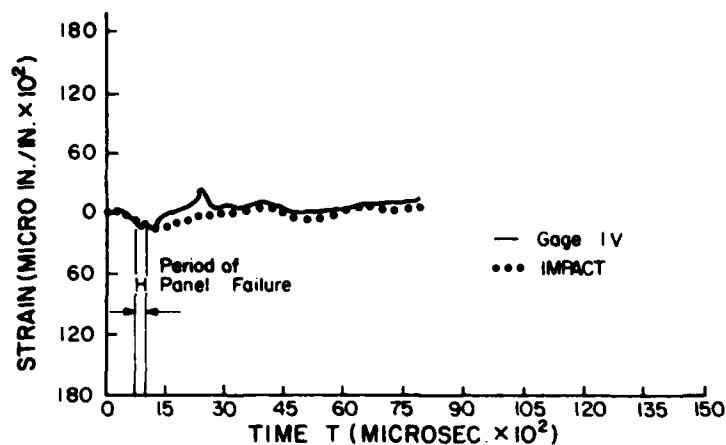


Figure 73. X Strain for the Outer Face of Cell Number 124.

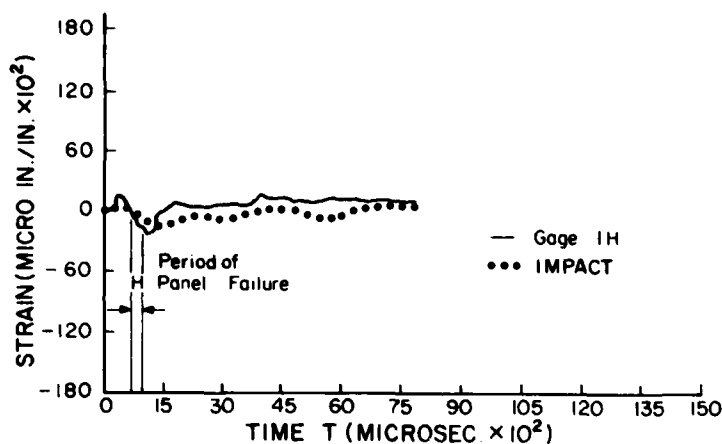


Figure 74. Y Strain for the Outer Face of Cell Number 124.

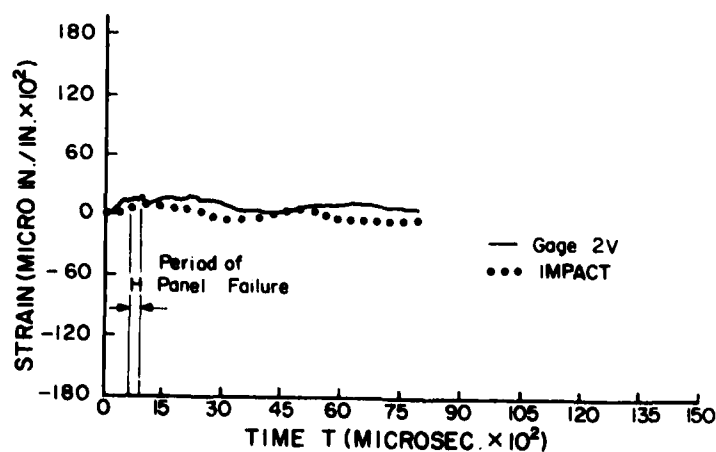


Figure 75. X Strain for the Inner Face of Cell Number 124.

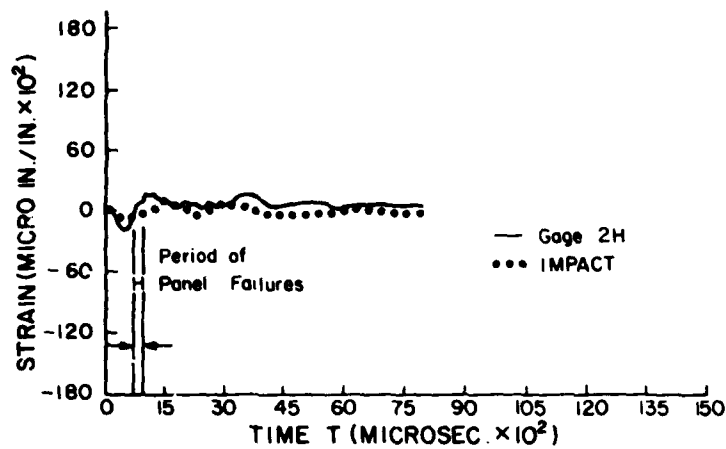


Figure 76. Y Strain for the Inner Face of Cell Number 124.

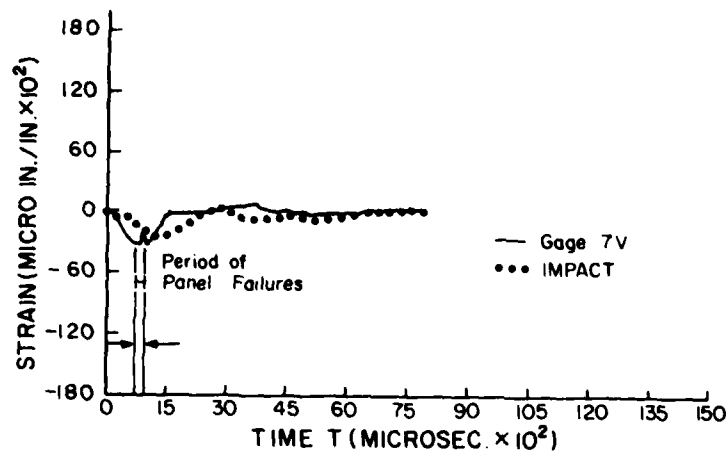


Figure 77. X Strain for the Outer Face of Cell Number 164.

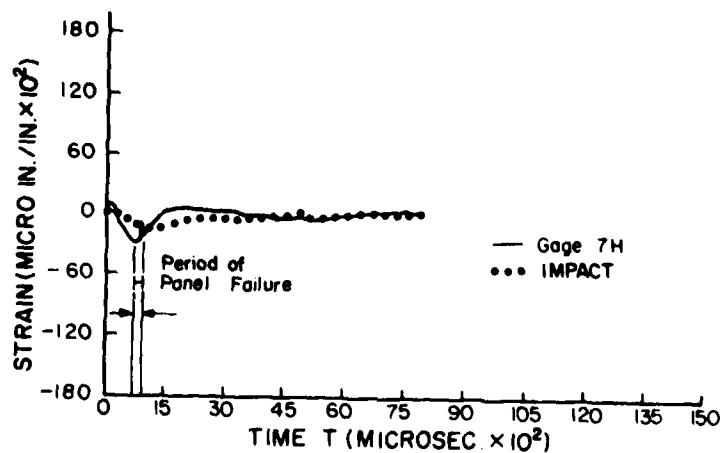


Figure 78. Y Strain for the Outer Face of Cell Number 164.

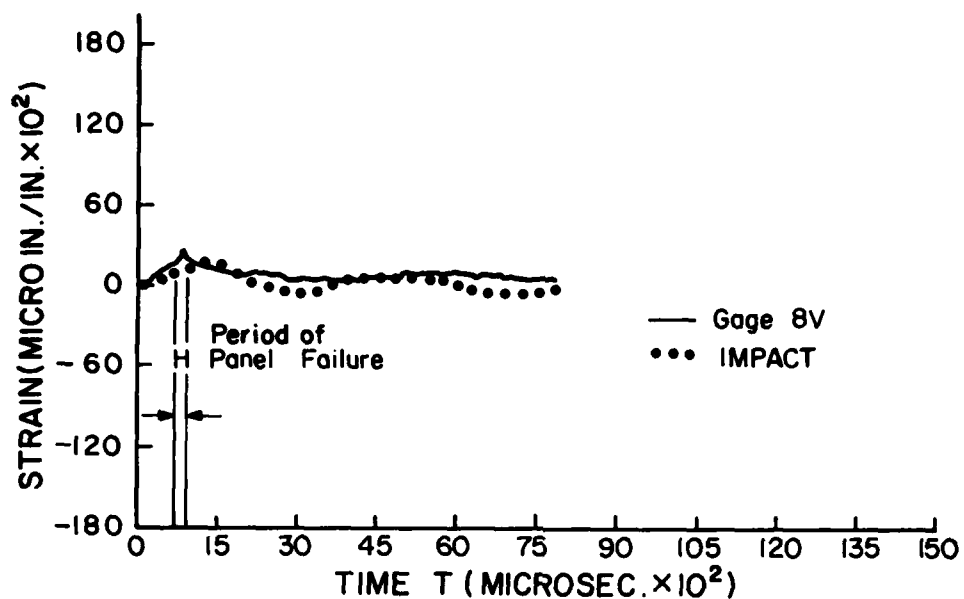


Figure 79. X Strain for the Inner Face of Cell Number 164.

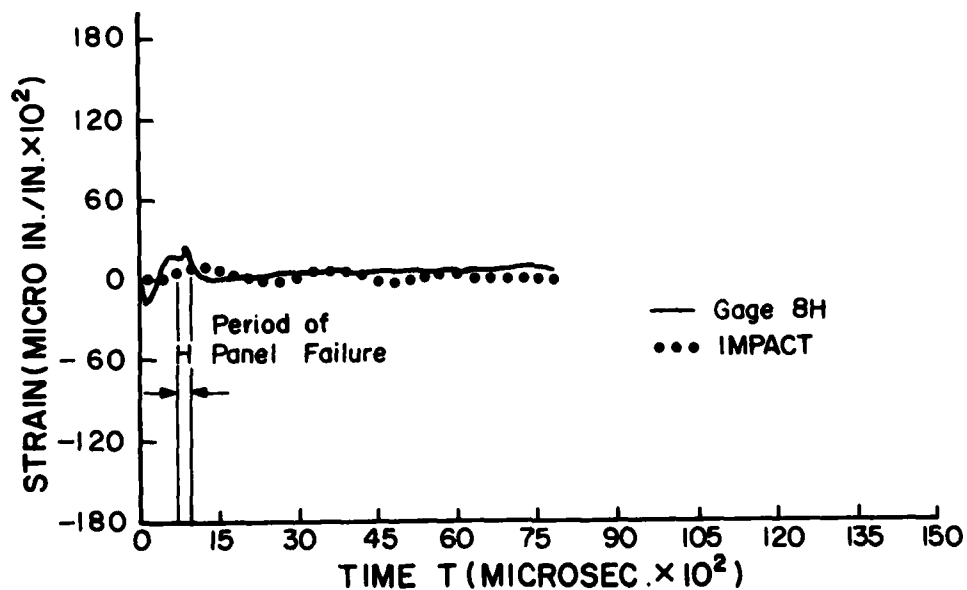


Figure 80. Y Strain for the Inner Face of Cell Number 164.

time and all inner gages showed tension. Initially, however, that is at times nearer zero time, all H gages registered strains of opposite sign. That is, the output of all H gages changed sign at some time between zero time and failure time from compression to tension or vice versa. Times of this sign change varied for different H gages, occurring earliest at locations near the initial bird impact point and later at locations farther away. For example, gages 7H, 5H, and 3H lie along a line in the general direction of bird travel over the surface. Gage output changed sign at -0.0002 sec for gage 7H, 0.0007 sec for gage 5H, and 0.0011 sec for gage 3H. All H gage data taken together can be interpreted as resulting from a bending wave propagating through the panel along the direction of bird travel. Figure 81 illustrates how a strain gage mounted on the outer surface of a transparency would first sense tensile strain as a bending wave generated by a bird impact neared the site. The same gage would later sense compression as the wave passed over the site. Interior gages would first sense compression, then tension. Gages far from the impact point would experience this sign reversal at times later than gages near the impact point. The BM14 data exhibits this same general pattern.

Of the five locations on soda lime glass plies chosen for strain gage installation, all showed tensile strains approaching 2,100 micro in/in, the tensile rupture strain for the soda lime glass. Another feature common to all the strain gage outputs was the fact that, after panel failure, all surviving gages showed some level of tensile strain ranging from 600 to 1,200 micro in/in. Such residual tensile strain would be expected in the surfaces of fragments of tempered glass as a result of the release of compressive strains existing in the surfaces before rupture occurred.

Figure 82 shows some of the locations on the panel at which the IMPACT analyses calculated strains. The locations shown are those closest to the strain gage sites illustrated in Figure 60. The orientation of the X and Y normal strains are also shown

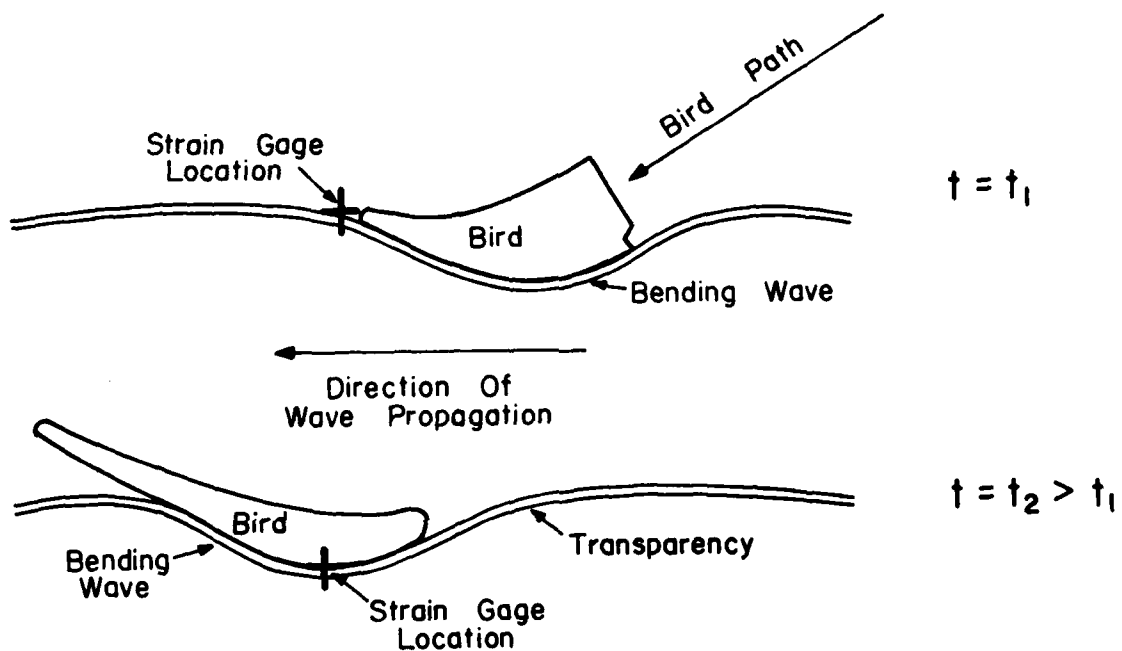


Figure 81. Bending Wave Propagation.

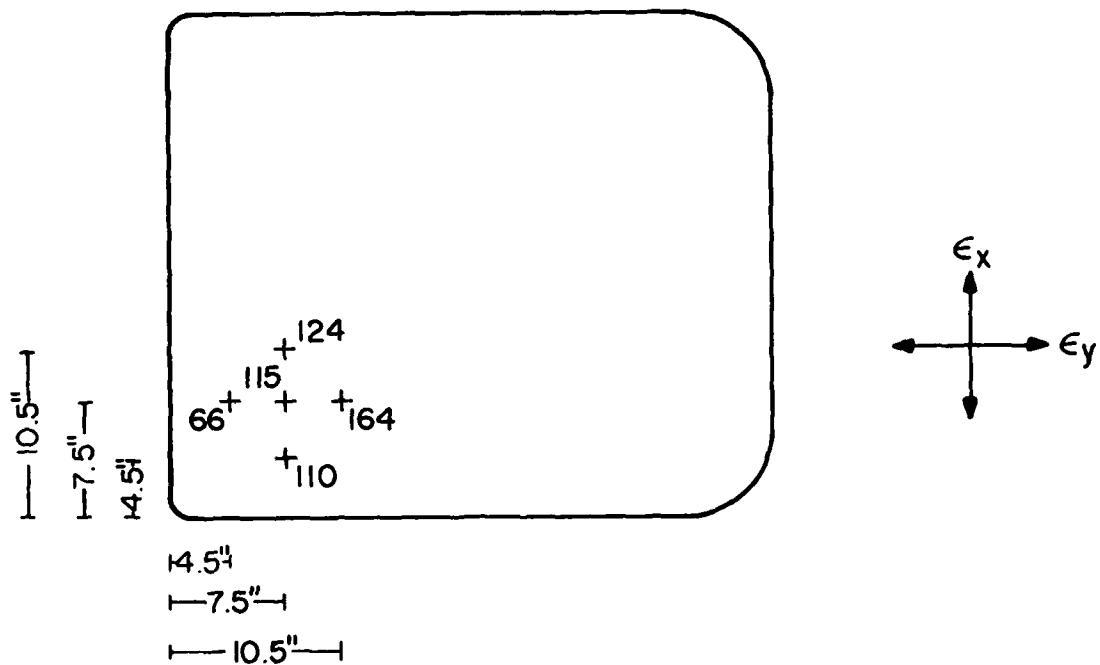


Figure 82. Locations for BM14 and BM19 at which IMPACT Calculated Strains.

in Figure 82 as are the cell element numbers corresponding to each data point. Cell numbers 66, 115, and 164 were part of the outer soda lime glass ply and cells 110 and 124 were part of the inner soda lime glass ply. For a given cell, normal strains were calculated for both inner and outer surfaces. Although the points at which strain data were measured were not identical to those points at which IMPACT calculated strains, the two sets of points were close enough together to permit the correlation between experimental and computed data to be established. Distance between respective pairs of points ranged from 0.72 to 1.56 in. Figures 61 through 80 show in addition to the strain gage data, the strain data computed by IMPACT.

Comparison between the respective pairs of experimental and computed strain data for Test BM14 reveals that the IMPACT results are quite realistic. The general pattern of strain histories calculated by IMPACT is the same as that recorded experimentally. The IMPACT strains in the X direction show compression on outer surfaces and tension on inner surfaces as do the strain gage data for the V direction. The computed strains in the Y direction show the same initial signs and the same sign reversals seen in the H direction strain gage data. The periods of motion in both sets of data agree very well. Comparison between the experimental and IMPACT data cannot be extended beyond the time of panel failure because after that time the BM14 finite element model does not physically represent the test article, the soda lime glass plies being modeled as intact and those in the test panel being completely fractured.

The only shortcoming apparent in the computed strain data is that, with one or two exceptions, the levels of strain predicted are very low compared to those measured. Most of the strains predicted by IMPACT were only half the recorded strains. This disagreement is significant and was the subject of some study to determine the most probable cause.

The assumptions made in the IMPACT analyses which were judged likely to have had major effects on the accuracy of results were broken down into four categories. First were those assumptions made in developing the finite element model of the structure. Second were those involving the mechanical properties of materials used in the structure. Third were those made in modeling the bird impact loads applied to the structure. Last were those assumptions inherent in the theoretical formulation of IMPACT itself.

In the first category, finite element modeling of the structure, the assumption judged most likely to have significantly affected results was that of pinned edges for the windshield panel. The possible effects of assuming pinned edges rather than edges having fixity in bending were considered by studying the results of the Boundary Conditions Study described in Section VI.5 of this report. Figure 83 illustrates static strains calculated at the central cross section of the pinned-pinned beam shown in Figure 58. Figure 84 illustrates static strains at the central cross section of the same beam but for the fixed-fixed case as illustrated in Figure 59. It is interesting to note that the soda lime glass structural plies act almost independently as individual beams in bending. The point of the two figures, however, is that strains in the soda lime glass plies are about 33 percent higher for the case of pinned ends than for the case of fixed ends. These static results were taken to imply that for Test BM14, the assumption of pinned edges of the windshield panel would have resulted in higher than actual strains being predicted by IMPACT, not lower as was the case. This means that modeling the windshield boundary conditions more realistically would have had the effect, if any at all, of lowering calculated strains. Apparently, modeling the windshield attachment as a pinned edge did not cause the calculated strains to be so low.

In the second category, the mechanical properties of materials used in the test article, the data judged to be the

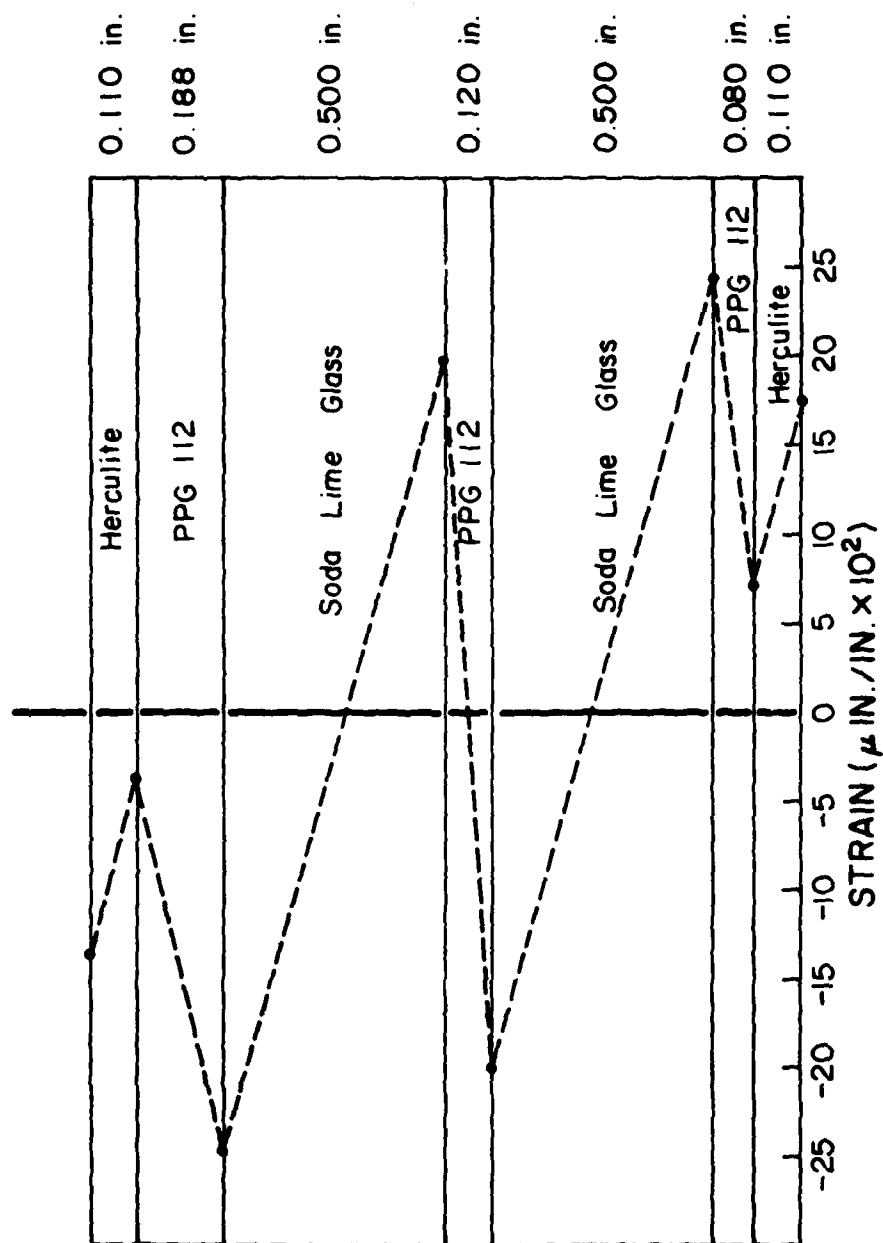


Figure 83. Static Strains at Center Cross Section of Pinned-Pinned Beam.

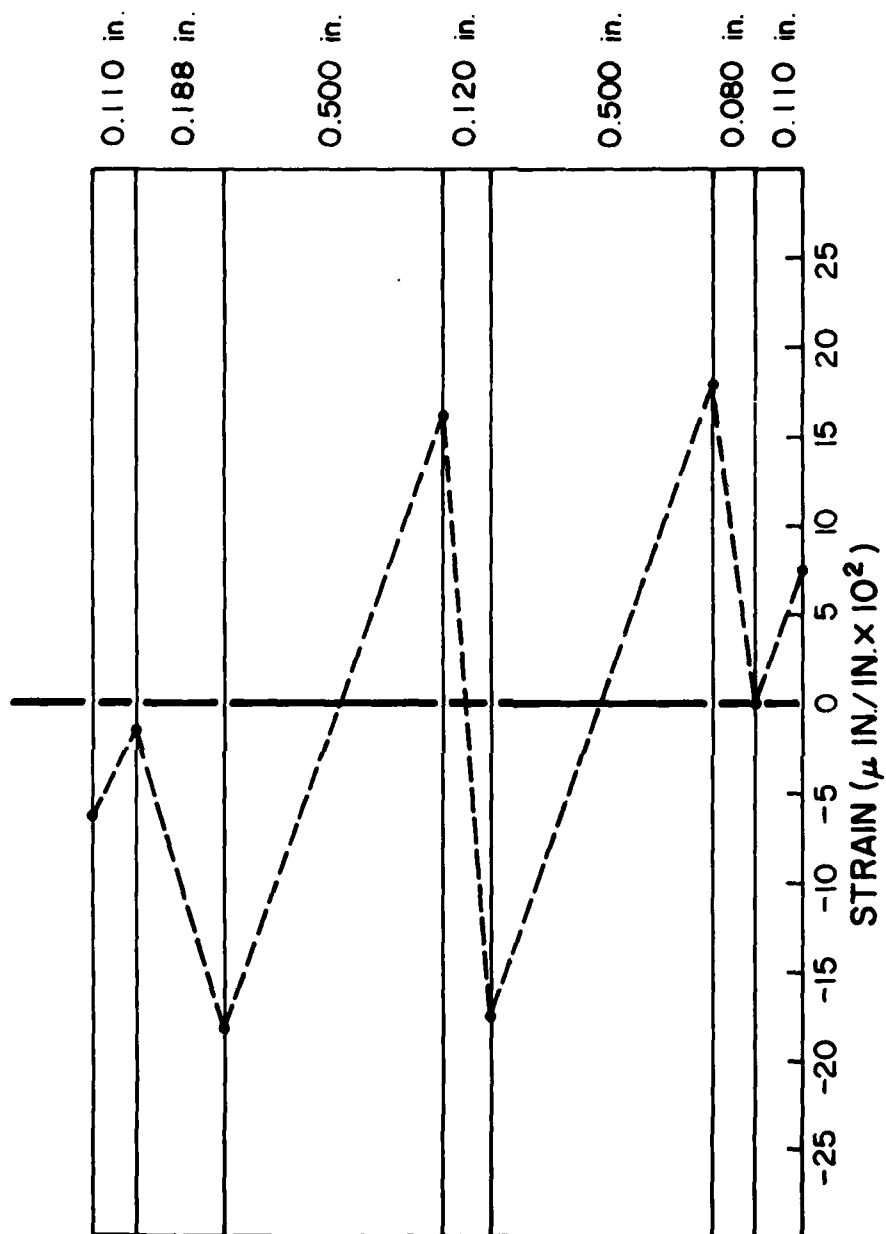


Figure 84. Static Strains at Center Cross Section of Fixed-Fixed Beam.

least well known were the properties of the PPG 112 interlayer material. The only other materials in the target structure were aluminum and titanium alloys and glasses, the mechanical properties of which are known more precisely than those of the PPG 112 interlayer. Sensitivity of strains in the laminated windshield panel to interlayer properties was considered by studying results of the Interlayer Properties Study discussed in Section VI.6 of this report. Figure 85 illustrates static strains at the central cross section of the pinned-pinned beam shown in Figure 58. The interlayer properties used in this beam analysis corresponded to a temperature of 195 deg F as reported in Reference 13. Results of the same analysis but for 75 deg F interlayer properties have already been shown in Figure 83. The effect of the high temperature interlayer properties was to increase levels of strain in the main structural plies of the laminated beam by over 50 percent. The value of Young's modulus used for the high temperature case was five times less than that used for the 75 deg F case. The results illustrated in Figures 83 and 85 were taken to imply that for the BM14 strains calculated by IMPACT to have been of the same magnitude as those measured experimentally, the Young's Modulus of the interlayer would have had to be ten times less than the value actually used. Even though the properties of PPG 112 are not known as precisely as those of other materials used in the model, this level of uncertainty (1,000 percent) is far in excess of the actual level. Therefore, the lack of precise mechanical data for PPG 112 cannot reasonably explain the very low levels of strain calculated by IMPACT.

In the third category of potential error sources, bird impact pressures, the aspect of modeling loads judged to be the most physically unrealistic was the manner in which the spatial distribution of pressures over the surface was determined. The method employed to distribute the net instantaneous bird impact force

(13) F. E. Greene, Testing for Mechanical Properties of Monolithic and Laminated Polycarbonate Materials, Air Force Flight Dynamics Laboratory, Wright-Patterson Air Force Base, Ohio 45433, AFFDL-TR-77-96, October 1977.

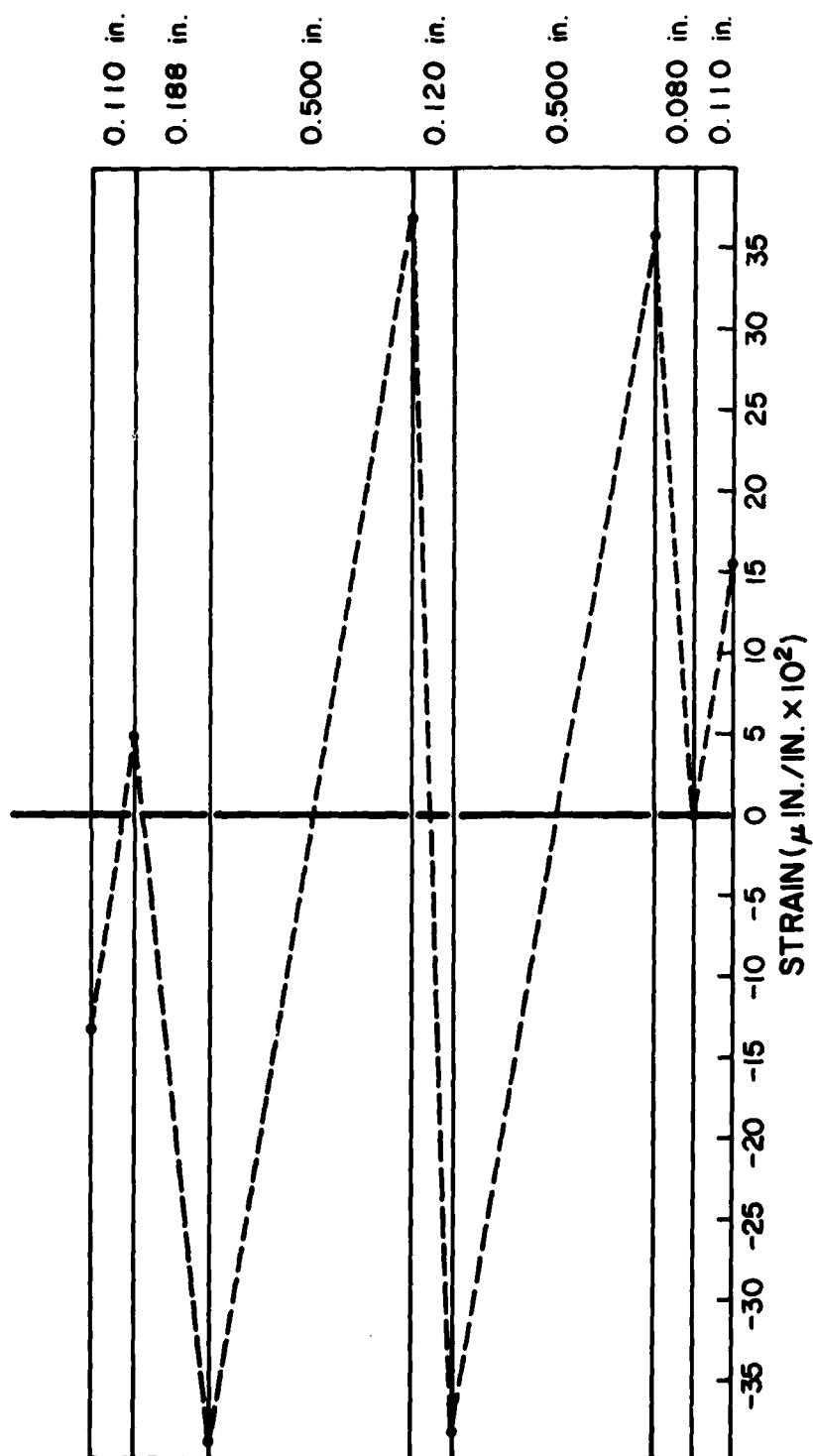


Figure 85. Static Strains at Center Cross Section of Hot Pinned-Pinned Beam.

over a given set of surface nodes affects only the near field response as long as the total impulse remains unchanged. Since the levels of strain calculated by IMPACT are uniformly low throughout the entire area of the bird impact footprint, the method used to distribute forces to surface nodes must have been relatively realistic. Otherwise, the near field response predicted by IMPACT would have differed in a more fundamental manner from that observed during the test. The spatial distribution of bird impact pressure over the surface of the BM14 finite element model, therefore, cannot reasonably explain the low levels of strain predicted by IMPACT. It should be noted here that the total impulse resulting from the individual node forces has been shown to be the component of linear momentum of the bird normal to the windshield surface, or $mv \sin \theta$ (Section V.1). This magnitude has been verified many times over as being physically realistic in References 15, 16, and 18. As a result, the value of the total impulse delivered to the structure in the BM14 IMPACT analyses has not been considered as a possible explanation of the errors in question.

The only category of possible error sources remaining after the above considerations had been made was that of those assumptions inherent in the theoretical formulation of IMPACT itself. One of these assumptions was that no significant geometric nonlinearities existed in the structure of interest. As has already been pointed out in Sections I.2 and VI.1, one goal of this work

(15) J. P. Barber and J. S. Wilbeck, Characterization of Bird Impacts on a Rigid Plate: Part I, Air Force Flight Dynamics Laboratory, Wright-Patterson Air Force Base, Ohio 45433, AFFDL-TR-75-5, January 1975.

(16) R. L. Peterson and J. P. Barber, Bird Impact Forces in Aircraft Windshield Designs, Air Force Flight Dynamics Laboratory, Wright-Patterson Air Force Base, Ohio 45433, AFFDL-TR-75-150, March 1976.

(18) J. P. Barber, J. S. Wilbeck, and H. R. Taylor, Bird Impact Forces and Pressures on Rigid and Compliant Targets, Air Force Flight Dynamics Laboratory, Wright-Patterson Air Force Base, Ohio 45433, AFFDL-TR-77-60, May 1978.

effort was to test the validity of this assumption for the B-1 windshield class of structures subject to bird impact loading.

The general characteristics of the geometric nonlinearity, if any, which might be expected to exist in the B-1 windshield panels are illustrated in Figures 86 and 87. The shallow spherical cap problem shown in these figures is often cited in the literature as an example of strong geometric nonlinearity. Both it and the B-1 windshield panels are thin, shallow, curved structures. Under apex loading the spherical cap exhibits first a softening behavior and then membrane stiffening.

Figure 88 shows that the panel height, h , of the BM14 windshield was 2.68 in. Since maximum linear deflection calculated by IMPACT was 0.31-in, the corresponding deflection ratio was 0.12. Figure 87 shows that for a linear deflection ratio of 0.12 the actual deflection of the spherical cap is twice that calculated from linear analysis. This result was taken to imply that if the effects of geometric nonlinearity are as strong for the B-1 windshield panels as they are for the shallow spherical cap, then it is possible that these effects account entirely for the fact that actual BM14 strains exceeded IMPACT strains by 100 percent. In other words, it seems reasonable that the assumption of geometric linearity inherent in IMPACT was entirely responsible for calculated strains being only half the observed strains. Of the potential sources of error considered, only this one can feasibly explain the results obtained.

Summarizing the strain data correlation obtained for Test BM14, it can be stated that the general characteristics of the panel response predicted by IMPACT are accurate. However, the magnitudes of strains measured during the test before panel failure were much greater than those predicted by IMPACT. The most probable cause, among those considered, of this disparity was the failure of the IMPACT analysis to account for significant effects of geometric nonlinearity present in the BM14 windshield test article.

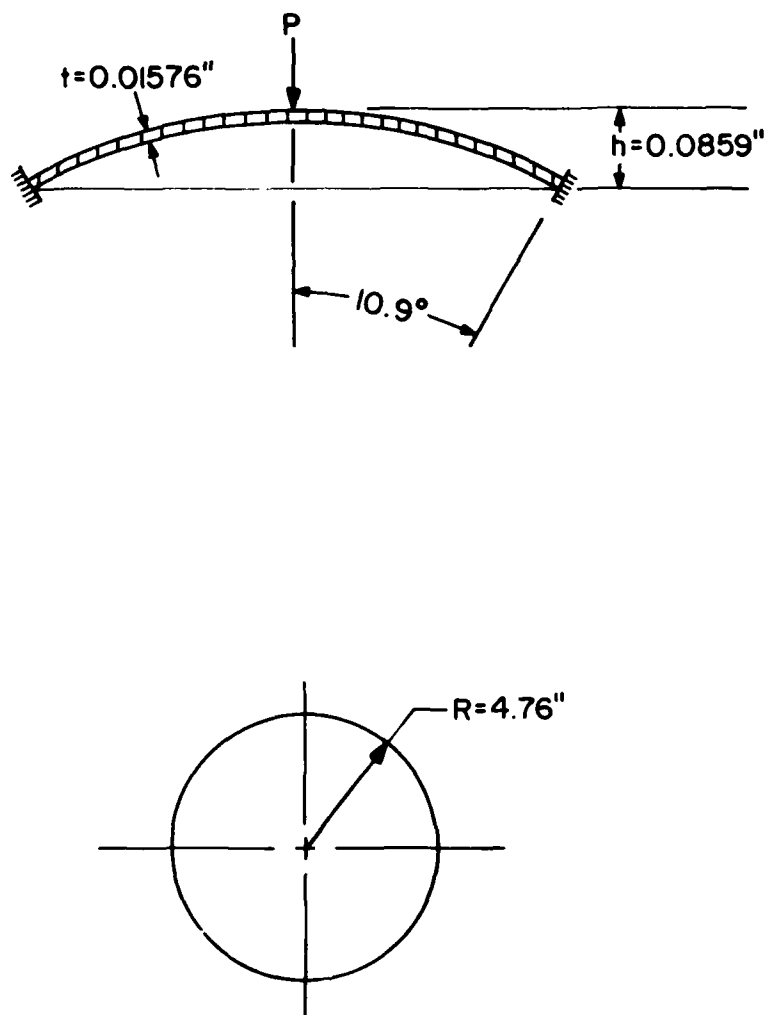


Figure 86. Shallow Spherical Cap Under Apex Loading.

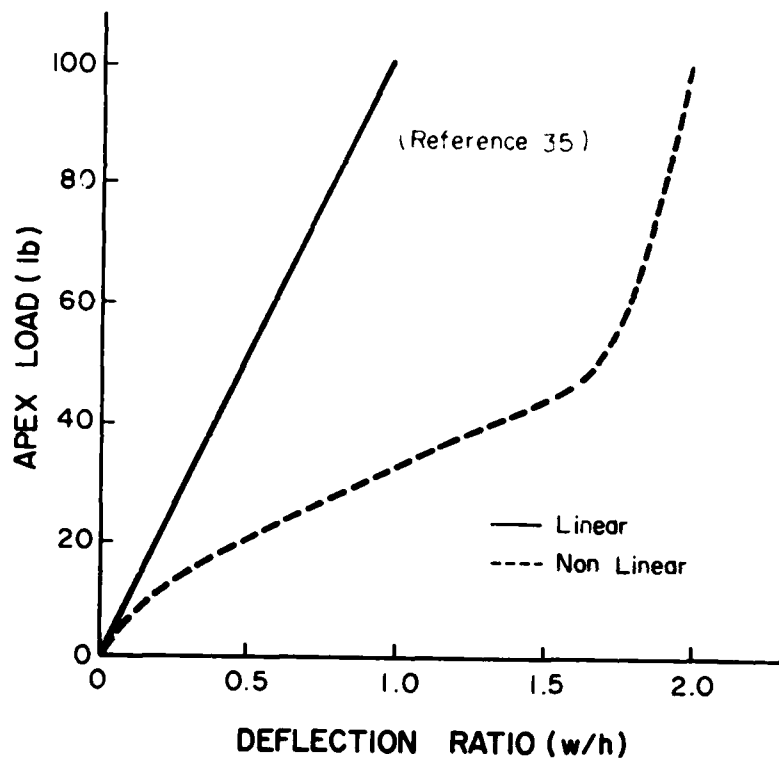


Figure 87. Linear and Nonlinear Analysis Results for Shallow Cap.

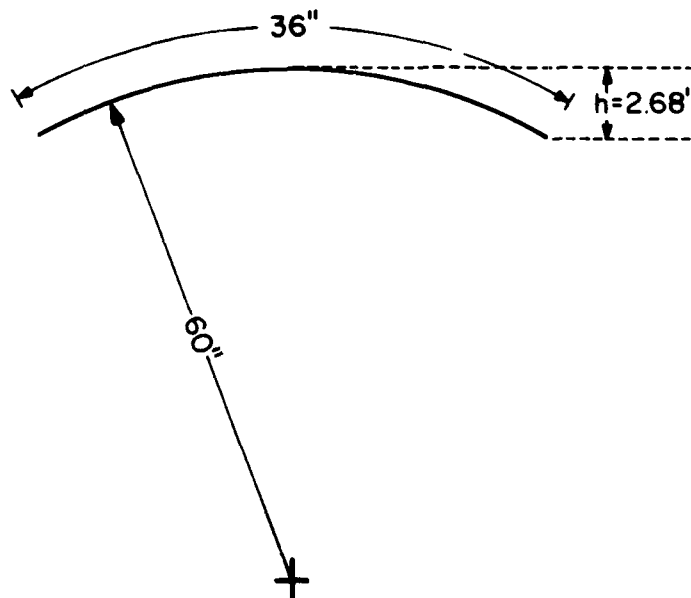


Figure 88. Cross Section of BM14 Windshield Panel.

Even though no experimental deflection data is available for BM14, it is interesting to note the deflections calculated by IMPACT. Figure 89 shows the deflection in a direction nearly normal to the surface of a node located within the bird impact footprint. The maximum inward deflection at the node during the impact event was 0.31 in, and during rebound was 0.21 in. The forced half period of motion is about 5,000 micro sec, the corresponding frequency is 200 Hz. Figure 90 shows the deflected shape of a longitudinal cross section of the BM14 structure taken through the node considered in Figure 89. Deflections are shown at six different times during the response; node numbers are indicated on the figure. At early times the deformation of the panel can be seen to be primarily local while at later times it has propagated throughout the panel.

Some correlation between experimental and computed results in terms of material failure is also possible. The material failure criterion adopted by the developers of IMPACT was the Prandtl-Reuss equivalent stress (Reference 5) which is twice the octahedral shearing stress (Reference 36). For a given finite element, when the equivalent stress exceeds the tensile rupture stress for the material involved, the element is considered to have failed. This consideration is entirely external to IMPACT, however; all elements are treated the same during IMPACT incremental solution regardless of whether or not their levels of equivalent stress are above or below the respective rupture stress.

IMPACT equivalent stresses were plotted as functions of time for 100 cell elements in the target corner of the BM14 windshield panel, 25 cells in each of the four glass plies.

(5) P. H. Denke, Aircraft Windshield Bird Impact Math Model, Part 1, Theory and Application, Air Force Flight Dynamics Laboratory, Wright-Patterson Air Force Base, Ohio 45433, AFFDL-TR-77-99, Part 1, December 1977.

(36) E. F. Bruhn, Analysis and Design of Flight Vehicle Structures, Tri-State Offset, 1965.

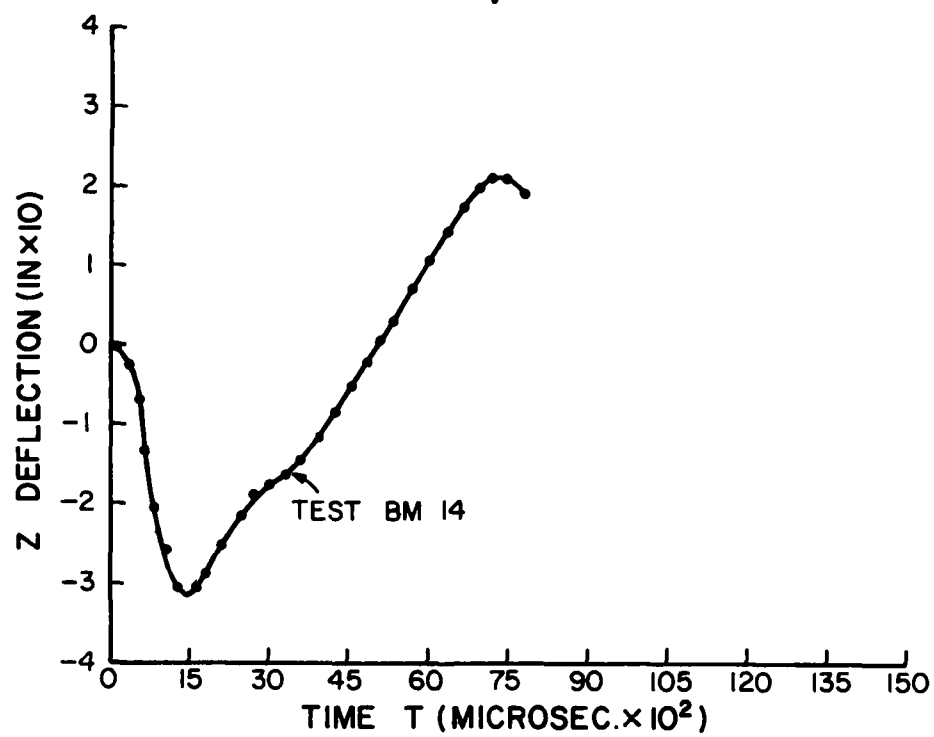


Figure 89. Z Deflection for Node 447.

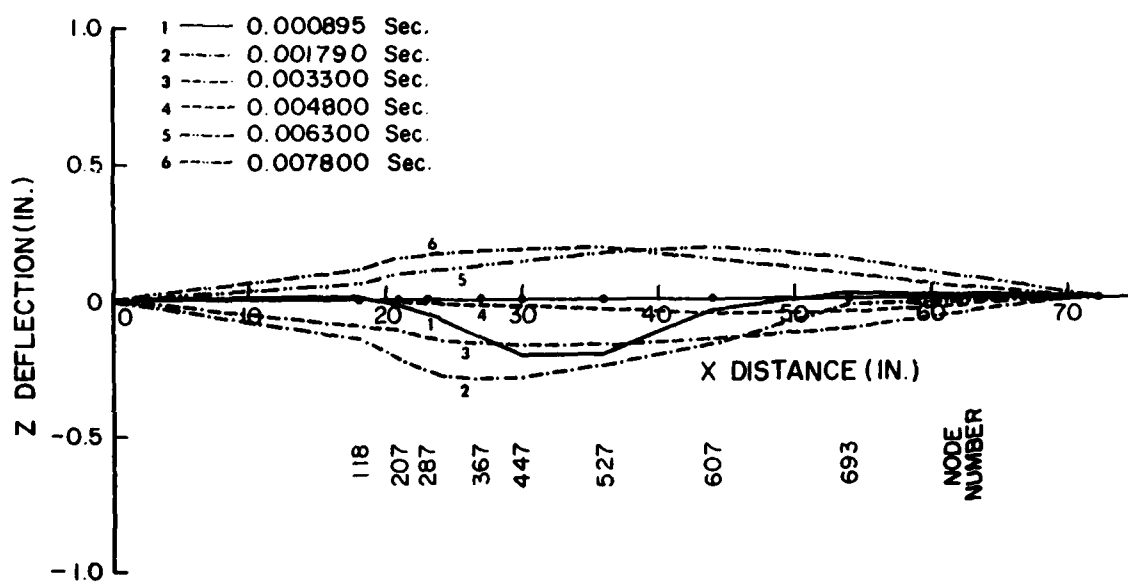


Figure 90. Z Deflection of Nodes Along Longitudinal Section for Test BM14.

Figure 91 illustrates those cells for which equivalent stress exceeded the rupture stress for the respective material. Small crosses in the center of each cell indicate the locations at which IMPACT calculated equivalent stress. The figure shows that IMPACT predicted two areas of main glass ply failure, one in the area of the bird impact footprint and one near the side post where only the inner soda lime glass ply failed. According to the IMPACT results, neither chemically strengthened Herculite glass face ply failed anywhere on the BM14 panel. In general, computed equivalent stresses were found to increase for the more inward levels. The Herculite cell nearest failure was that at the aft right corner of the inner face ply where IMPACT calculated a level of equivalent stress equal to 95 percent of the rupture stress. The equivalent stresses predicted everywhere in the outer Herculite face ply were very low as would be expected for the BM14 panel design which allows the outer face ply to float on top of the remainder of the laminate.

These IMPACT results translate, of course, into complete fracture of both soda lime glass plies since the thermally tempered material is incapable of failing in only a local manner, and into both Herculite face plies remaining intact. This is, in fact, the same result observed during the test and as such lends more credence to the IMPACT results. The area of heaviest, or finest, dicing of the soda lime glass plies observed after the test is also shown on Figure 91 and corresponds roughly in size to the area of initial failure predicted by IMPACT.

Turning now to the discussion of the BM19 analysis, Figures 92 through 104 show the strain gage data acquired for that test. Figure 60 may be used to determine the locations of the strain gages used because they were the same as for Test BM14. All four glass plies, both Herculite face plies and both soda lime glass structural plies, were reported to have failed during this test. This result might have been anticipated during the test program due to the decreased shear strength of the PPG 112 interlayer material at elevated temperatures.

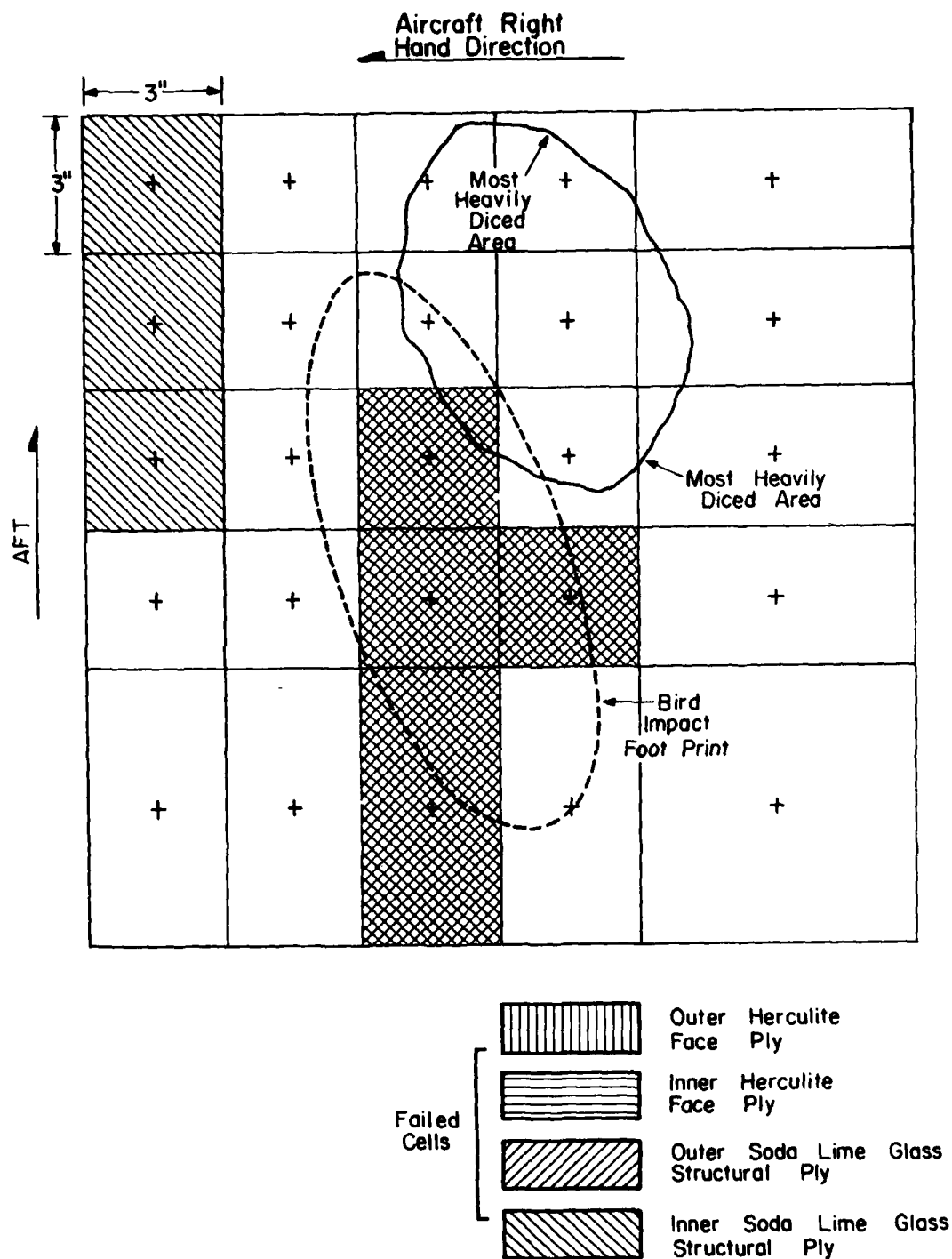


Figure 91. BM14 Structural Failure Predicted by IMPACT.

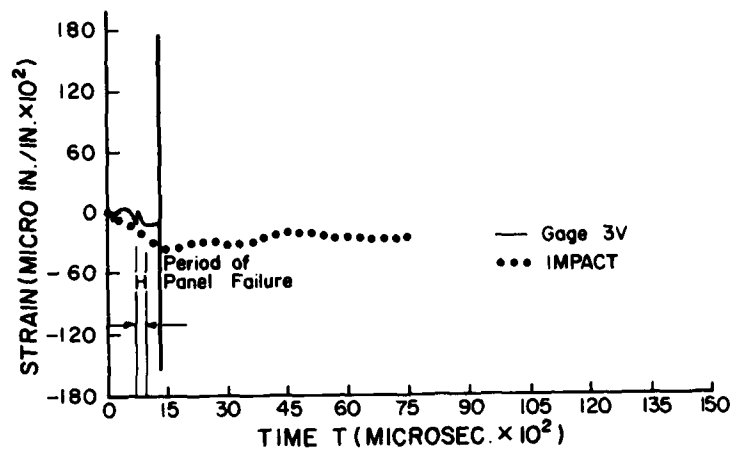


Figure 92. X Strain for the Outer Face of Cell Number 66.

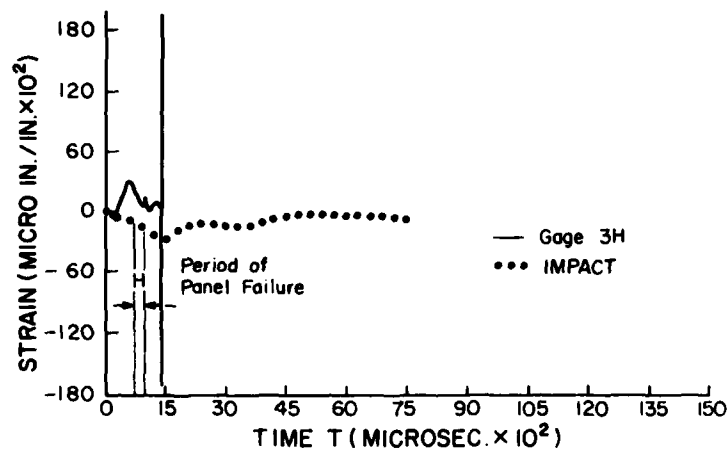


Figure 93. Y Strain for the Outer Face of Cell Number 66.

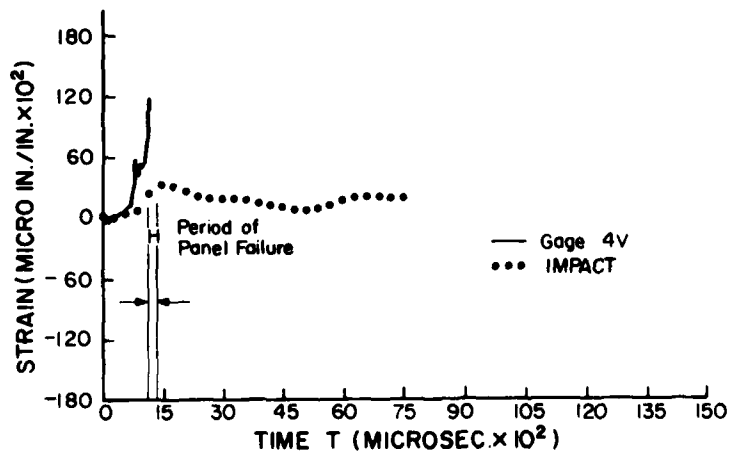


Figure 94. X Strain for the Inner Face of Cell Number 66.

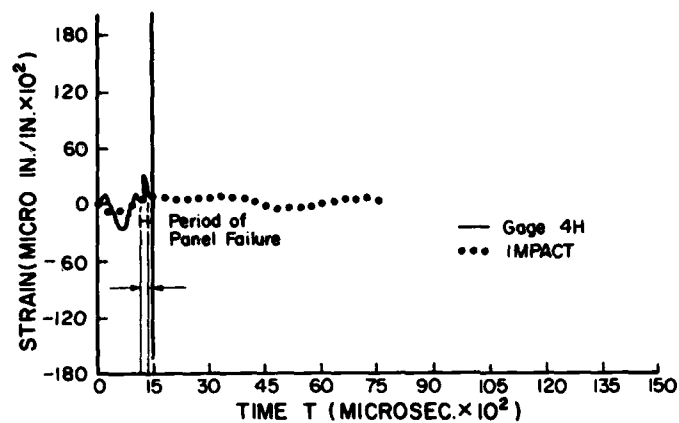


Figure 95. Y Strain for the Inner Face of Cell Number 66.

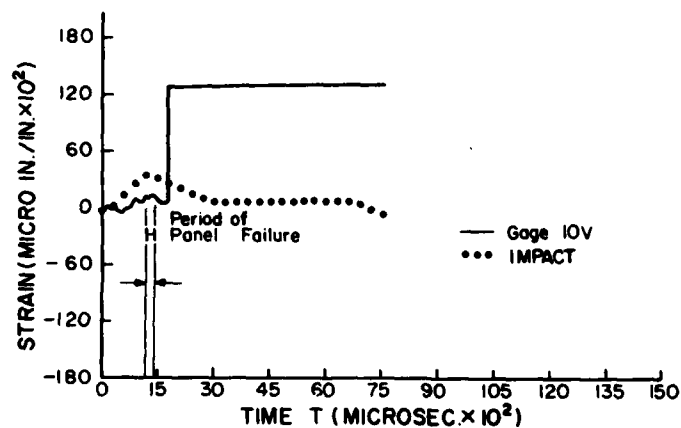


Figure 96. X Strain for the Inner Face of Cell Number 110.

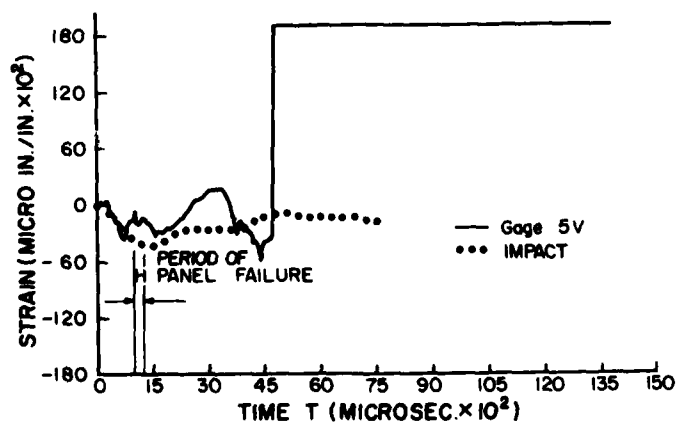


Figure 97. X Strain for the Outer Face of Cell Number 115.

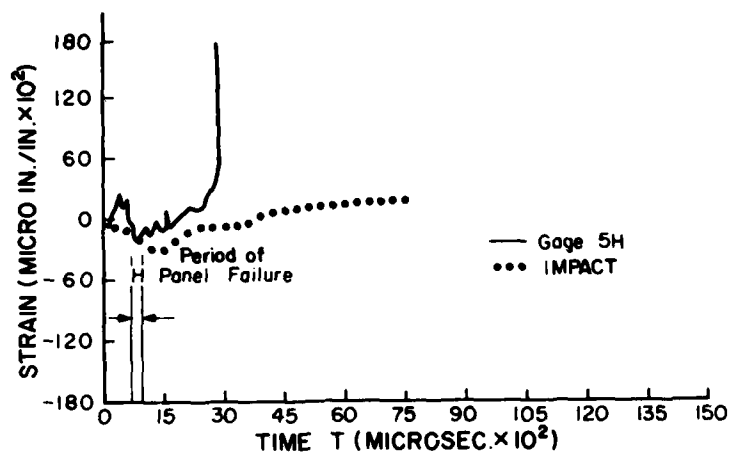


Figure 98. Y Strain for the Outer Face of Cell Number 115.

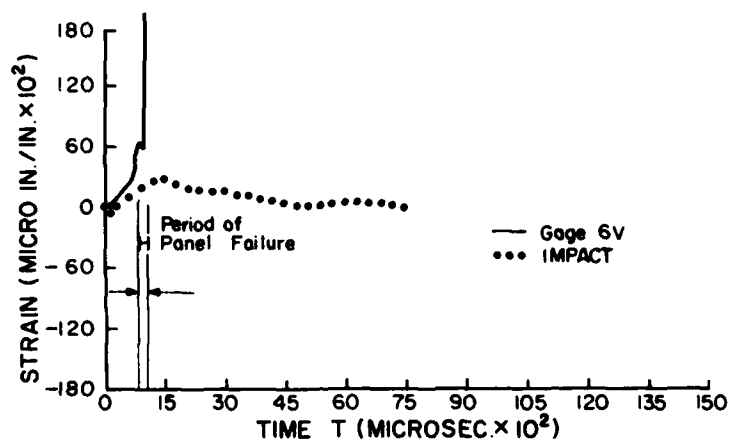


Figure 99. X Strain for the Inner Face of Cell Number 115.

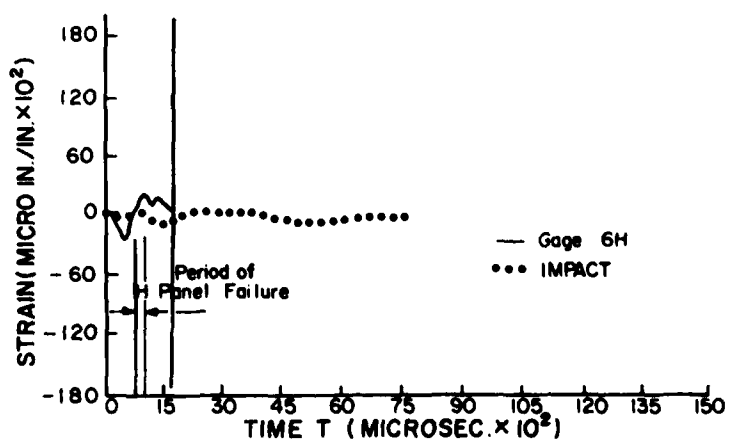


Figure 100. Y Strain for the Inner Face of Cell Number 115.

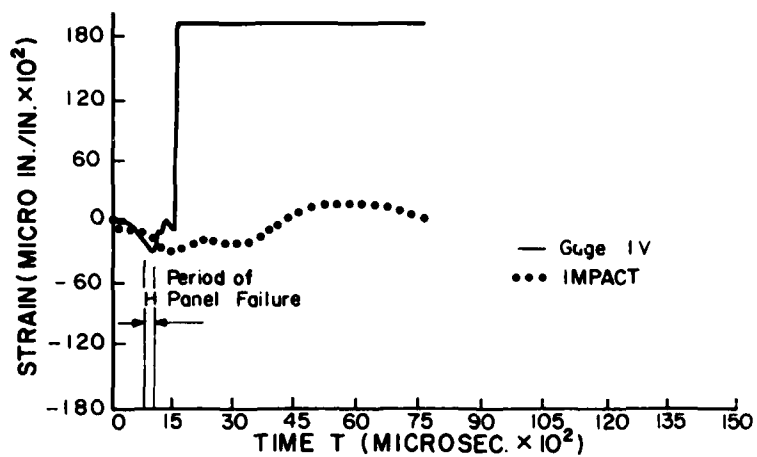


Figure 101. X Strain for the Outer Face of Cell Number 124.

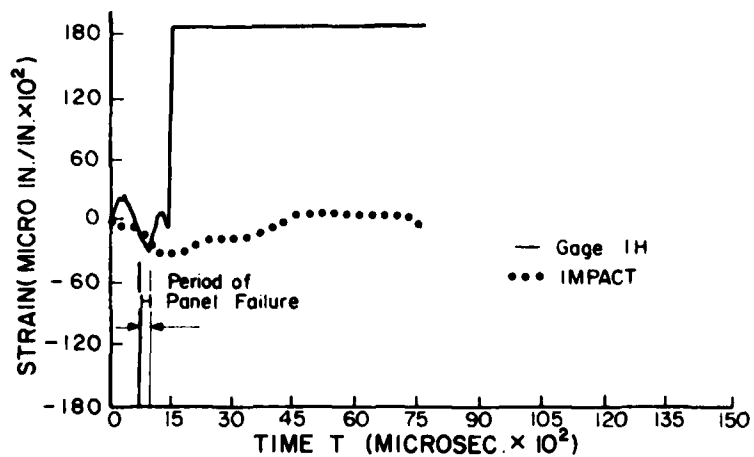


Figure 102. Y Strain for the Outer Face of Cell Number 124.

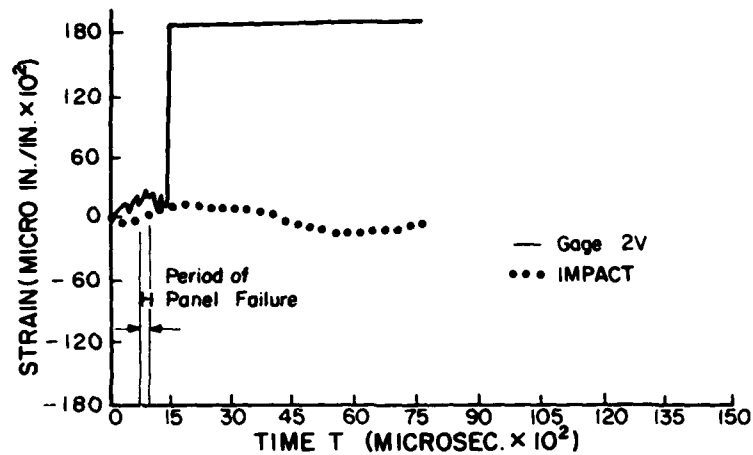


Figure 103. X Strain for the Inner Face of Cell Number 124.

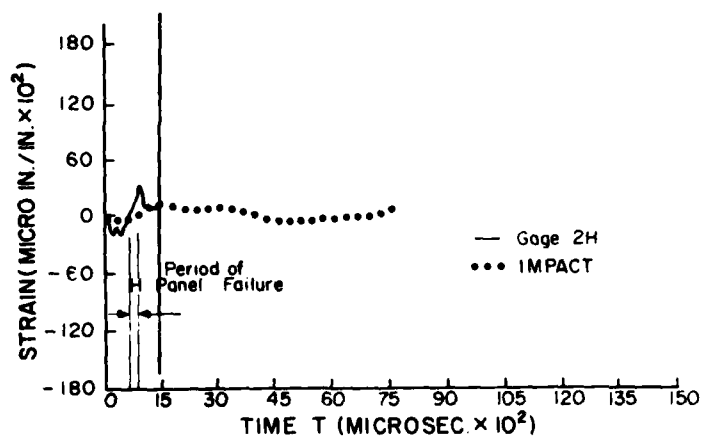


Figure 104. Y Strain for the Inner Face of Cell Number 124.

First dicing of a glass ply was observed in high-speed film records of the test to occur at 0.0012 sec after initial bird impact; the target became completely translucent at about 0.0015 sec. This period of time has been indicated on Figures 92 through 104. The general nature of the panel response represented by the BM19 strain data is the same as that for BM14. All H channels show evidence of a bending wave traveling in the direction of bird motion, and all V channels show a simple bending response.

All strain gage locations for BM19 exhibited tensile strains approaching 2100 micro in/in/, the tensile rupture strain for soda lime glass. Most of the strain gage signals were interrupted permanently during the panel failure; none survived longer than 4800 micro sec after initial impact. This serves as more evidence of the greater severity of the BM19 panel response compared to that for BM14.

Figure 82 may be used to determine the locations in the BM19 panel at which IMPACT calculated strains, again because these were the same as for BM14. Figures 92 through 104 show the strain data calculated at these points. As for BM14, the IMPACT results for BM19 seem to show the same signs, the same sign reversals, and the same periods of motion observed in the data. The magnitudes of the individual strain histories, however, differ even more from the observed data than did those calculated for the BM14 case. Instead of being uniformly low as was the case for BM14, the IMPACT strain data for BM19 is much too great at some locations and much too low at others. With the exception of the inner face of cell element 110, the calculated strains are too great on all cell outer surfaces (too much compression) and too low on all cell inner surfaces (too little tension). The calculated strains seem to correspond to a strong field of compressive strains being superposed over the normal bending strains which would result from bird impact. Some overall field of compressive strains might be expected to result from the elevated temperature of the structure for this test. Heating should have resulted

in a (compressive) thermal strain field being induced throughout the test article. However, the level seen in the IMPACT dynamic response data is much greater than would be expected as a result of temperature gradients in the structure, the IMPACT compressive strains being as much as four times those measured and the tensile strains as little as one-fourth of those measured. This strong overall compression is not evident at zero time but develops during the response of the panel.

In an attempt to clarify the BM19 strain data correlation, the IMPACT deflection data was studied. Figure 105 illustrates deflection in the Z direction of a node located within the bird impact footprint. The deflection history for the BM19 node is compared to that for the BM14 node considered in Figure 89. The two deflection histories are almost identical during load rise as would be expected for such similar cases. But near the time of peak bird impact force, the BM19 response abruptly departs from the BM14 response, rebounding at a rate eight times higher. Figure 106 shows the deflection of the same node at later times; the deflections grow to completely unreasonable levels in excess of 3 in in the outward direction. Figure 107 shows the deflected shape of the BM19 panel at six different times during the calculated response. Deflections in the area of bird impact are very nearly the same as for BM14 during the first 1,500 micro sec. Even at these early times, however, the deflections of the support structure are physically unrealistic, reaching nearly 1 in in the outward direction. At this same time during the BM14 panel response, all points on the surface of the test structure was moving inward. After the rebound of the panel begins, the BM19 data shows outward deflections approaching 4 in. No evidence of deflections even a fraction of this level are evident from high-speed film records of the test. Peak deflections calculated by IMPACT after panel failure time should have been less than the actual deflections instead of greater because all four structural plies are treated as being intact and load-bearing throughout the IMPACT solution.

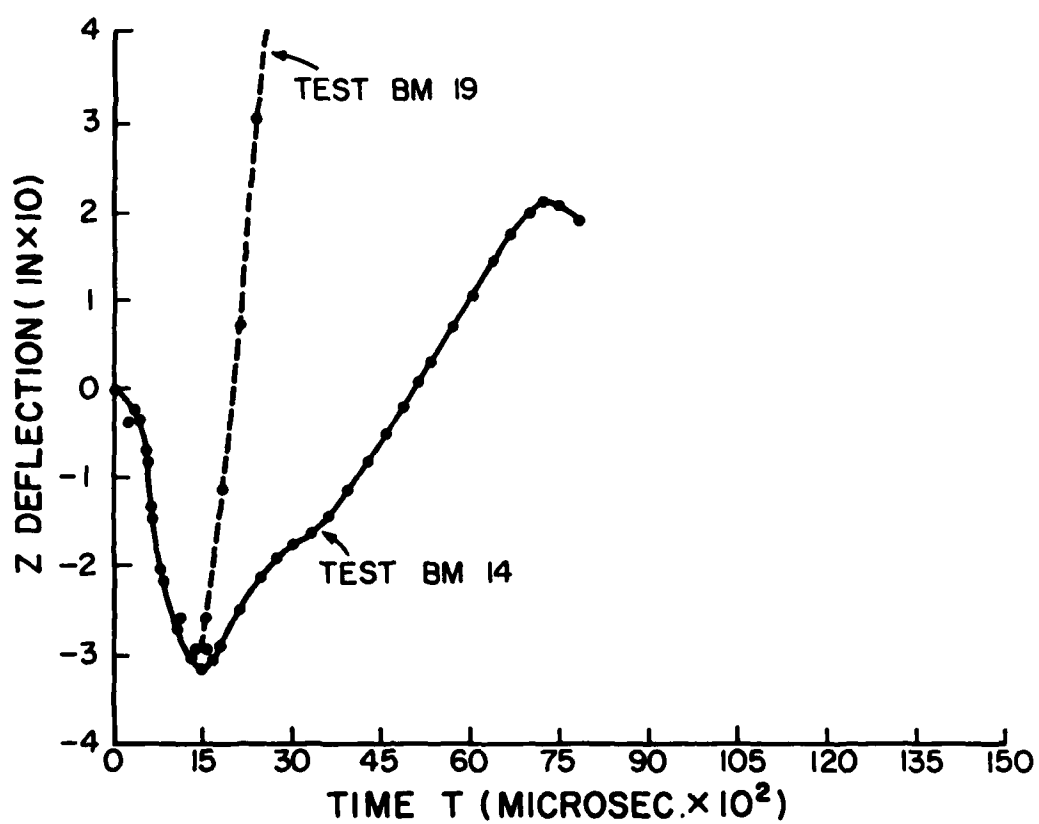


Figure 105. Z Deflection for BM14 Node 447 and BM19 Node 359.

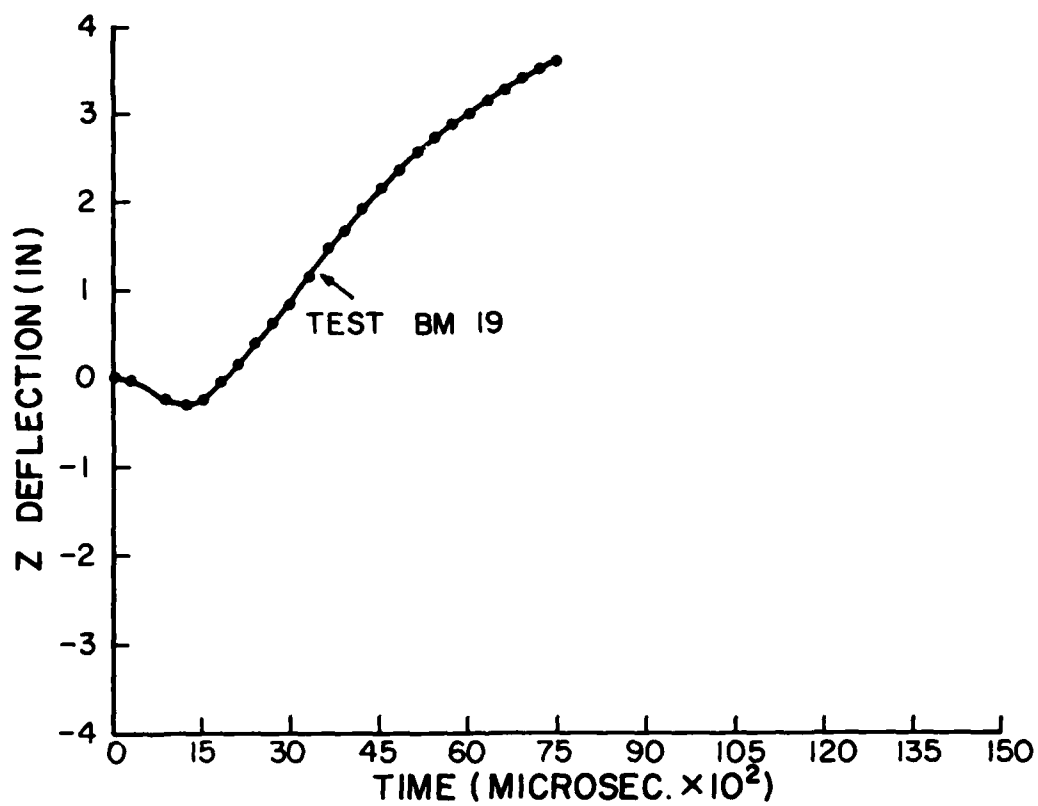


Figure 106. Z Deflection for Node 359.

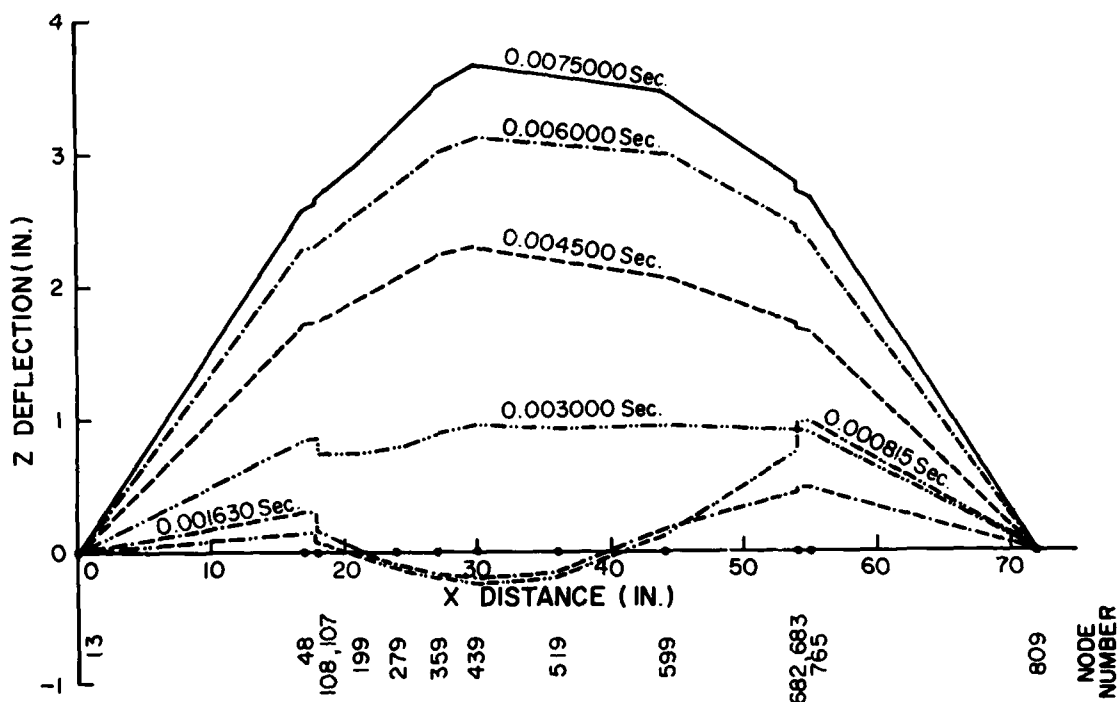


Figure 107. Z Deflection of Nodes Along a Longitudinal Section for Test BM19.

The final evidence of gross error in the BM19 IMPACT results was obtained from the equivalent stress data calculated. The same 100 cell elements were studied as for BM14. The IMPACT data indicates material rupture in every cell element representing a glass ply. This result in itself does not disagree with experimental observation, but plots of equivalent stress for other cell elements in the BM19 model were also plotted and two of these are shown in Figures 108 and 109. The cell element involved, number 394, is located in the windshield sidepost near the forward right corner of the transparency. An equivalent stress more than ten times the rupture stress for the material in the cell, 2024-T3 aluminum alloy, was calculated by IMPACT. This result is totally unrealistic because the test records show that no plastic deformation, and certainly no material rupture, occurred anywhere in the metallic support structure during Test BM19 (Reference 8).

At this point two explanations of the unrealistic BM19 results were being entertained, one being errors committed in the preparation of input data for the IMPACT analyses and the second being theoretical or coding errors within IMPACT related to the calculation of strain fields resulting from temperature gradients in the structure. The fundamental difference between BM14 and BM19 was the attempt to use the thermal stress capability for the latter case. For BM19 the temperature field in the structure, a linear gradient through the windshield, was specified at time zero. IMPACT was to have calculated strains resulting from the static temperature field and then to have proceeded with the solution of the transient response.

Repeated attempts to uncover errors in the BM19 input data proved fruitless. The portions of the model most suspect were the data describing the mechanical properties of materials (in

(8) R. H. Magnusson, High Speed Bird Impact Testing of Aircraft Transparencies, Air Force Flight Dynamics Laboratory, Wright-Patterson Air Force Base, Ohio 45433, AFFDL-TR-77-98, February 1978.

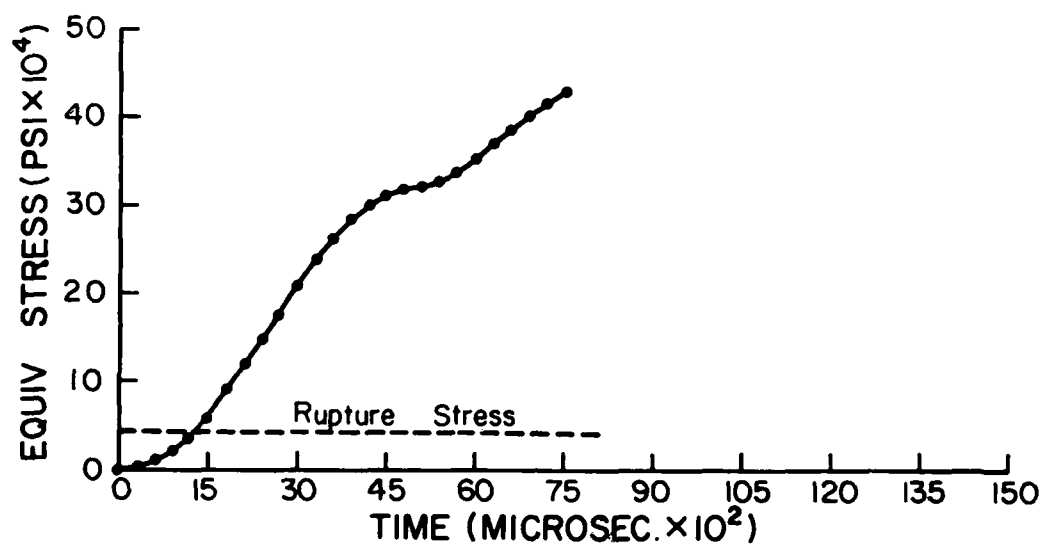


Figure 108. Equivalent Stress for Outer Surface of Cell 394.

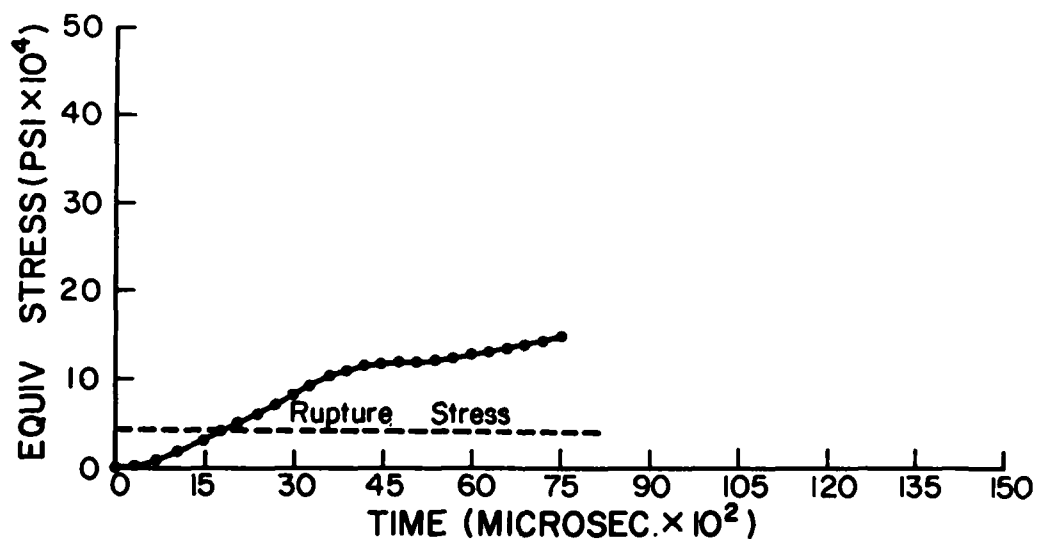


Figure 109. Equivalent Stress for Inner Surface of Cell 394.

particular the coefficients of thermal expansion), the data describing the temperatures of all nodes in the model, and the data describing the bird impact forces. These are the only areas differing from the BM14 model which apparently was analyzed successfully.

A query was made to the developers of IMPACT regarding the possibility of error in the thermal strain formulation in IMPACT (Reference 37). The response revealed that this feature of IMPACT had never been tested by its developers.

In light of all the above considerations, the most probable explanation of the physically unrealistic IMPACT results obtained for Test BM19 is that coding or theoretical errors exist in the formulation of IMPACT which render its thermal strain capability ineffectual. No resources were available under the subject work effort to test this hypothesis further.

2. EFFICIENCY OF IMPACT

In the application of any analytical tool or method in the solution of engineering problems, it is always necessary to trade off the resources required to accomplish the analysis against the benefits of having done so. An analysis which is costly to perform in terms of time, money, or manpower may not provide results or benefits which are worth the effort involved. In finite element dynamic analysis, the costs of performing the analysis may be measured in terms of manpower and calendar time required to prepare the structural and loading models, manpower and calendar time required to setup and run analysis jobs on a computer, cost of computer time required to calculate problem solutions, and the manpower and calendar time required to analyze computed results.

(37) Personal Communication, 14 May 1979, R. C. Morris, Douglas Aircraft Company, Cl-253, 3855 Lakewood Boulevard, Long Beach, California 90846.

In Section I.2 of this report it was pointed out that the finite element models used in these analyses were prepared under contract by the Douglas Aircraft Company. The man-hours actually required by Douglas to complete the BM14 model were not available at the time of this writing, but may be estimated as 300 man-hours. Another 200 AFFDL/FER man-hours were required to generate the BM19 model from the BM14 model and to prepare loading data for both. Another 200 hours were required to run the IMPACT analyses for Tests BM14 and BM19. The computer costs associated with these analyses have been presented in Tables 5 and 6. About 200 man-hours were required to reduce the calculated data. Plots had to be drawn by hand due to the lack of plotting capability in the IMPACT postprocessor. The elapsed calendar time from the initiation of AFFDL/FER studies to the completion of data reduction was 14 months. An unknown number of additional months had been required by Douglas Aircraft Company to prepare the BM14 finite element model.

At an average of \$12 per hour, all these activities related to BM14/19 IMPACT analyses add up to nearly \$11,000. The total computing costs for the two analyses exceeded \$3,000 and roughly one and one-half years were required to complete the overall study. These values may be compared respectively with the approximate cost of fabricating the two test articles \$15,000; the cost of actually performing the two bird impact tests at AEDC, \$3,000; and the calendar time required to design, fabricate, and test the panels, about 12 months.

It is apparent from the discussion above that the resources required to utilize IMPACT as an aircraft transparency design and analysis tool are significant when compared to those required by current more empirical methods for accomplishing the same task.

In the form used for the work reported here, the most costly aspect of IMPACT was its lack of effective pre- and post-processors. This required, as a result, a great deal of time for manual data manipulation.

The next most costly aspect of IMPACT was probably the large size which was typical of all the FORMAT Setup 1 and 2 jobs. The cost to accomplish each was three or four times that of the next most expensive computational step, the Incremental Solution. The calendar time required for these FORMAT steps was also significant because jobs this size could be turned around only once per week on the Wright-Patterson Air Force Base ASD computer system. The benefits of reducing the size of these jobs, if possible, could be very significant; for example, reducing CPU and I/O times by a factor of two might increase the job turn-around rate by a factor of 20.

It is apparent that additional development of IMPACT might greatly enhance its efficiency and hence its desirability as an aircraft transparency design analysis tool.

3. USABILITY OF IMPACT

At the time that these IMPACT analyses were initiated, personnel of AFFDL/FER had a working knowledge of the operating system for the ASD computer system at Wright-Patterson Air Force Base, but little experience with finite element analysis computer programs. The dates shown on Tables 5, 6, and 7 represent the learning curve experienced by FER personnel in the utilization of IMPACT. Other than those incidents made reference to in the text of this report, no contracts were made with the developers of IMPACT during the period of these studies. The dates referred to represent therefore the time required for FER personnel to read, understand, and successfully implement the written guidance contained in the IMPACT User's Manual (Reference 6). Two months were required to complete the first (BM14) analysis, but only 15 days for the second. It should be noted that 15 days represent nearly minimum time required for a problem of this size because

(6) G. R. Eide, Aircraft Windshield Bird Impact Math Model -Part 2 - User's Manual, Air Force Flight Dynamics Laboratory, Wright-Patterson Air Force Base, Ohio 45433, AFFDL-TR-77-99, Part 2, December 1977.

of the one-per-week turnaround rate for the large FORMAT jobs involved.

The fact that FER personnel were able to accomplish the second analysis in so short a time speaks well for the quality of the written program documentation. No significant problems were encountered in preparing the input data and executing the jobs desired. The written guidance was found to be straight forward and understandable. If, however, both the pre- and postprocessors are included under the category of usability, the overall usability of IMPACT must be rated on the cumbersome side. A user planning to conduct studies must either adapt other existing processors for use with IMPACT or face the considerable penalty of preparing models and plotting results by hand. The scope of these manual tasks is such that it might limit the acceptance and use of IMPACT by the transparency design community, at least the edition of IMPACT used in the B-1 windshield studies reported here.

The next section of this report summarizes the conclusions which were drawn from the results presented in this section.

SECTION VIII

CONCLUSIONS

As stated in Section I.1 of this report, the IMPACT finite element transient response computer program was developed in an attempt to provide a birdstrike analysis tool which would find application in the aircraft transparency design community. It was anticipated that this tool would aid in reducing the time and costs associated with transparency design by eliminating the need for some of the developmental fabrication and testing required by current, more empirical, design methods.

Since IMPACT, as delivered to the Air Force in December 1977, was strictly a linear analysis program, the primary objective of the work reported here was to determine whether or not aircraft transparency systems employing relatively stiff structure might be designed with such a linear analysis tool. It was assumed that more compliant, or flexible, aircraft transparencies such as the F-16 clear-view canopy would necessarily require non-linear analysis in order to take into account the effects of the larger deflections in the structure resulting from bird impact. The B-1 aircraft was selected as an example of stiff windshield structure and as such to serve as a test case for IMPACT correlation studies. Secondary objectives of the work were to evaluate the efficiency and usability of IMPACT.

The results of the B-1 IMPACT analyses accomplished may be summarized from Section VII as follows.

Although IMPACT was able to qualitatively simulate the bird impact response of a simulated B-1 windshield panel quite realistically, it failed to predict accurately the magnitudes of the strains and deflections observed during the actual bird impact test. The levels of strain measured in the main glass plies of the test panel exceeded those calculated by IMPACT by as much as 100 percent.

IMPACT simulation for the bird impact response of a second B-1 windshield panel which had been heated to an outer surface temperature of 220 deg F was accomplished but the results were not realistic. Deflections calculated by IMPACT for this case reached levels ten times those observed during the actual test.

Attempts to simulate the bird impact response of a prototype B-1 windshield mounted in the B-1 X-5 crew module were unsuccessful when the IMPACT jobs proved to be too large to run on the Wright-Patterson Air Force Base CDC Cyber 74 computer. The cause of the failure was the fact that decomposition of the structural stiffness matrix for the B-1 X-5 finite element model was not possible within the central memory space available on the computer (275,000 octal words).

The overall cost and time required to complete the IMPACT analysis of two simulated B-1 windshield panel designs were roughly equivalent to the cost and time required for fabrication and test of the actual windshield panels excluding development cost and time. Ten months alone were required to manually reduce IMPACT results to plotted form for data analysis since no plotting capability was provided by the IMPACT postprocessor.

The conclusions regarding the objectives of this work which may be drawn from these results are as follows:

1. The most probable cause, among those considered, of the large strain errors observed in the BM14 IMPACT results was the fact that IMPACT did not account for the effects of geometric nonlinearity which apparently were present in the curved test panel.
2. The magnitude of the strain errors observed in the IMPACT results is great enough to prevent the successful application of IMPACT to the design and birdstrike analysis of this class of structures—large, curved windshields of laminated glass or plastic construction.

3. The only type of aircraft transparency which might be expected to behave in a more linear fashion than the B-1 windshield is that of flat, laminated glass panels like those used in some transport and bomber aircraft. The bird impact response of this type transparency may prove to be sufficiently linear to permit successful application of IMPACT.
4. Apparently some theoretical or coding errors exist in the formulation of the December 1977 edition of IMPACT which render it incapable of correctly accounting for the effects of elevated temperatures and/or temperature gradients in the structure of interest.
5. The formulation of IMPACT prevents the analysis of finite element models having more than 4,000 unconstrained degrees of freedom unless the geometry of the structure is quite simple and regular.
6. The efficiency of IMPACT suffers due to the long time and high cost associated with some of the steps required, in particular the FORMAT Setup 1 and Setup 2 jobs. These jobs accomplish decomposition of the structural stiffness matrix and the extraction of an arbitrary number of free vibration modes for the structure, respectively. Any development which would reduce the size of these steps or, in the case of the Setup 2 job, remove the need for the step (a nonmodal approach) would greatly enhance the efficiency and desirability of IMPACT as an aircraft transparency design and analysis tool.
7. The lack of effective pre- and postprocessors with the December 1977 edition of IMPACT poses a severe penalty to the usability of the program. As a result, the only practical method for applying IMPACT would seem to be by interfacing it with other currently available pre- and postprocessors. The development of effective pre- and postprocessors for IMPACT would greatly enhance its utility as an aircraft transparency design and analysis tool.

8. The program documentation available for IMPACT users is written in a straightforward and understandable manner (References 5, 6, and ...).

(5) P. H. Denke, Aircraft Windshield Bird Impact Math Model, Part 1 Theory and Application, Air Force Flight Dynamics Laboratory, Wright-Patterson Air Force Base, Ohio 45433, AFFDL-TR-77-99, Part 1, December 1977.

(6) G. R. Eide, Aircraft Windshield Bird Impact Math Model - Part 2 - User's Manual, Air Force Flight Dynamics Laboratory, Wright-Patterson Air Force Base, Ohio 45433, AFFDL-TR-77-99, Part 2, December 1977.

(7) R. C. Morris, Aircraft Windshield Bird Impact Math Model, Part 3: Programming Manual, Air Force Flight Dynamics Laboratory, Wright-Patterson Air Force Base, Ohio 45433, AFFDL-TR-77-99, Part 3, December 1977.

SECTION IX RECOMMENDATIONS

The following recommendations may be made in view of the conclusions presented in Section VIII.

Even though the IMPACT computer program was not found to be useful for the B-1 windshield, the development and application of the finite element method for birdstrike analysis and design of aircraft transparency systems should be pursued further as a cost-saving alternative to more empirical analysis and design techniques.

The computer program involved should provide the capability to accurately account for the effects of both geometric and material nonlinearity.

The capability to more realistically model bird impact pressures should be developed and incorporated into the computer program used.

The most efficient problem solution approaches, numerical methods, and programming techniques available should be incorporated into the computer program used in order to reduce to a minimum the computer resources required to run it.

Capable pre- and postprocessors should be developed along with the code used. The utility of the overall analysis tool hinges upon the availability of powerful pre- and postprocessors which will preclude the need for manual data preparation and reduction.

To accomplish these improvements for IMPACT would require an extensive effort. This should not be accomplished because other computer programs are currently available which provide these capabilities. In particular, the nonlinear finite element program which should be developed for aircraft transparency birdstrike analysis and design is the code named MAGNA (Materially and Geometrically Nonlinear Analysis) which has been developed by

the University of Dayton Research Institute, Dayton, Ohio (Reference 38). Of all the nonlinear and finite element programs currently available, MAGNA has shown the most promise as a birdstrike analysis tool. MAGNA has features which make it especially well-suited to the transparency birdstrike problem including a preprocessor for laminated transparency structures (Reference 39). The preprocessor provides interactive plotting to permit viewing of the finite element model being generated. A postprocessor is currently under development for MAGNA which offers two-dimensional plots of any one parameter in the finite element solution against any other, deformed structure plotting, and relief and contour plotting.

In view of the recent significant advances with MAGNA, further Air Force development of the IMPACT computer program is not recommended. It should be noted here that a version of IMPACT is still under development at Douglas Aircraft Company, Long Beach, California. At the time of this writing, improvements have been made in the Douglas version of IMPACT, especially regarding its capability to take into account the effects of geometric nonlinearities (Reference 37).

Success in the development of a nonlinear finite element code for transparency birdstrike analysis and design will lead to a requirement for better data on the mechanical properties of transparent materials used in current systems. The properties

(38) R. A. Brockman, MAGNA: A Finite Element Program for the Materially and Geometrically Nonlinear Analysis of Three Dimensional Structures Subjected to Static and Transient Loading, University of Dayton Research Institute, Dayton, Ohio 45469, UDR-TR-79-45, November 1979.

(39) H. C. Rhee, Finite Element Discretization Program for Aircraft Windshield Systems: Theoretical Development and User's Guide, University of Dayton Research Institute, Dayton, Ohio 45469, UDR-TR-78-122, January 1979.

(37) Personal Communication, 14 May 1979, R. C. Morris, Douglas Aircraft Company, C1-253, 3855 Lakewood Boulevard, Long Beach, California 90846.

of plastic and interlayer materials in particular are poorly known as are the strong effects which temperature and strain rate have upon these properties. It is recommended that, as development of the finite element method continues and as the definition of materials data required as a result becomes more and more clear, programs be planned and accomplished to acquire the required data. Some work along these lines has already been accomplished (References 13, 40, and 41), but a great deal more remains to be done.

(13) F. E. Green, Testing for Mechanical Properties of Monolithic and Laminated Polycarbonate Materials, Air Force Flight Dynamics Laboratory, Wright-Patterson Air Force Base, Ohio 45433, AFFDL-TR-77-96, October 1977.

(40) R. J. Reid, and A. H. Jones, High Rate Tension and Compression on Selected Candidate Windshield Materials, Terra Tek Inc., Salt Lake City, Utah 84108, TR-77-25, April 1977.

(41) R. Lingle, K. L. DeVries, and A. H. Jones, Performance Evaluation of Candidate Windshield and Interlayer Materials, Terra Tek Inc., Salt Lake City, Utah 84108, TR-77-109, November 1977.

REFERENCES

1. H. E. Littel, Improved Windshield and Canopy Protection Development Program, Air Force Flight Dynamics Laboratory, Wright-Patterson Air Force Base, Ohio 45433, AFFDL-TR-74-75, June 1974.
2. A. L. Lewis and K. W. Cooke, F-111 Bird Resistant Windshield Support Structure, Air Force Flight Dynamics Laboratory, Wright-Patterson Air Force Base, Ohio 45433, AFFDL-TR-74-40, 10 May 1974.
3. B. S. West, Design and Testing of F-111 Bird Resistant Windshield/Support Structure: Volume 1 - Design and Verification Testing, Air Force Flight Dynamics Laboratory, Wright-Patterson Air Force Base, Ohio 45433, AFFDL-TR-76-101, October 1976.
4. J. B. Olson, Design, Development and Testing of a Light-Weight-Bird-Proof Cockpit Enclosure for the F-111, 1978 Conference on Aerospace Transparent Materials and Enclosures, Air Force Flight Dynamics Laboratory, Wright-Patterson Air Force Base, Ohio 45433, AFFDL-TR-78-168.
5. P. H. Denke, Aircraft Windshield Bird Impact Math Model, Part 1 Theory and Application, Air Force Flight Dynamics Laboratory, Wright-Patterson Air Force Base, Ohio 45433, AFFDL-TR-77-99, Part 1, December 1977.
6. G. R. Eide, Aircraft Windshield Bird Impact Math Model -Part 2- User's Manual, Air Force Flight Dynamics Laboratory, Wright-Patterson Air Force Base, Ohio 45433, AFFDL-TR-77-99, Part 2, December 1977.
7. R. C. Morris, Aircraft Windshield Bird Impact Math Model, Part 3: Programming Manual, Air Force Flight Dynamics Laboratory, Wright-Patterson Air Force Base, Ohio 45433, AFFDL-TR-77-99, Part 3, December 1977.
8. R. H. Magnusson, High Speed Bird Impact Testing of Aircraft Transparencies, Air Force Flight Dynamics Laboratory, Wright-Patterson Air Force Base, Ohio 45433, AFFDL-TR-77-98, February 1978.
9. E. J. Sanders, Results of Further Tests to Evaluate the Bird Impact Resistance of Windshields for the B-1 Aircraft, AEDC-DR-76-43, Arnold Engineering Development Center, Arnold Air Force Station, Tennessee 37389.
10. E. J. Sanders, Results of Bird Impact Testing of Prototype B-1 Windshields and Supporting Structure Design, AEDC-DR-76-100, Arnold Engineering Development Center, Arnold Air Force Station, Tennessee 37389.

11. Military Standardization Handbook - Metallic Materials and Elements for Aerospace Vehicle Structures, Volumes 1 and 2, MIL-HDBK-5C, 15 September 1976.
12. Military Standardization Handbook-Plastics for Aerospace Vehicles, Part II Transparent Glazing Materials, MIL-HDBK-17A, Part II, 8 June 1977.
13. F. E. Greene, Testing for Mechanical Properties of Monolithic and Laminated Polycarbonate Materials, Air Force Flight Dynamics Laboratory, Wright-Patterson Air Force Base, Ohio 45433, AFFDL-TR-77-96, October 1977.
14. J. Pickard, FORMAT - Fortran Matrix Abstraction Technique Volume V, Engineering User and Technical Report, Air Force Flight Dynamics Laboratory, Wright-Patterson Air Force Base, Ohio 45433, AFFDL-TR-66-207, Volume V, October 1968; Volume V Supplement I, June 1970; Volume V Supplement II, April 1973; Volume V Supplement III, December 1977.
15. J. P. Barber and J. S. Wilbeck, Characterization of Bird Impacts on a Rigid Plate: Part I, Air Force Flight Dynamics Laboratory, Wright-Patterson Air Force Base, Ohio 45433, AFFDL-TR-75-5, January 1975.
16. R. L. Peterson and J. P. Barber, Bird Impact Forces in Aircraft Windshield Designs, Air Force Flight Dynamics Laboratory, Wright-Patterson Air Force Base, Ohio 45433, AFFDL-TR-75-150, March 1976.
17. Y. M. Ito, G. E. Carpenter, and F. W. Perry, Bird Impact Loading Model for Aircraft Windshield Design, CRT 3090-2, California Research & Technology, Inc., Woodland Hills, California 91364, July 1977.
18. J. P. Barber, J. S. Wilbeck, and H. R. Taylor, Bird Impact Forces and Pressures on Rigid and Compliant Targets, Air Force Flight Dynamics Laboratory, Wright-Patterson Air Force Base, Ohio 45433, AFFDL-TR-77-60, May 1978.
19. J. S. Wilbeck, Impact Behavior of Low Strength Projectiles, Air Force Materials Laboratory, Wright-Patterson Air Force Base, Ohio 45433, AFML-TR-77-134, July 1978.
20. E. J. Sanders, The Von Karman Gas Dynamics Facility Range S-3- Description and Capabilities, Arnold Engineering Development Center, Arnold Air Force Station, Tennessee 37389, AEDC-TR-76-9, January 1976.
21. Drawing Number Z5942639-501, Z5942642-1, Z5942694-1, Z5942643-2, Z5942643-1, and Z5942638-1, Douglas Aircraft Company, Long Beach, California.

22. S. H. Crandall and N. C. Dahl, An Introduction to the Mechanics of Solids, McGraw Hill, 1959.
23. G. F. Rhodes, Damping, Static, Dynamic and Impact Characteristics of Laminated Beams Typical of Windshield Construction, Air Force Flight Dynamics Laboratory, Wright-Patterson Air Force Base, Ohio 45433, AFFDL-TR-76-156, December 1977.
24. A. S. Saada, Elasticity: Theory and Applications, Pergamon Press, 1974.
25. Personal Communication, 24 May 1978, Merle J. Coker, Douglas Aircraft Company, Cl-253, 3855 Lakewood Boulevard, Long Beach, California 90846.
26. A. Challita and J. P. Barber, The Scaling of Bird Impact Loads, Air Force Flight Dynamics Laboratory, Wright-Patterson Air Force Base, Ohio 45433, AFFDL-TR-79-3042, March 1979.
27. J. Y. Parker, Measurement of Impact Bird Pressure on a Flat Plate, Arnold Engineering Development Center, Arnold Air Force Station, Tennessee 37389, AEDC-TR-79-14.
28. G. B. Thomas, Calculus and Analytic Geometry, Addison-Wesley, 1965.
29. R. H. Hammond, C. P. Buck, W. B. Rogers, G. W. Walsh, Jr., and H. P. Ackert, Engineering Graphics for Design and Analysis, The Ronald Press Company, 1964.
30. R. L. Ketter and S. P. Prawel, Jr., Modern Methods of Engineering Computation, McGraw-Hill, 1969.
31. P. H. Denke and J. B. Hoffman, The Determination of Deflection and Stress Distribution for a Laminated Transparent Beam, Air Force Flight Dynamics Laboratory, Wright-Patterson Air Force Base, Ohio 45433, AFFDL-TR-76-114, November 1976.
32. G. Murphy, Advanced Mechanics of Materials, McGraw-Hill, 1946.
33. Personal Communication, 5 June 1978, R. C. Morris and G. R. Eide, Douglas Aircraft Company, Cl-253, 3855 Lakewood Boulevard, Long Beach, California 90846.
34. NOS/BE Version 1 Reference Manual, Publication Number 60493800, Control Data Corporation, Publications and Graphics Division, ARH219, 4201 North Lexington Avenue, St. Paul, Minnesota 55112.

35. D. P. Mondkar and G. H. Powell, "Finite Element Analysis of Nonlinear Static and Dynamic Response," International Journal for Numerical Methods in Engineering, Vol II, pp 499-520, 1977.
36. E. F. Bruhn, Analysis and Design of Flight Vehicle Structures, Tri-State Offset, 1965.
37. Personal Communication, 14 May 1979, R. C. Morris, Douglas Aircraft Company, Cl-253, 3855 Lakewood Boulevard, Long Beach, California 90846.
38. R. A. Brockman, MAGNA: A Finite Element Program for the Materially and Geometrically Nonlinear Analysis of Three Dimensional Structures Subjected to Static and Transient Loading, University of Dayton Research Institute, Dayton, Ohio 45469, UDR-TR-79-45, November 1979.
39. H. C. Rhee, Finite Element Discretization Program for Aircraft Windshield Systems: Theoretical Development and User's Guide, University of Dayton Research Institute, Dayton, Ohio 45469, UDR-TR-78-122, January 1979.
40. R. J. Reid and A. H. Jones, High Rate Tension and Compression on Selected Candidate Windshield Materials, Terra Tek Inc., Salt Lake City, Utah 84108, TR-77-25, April 1977.
41. R. Lingle, K. L. DeVries, and A. H. Jones, Performance Evaluation of Candidate Windshield and Interlayer Materials, Terra Tek Inc., Salt Lake City, Utah 84108, TR-77-109, November 1977.